

LIGHT ADAPTATION AND SENSITIVITY CHANGE
PROCESSES IN THE HUMAN RETINA –
INVESTIGATING OPTO-ELECTRONIC APPLICATIONS

by

Tomasz Waldemar Wysokinski

M.Sc., Eng. (Physics) Technical University of Gdansk – Poland, 1989

A THESIS SUBMITTED IN PARTIAL FULFILLMENT OF
THE REQUIREMENTS FOR THE DEGREE OF
DOCTOR OF PHILOSOPHY
in the School
of
Engineering Science

© Tomasz W. Wysokinski 1996
SIMON FRASER UNIVERSITY
May 1996

All rights reserved. This work may not be
reproduced in whole or in part, by photocopy
or other means, without the permission of the author.

Approval

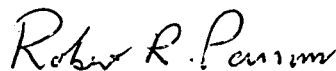
Name: Tomasz Waldemar Wysokinski
Degree: Doctor of Philosophy (Engineering)
Title of Thesis: *Light Adaptation and Sensitivity Change Processes in the Human Retina – Investigating Opto-Electronic Applications*
Examining Committee: Dr. John S. Bird
Chairman

Dr. Andrew H. Rawicz
Senior Supervisor

Dr. Romuald Lakowski
Supervisor

Dr. M. Parameswaran
Supervisor

Dr. Robert F. Frindt
Internal External Examiner



Dr. Robert R. Parsons
External Examiner
University of British Columbia

Date Approved: May 8, 1996

PARTIAL COPYRIGHT LICENSE

I hereby grant to Simon Fraser University the right to lend my thesis, project or extended essay (the title of which is shown below) to users of the Simon Fraser University Library, and to make partial or single copies only for such users or in response to a request from the library of any other university, or other educational institution, on its own behalf or for one of its users. I further agree that permission for multiple copying of this work for scholarly purposes may be granted by me or the Dean of Graduate Studies. It is understood that copying or publication of this work for financial gain shall not be allowed without my written permission.

Title of Thesis/Project/Extended Essay

LIGHT ADAPTATION AND SENSITIVITY CHANGE

PROCESSES IN THE HUMAN RETINA —

INVESTIGATING OPTO-ELECTRONIC APPLICATIONS

Author:

(signature)

Tomasz W. WYSOKINSKI

(name)

May 8th, 1996

(date)

Abstract

Real-world image acquisition systems, such as the charge coupled device with frame grabber and computer, are still very limited in overall performance compared with the biological visual systems. The work done in this thesis originates from the fact that the solutions implemented by nature are both elegant and efficient, and that they should be the inspiration for designers to enhance the performance of artificial visual systems.

In the first part of this research, we investigate the phenomena of light adaptation and sensitivity change processes that allow an eye to operate over 12 decades of light intensity range. Different adaptation mechanisms are scrutinised, and a model of those mechanisms is developed. Next we investigate how the visual system copes with light intensities beyond its dynamic range when glare occurs. The signal saturation in glare phenomena is used to reveal the highly complex structure of the retina. By applying a developed model of signal propagation in the Outer Plexiform Layer and by relating it to the experimental psychophysical data, we obtain a formula for the density of horizontal cell connections along the diameter of the human retina.

By studying the architecture, neurology and physiology of the retina, we develop an equivalent Adaptive Filter/Photosensitive Device Array system capable of coping with a

wide range of light conditions. The Adaptive Filter mimics some adaptation mechanisms of the human eye and offers the possibility of extending the dynamic range of operation of any image-acquiring system without affecting the electronic circuitry of the photo-sensor array.

In the third part, we describe efforts to build one of the possible implementations of the adaptive filter, namely an optically addressed Photochromic Adaptive Filter (PAF), which utilizes photochromic material embedded in a polymeric environment. We successfully test the concept of extending the operating range of the constructed image-acquiring system by using optically-addressed PAF's. The system is modified to determine a Transformation Function of these filters using a simple, fast and easy-to-automate method.

In the appendix we discuss several problems related to this research program. We estimate the measurement errors in detail. We also present a new method of preparing thin-layer silver-halide film and describe other possible implementations of the adaptive filter using active opto-electronic devices.

“To suppose that the eye, with all its inimitable contrivances for adjusting the focus to different distances, for admitting different amounts of light, and for the correction of spherical and chromatic aberration, could have been formed by natural selection, seems, I freely confess, absurd in the highest possible degree.”

Charles Darwin: *On the Origin of Species*

Acknowledgements

I wish to thank my advisor, Dr. Andrew Rawicz, the members of my committee, Dr. Romuald Lakowski and Dr. M. Parameswaran, and all my friends for their many helpful comments and advice. I also owe a great deal of thanks to Brigitte Rabold and Susan Stevenson.

Last but not least, I wish to acknowledge my most important supporter, Hania, my wife.

Contents

Abstract iii

Acknowledgements vi

Contents vii

List of Equations xi

List of Tables xii

List of Figures xiii

List of Symbols and Abbreviations xv

Introduction 1

 Motivation 1

 Adaptation and Glare 2

 Adaptive Filter: Concept and Implementation 3

 Contributions 4

 Outline 4

Part I Light adaptation in biological visual systems 6

| | |
|--|----|
| Introduction | 7 |
| The retina – part of the visual system | 7 |
| Signal Flow in the Outer Plexiform Layer (OPL) | 9 |
| Adaptation and Sensitivity | 13 |
| Adaptation Mechanisms | 14 |
| Sensitivity Change Mechanisms | 17 |
| Conclusions | 18 |
| Glare | 20 |
| Neuronal Model of “Dazzling Glare” | 21 |
| Summary | 31 |

Part II Adaptive Filter: the concept 33

| | |
|--|----|
| Introduction | 34 |
| The concept | 34 |
| Transformation Function (TF) | 37 |
| Modelling | 39 |
| Modelling Image Transformation by Different Transformation Functions | 39 |
| Discussion of a few special cases of adaptive filters | 41 |
| Summary | 48 |

Part III Photochromic Adaptive Filter 49

| | |
|--|----|
| Introduction | 50 |
| Photochromic Systems | 50 |
| Photochromic systems – general description | 51 |
| Inorganic photochromic systems | 51 |

| | |
|---|-----------|
| Organic photochromic systems | 52 |
| Applications of photochromic systems | 54 |
| Development of a Photochromic Adaptive Filter (PAF) | 55 |
| Polymeric matrices | 56 |
| Photochromes | 57 |
| Design and fabrication | 59 |
| Spectral properties of photochromic filters | 61 |
| Thin film thickness estimation | 66 |
| Photochromic Filter – Implementation | 73 |
| Developing of the test bench | 73 |
| Experimentation | 76 |
| Typical image quality improvements | 77 |
| Determination of the Transformation Function of PAF | 83 |
| Introduction | 84 |
| Experimental | 84 |
| Transformation Function | 85 |
| Results and Discussion | 85 |
| Summary | 88 |
| Conclusions | 91 |
| Contributions | 92 |
| Advantages of photochromic systems | 93 |
| Limitations of organic photochromic systems | 94 |
| Future work | 95 |
| Design improvements | 95 |
| Technological improvements | 96 |
| Applications of photochromic systems | 97 |
| Related studies | 98 |

| | |
|---|------------|
| Appendix | 99 |
| Errors discussion and summary | 100 |
| Development of the inorganic PAF | 103 |
| Photochromic process | 103 |
| Spectral properties of inorganic photochromic film | 104 |
| Formation of Photochromic Glasses | 106 |
| Sputtering deposition of inorganic PAF | 106 |
| Preparation of a Photochromic Glass via a Sol-Gel process | 108 |
| Summary | 109 |
| Investigating possible implementation of the Active Adaptive Filter | 110 |
| Liquid Crystal Displays (LCD's) | 110 |
| Digital Micromirror Device (DMD) | 112 |
| Summary | 115 |
| Bibliography | 116 |

List of Equations

| | | |
|-----------|-------|-----|
| (Eq. 1.1) | | 23 |
| (Eq. 1.2) | | 25 |
| (Eq. 1.3) | | 26 |
| (Eq. 1.4) | | 26 |
| (Eq. 1.5) | | 27 |
| (Eq. 1.6) | | 28 |
| (Eq. 1.7) | | 29 |
| (Eq. 1.8) | | 29 |
| (Eq. 1.9) | | 29 |
| | | |
| (Eq. 2.1) | | 40 |
| (Eq. 2.2) | | 40 |
| (Eq. 2.3) | | 40 |
| (Eq. 2.4) | | 41 |
| (Eq. 2.5) | | 41 |
| (Eq. 2.6) | | 41 |
| (Eq. 2.7) | | 42 |
| (Eq. 2.8) | | 45 |
| | | |
| (Eq. 3.1) | | 51 |
| (Eq. 3.2) | | 67 |
| (Eq. 3.3) | | 69 |
| (Eq. 3.4) | | 69 |
| (Eq. 3.5) | | 70 |
| (Eq. 3.6) | | 71 |
| (Eq. 3.7) | | 71 |
| (Eq. 3.8) | | 87 |
| | | |
| (Eq. A.1) | | 100 |
| (Eq. A.2) | | 101 |
| (Eq. A.3) | | 101 |
| (Eq. A.4) | | 104 |

List of Tables

| | | |
|-----------|--|-----|
| Table 1.1 | Selected biological adaptation processes compared with equivalent opto-electronic implementation | 19 |
| Table 3.1 | Product names and acronyms of investigated polymers | 56 |
| Table 3.2 | Solvents used in trial experiments | 57 |
| Table 3.3 | Structure and conventional names of investigated photochromes | 57 |
| Table 3.4 | Typical photochrome-polymer solution formulation | 60 |
| Table 3.5 | Sample composition | 60 |
| Table 3.6 | Spectral and temporal properties of photochromic filters | 62 |
| Table 3.7 | Spectral parameters for different photochromic systems | 66 |
| Table 3.8 | Calculated values of time constant – first approximation | 66 |
| Table A.1 | Errors overview | 102 |

List of Figures

| | | |
|------------|---|----|
| Figure 1.1 | Human eye: schematic cross-section | 8 |
| Figure 1.2 | Synaptic connections of cells in the peripheral retina | 9 |
| Figure 1.3 | Dazzling glare models: a. lateral inhibition in the OPL, b. light scattering | 22 |
| Figure 1.4 | Electrical circuit model of one dimensional resistive network | 24 |
| Figure 1.5 | Experimental glare function vs. angular distance from the glare source derived from Equation 1.3 | 27 |
| Figure 1.6 | Normalized lateral inhibition spread function calculated from Equation 1.5 with $a = 46$ and $b = 0.112$ | 28 |
| Figure 1.7 | Horizontal cells and horizontal cell connection density distribution | 30 |
| | | |
| Figure 2.1 | Utilization of the adaptive filter in a. global and b. local operating mode | 36 |
| Figure 2.2 | Block diagram of the image processing system utilizing active and passive types of the Adaptive Filter | 37 |
| Figure 2.3 | Selected image transformation types: a. proportional reconstruction b. nonlinear reconstruction c. optimal proportional reconstruction d. proportional reconstruction with part of the image saturated e. exact reconstruction | 38 |
| Figure 2.4 | Global adaptation modelling – “Model 1”, a. initial (overexposed) image, b. transformed image (the forest in the background clearly visible) | 43 |
| Figure 2.5 | Local adaptation modelling – “Model 2”, a. initial (overexposed) image, b. transformed image (many more details are clearly visible) | 44 |
| Figure 2.6 | Local adaptation modelling – “Model 4”, a. initial (overexposed) image, b. transformed image (note the hot air above the chimney, the license plate) | 46 |
| Figure 2.7 | Investigated transformation functions | 47 |
| | | |
| Figure 3.1 | Heterolytic bond cleavage mechanism in spiroxazine “N” | 52 |
| Figure 3.2 | Heterolytic bond cleavage mechanism in naphthopyran “Y” | 53 |
| Figure 3.3 | Block diagram of an optic-optic light modulator unit | 55 |
| Figure 3.4 | Spectral properties of multi-component photochromic systems | 65 |
| Figure 3.5 | Kinetic properties – thermal decay of the colored forms of samples | 67 |
| Figure 3.6 | Spectral transmittance for bare glass plate and a plate coated with thin film: Red photochrome in B-725 matrix, N #9 | 68 |
| Figure 3.7 | Reflectance and transmittance of a. a thick substrate, and b. system of the substrate and a thin layer | 69 |

| | | |
|-------------|--|-----|
| Figure 3.8 | Interference phenomena in a thin film | 70 |
| Figure 3.9 | Graphical method of estimating thin film thickness: Yellow photochrome in B-725 matrix, PL #20 | 72 |
| Figure 3.10 | Experimental set-up for testing photochromic filter (for clarity, housing has been removed; spectral properties presented in: T. 3.6 & F. 3.12) | 73 |
| Figure 3.11 | Block diagram of the experimental set-up for testing local adaptation | 74 |
| Figure 3.12 | Transmittance of Modification and IPB Filters | 75 |
| Figure 3.13 | Block diagram of the experimental set-up for testing global adaptation | 76 |
| Figure 3.14 | Experimentally observed image transformation types | 77 |
| Figure 3.15 | Image quality improvement a. before and b. after global adaptation: Yellow photochrome in B-725 matrix, PL #20; MOD – 420 nm | 78 |
| Figure 3.16 | Image quality improvement a. before and b. after global adaptation: Red photochrome in B-725 matrix, N #9; MOD – 560 nm | 79 |
| Figure 3.17 | Picture taken a. before adaptation, b. after adaptation and c. after normalization: Red photochrome in B-725 matrix, NN #7; MOD – 560 | 80 |
| Figure 3.18 | Image quality improvement a. before and b. after local adaptation: Yellow photochrome in B-725 matrix, NN #6; MOD – 420 nm | 81 |
| Figure 3.19 | Image quality improvement a. before and b. after local adaptation: CI-P & P photochromes in B-725 matrix, NN #4; MOD – 582 nm | 81 |
| Figure 3.20 | Image quality improvement a. before and b. after local adaptation: Yellow photochrome in B-725 matrix, NN #3; MOD – 420 nm | 82 |
| Figure 3.21 | Cross section of the image of the light source | 86 |
| Figure 3.22 | Transformation Function of a photochromic filter, calculated from data in inset in Figure 3.21 | 87 |
| Figure 3.23 | Reciprocal transmittance as a function of light intensity, calculated from Figure 3.21 | 88 |
| Figure 3.24 | Optical Density of the filter as a function of light intensity, calculated from Figure 3.21 | 89 |
| Figure 3.25 | Transformation function for a. spectrally and spatially uniform (point-like) and b. non-uniform light sources, NN #2 | 90 |
| Figure 4.1 | Organic photochromes based color image processing | 96 |
| Figure A.1 | Spatial separation of image processing and display | 100 |
| Figure A.2 | Spectral characteristic data for SOLA PhotoGray Extra [®] lens | 105 |
| Figure A.3 | Multilayered structures fabricated using sputtering technique | 107 |
| Figure A.4 | General layout of an image processing system utilizing LCD as an Active Adaptive Filter | 111 |
| Figure A.5 | General layout of an image processing system utilizing DMD as an Active Adaptive Filter | 113 |

List of Symbols and Abbreviations

Photochromic Systems

| | |
|---------------|-------------------------------------|
| B-725 | Butyl Methyl Methacrylate Copolymer |
| NN #20 | Sample NN #20 abbreviation* |
| PC | Poly(Carbonate) |
| PMMA | Poly(Methyl Methacrylate) |
| PS | Poly(Styrene) |
| PVA | Poly(Vinyl-Alcohol) |
| $C_{wt} [\%]$ | weight percent concentration |

Experimental Techniques

| | |
|------------------|-------------------------------|
| A | absorption |
| cm | centimeter (10^{-2} meter) |
| ϵ_{max} | extinction coefficient |
| IR | infra-red region |
| λ_{max} | absorption/transmission peak |
| μm | micrometer (10^{-6} meter) |
| min | minute (60 seconds) |
| nm | nanometer (10^{-9} meter) |
| RF | radio frequency |
| UV | ultra-violet region |
| VIS | visible region |
| wav | wavelength |

Miscellanea

| | |
|----------|---------------------------------------|
| 2-D | Two-Dimensional |
| 3-D | Three-Dimensional |
| α | in proportion to |
| AAF | Active Adaptive Filter |
| AF | Adaptive Filter |
| AMLCD's | Active Matrix Liquid Crystal Displays |
| arc min | minutes of arc |
| a.u. | arbitrary units |

* For details regarding other samples see *Table 3.5*.

| | |
|-------------|---|
| BNS | Boulder Nonlinear Systems |
| B/W | black & white |
| CCD | Charge Coupled Device |
| CPU | Central Processing Unit |
| CR | Contrast Ratio |
| d | thickness |
| DLP | Digital Light Processing |
| DMD | Digital Micromirror Device |
| e- | electrons |
| E-O | Electro-Optic |
| Φ_R | quantum yield |
| FLC | Ferro-electric Liquid Crystal |
| FPD | Flat Panel Display |
| GC | Glare Constant formula (see Equation 1.3) |
| IC | Integrated Circuit |
| IF | Interference Filter |
| IPL | Inner Plexiform Layer |
| lp | line pairs |
| m | integer (0,1,2,3, ...) |
| mln | million |
| MOD | Modification Filter |
| ND Filter | Neutral Density Filter (grey-color) |
| OD | Optical Density |
| ΔOD | photochromic response |
| O-M | Opto-Mechanical |
| OPL | Outer Plexiform Layer |
| PAF | Photochromic Adaptive Filter |
| Θ | eccentricity |
| rpm | revolutions per minute |
| ρ_s | surface density [mm^{-2}] (density projected on the unit of surface) |
| ΔS | sensitivity (the smallest noticeable differences) |
| s | second |
| SLM | Spatial Light Modulator |
| SOG | Spin on Glass |
| T | Transmittance |
| TF | Transformation Function |
| TFT's | Thin-Film Transistors |
| VLSI | Very Large Scale Integration |
| [-] | dimensionless quantity |

Introduction

This thesis describes the results of an investigation into the functions of the human visual system that led us to propose and develop a novel photonic device – Adaptive Filter. This work presents experimental results and documents the theory, design and implementation of the Adaptive Filter. The Adaptive Filter is implemented as a photosensitive device, the Photochromic Adaptive Filter, a device that controls and modifies images in a parallel fashion. By studying and understanding nature we get new ideas for improving existing man-made systems.

Motivation

The work described in the thesis was motivated by a desire to improve the limited dynamic range of modern artificial vision systems. The purpose of the thesis is to investigate and observe phenomenological effects in a living visual system, namely the human vision system, that responds to changing ambient light conditions. We believe that biological structures are designed optimally and that studying them may help to advance existing artificial systems.

Many modern vision systems work in conditions where the light intensity changes in the range of 12 decades – but only biological visual systems, such as the human eye, can efficiently operate under such conditions. Even so-called intelligent vision systems with

built-in adaptive properties can operate only in part (max. 7 decades) of this range. Human photoreceptors are very sensitive to extremely weak sources of light. It is well established that the photoreceptor cells are sensitive enough to detect a few photons, and with more light coming in, the sensitivity (defined as the smallest noticeable contrast difference) of the visual system decreases due to a variety of adaptation mechanisms. Based on the results of this research we suggest, analyze and implement new solutions in the optoelectronic field.

We have chosen to study the adaptation processes of the human eye across a very wide range of scientific disciplines, including anatomy, psychophysics, psychophysiology and psychology. All disciplines deal with the mechanism of light adaptation in different ways. Each of these disciplines may suggest different solutions and explanations for the same phenomena. Our role was to look at a broader picture and, based on that, propose a general description of the light adaptation mechanism. We did our best to find a common ground and we proposed the solutions based on the principles of physics. In an eclectic way we have looked at the many ways nature has solved the problem of detecting images within a very wide range of light intensities. Based on that knowledge we propose a novel artificial vision system that is superior to ordinary cameras. Although the idea of image modification by means of a Two Dimensional Spatial Light Modulator has been described previously, this dissertation provides the general framework, and analysis required to support the concept that originates from biological image processing. Our concept of applying the organic photochromic thin-layer filter in the image acquisition systems as an optically addressed spatial light modulator is a new one.

The material presented here is interesting because it provides a link between the biological and artificial visual systems. The adaptive system with photochromes is similar in many aspects to the human eye – photosensitive molecules in the eye (e.g. rhodopsin molecules) are members of the family of organic photochromes. As a result relaxation and excitation times of these two systems are comparable. This work originates from the biological implementations and leads to a new concept for the design of artificial visual systems.

Adaptation and Glare

In the first part of this research, different adaptation mechanisms are introduced, and models connecting those mechanisms to the psychophysics of the eye are developed. We

present a comprehensive overview of different adaptation and sensitivity change mechanisms based on modern classification and we propose solutions to human-made visual systems. Next we concentrate on the glare phenomenon – we investigate how the visual system copes with the light intensities beyond its dynamic range. Because of the shortcomings of the glare model based on stray light in the intraocular media, we further develop the glare model originating in the spread of the lateral inhibition in the Outer Plexiform Layer of the retina. The saturation of the signal in glare phenomena is used by us to reveal the highly complex structure of the retina. By applying a developed model of signal propagation in the Outer Plexiform Layer and by relating it to the experimental psychophysical data, we obtained a formula for the density of horizontal cell connections along the diameter of the human retina and the space constant of the horizontal cell lattice.

Adaptive Filter: Concept and Implementation

We have chosen to observe the response of the human eye to different light conditions and to propose new solutions to the problem of limited dynamic range in artificial vision systems. For example, CCD images resulting from extremely high irradiation suffer localized charge overflow known as blooming. After reaching a level of nearly 200,000 [e-/pixel] (in the partially inverted mode) blooming will occur, destroying parts of the picture. Blooming happens when the additional charges leave the area along the columns of the CCD, deforming the shape of a bright spot (as compared to reality) and making it impossible to reconstruct the whole image. (cf. Figure 3.18a).

By analyzing different adaptation mechanisms and sensitivity change processes in the human retina, we come to the idea of a novel photonic device: an Adaptive Filter. We propose to apply the Adaptive Filter in combination with an extremely sensitive photodetector array to implement local and/or global adaptation in a novel image acquiring system. This device modelled on the human eye offers the possibility of extending the dynamic range of operation of any standard video camera without affecting the electronic components of the system. Models of adaptive filters are investigated to extend global light intensity operation range, as well as to enhance detection of less illuminated regions of the image.

Next we undertake the research effort towards implementing the photochromic filter as an adaptive filter. We describe how to build one of the possible implementations of the adaptive filter – an optically addressed Photochromic Adaptive Filter (PAF), which utilizes

photochromic material embedded into a polymeric environment. This optically induced processing utilizes light to affect optical properties in the photo-reactive filter which is subsequently used for image processing. We present the theory of photochromic adaptive filters in general and describe the properties of several types of PAF that we designed and fabricated from common polymers containing photochromes. We design and develop a test bench for evaluating Photochromic Adaptive Filters, and successfully test the concept of operating range extension by using optically-addressed PAF's. The modified test bench is used to determine a Transformation Function of those filters by means of a simple, fast and easy-to-automate method.

Contributions

The major contribution made by this thesis is the presentation of a novel photonic device, called the Adaptive Filter. This device modifies the state of an input light beam according to pre-defined pattern. Very detailed and multilevel investigation of the adaptation processes found in the human visual system leads to the development of the novel man-made vision acquisition system. The same investigation gives the estimate of the horizontal cell connection density, yet to be confirmed experimentally. We also postulate other possible solutions that might be implemented using standard IC technology to manufacture imaging systems with enhanced properties.

We develop various fabrication techniques required to realize thin film photochromic filters and present physical characteristics of the developed filters. The aim of this thesis is not to prove or claim that the photochromic adaptive systems are optimal for all image scenarios, but to demonstrate that the system operating under our principles does work. While the emphasis of this thesis is on the application part of the project, we also present a very fast and efficient method for evaluating properties of the photosensitive materials that were developed as part of the research. Last but not least we detail experimental results using several developed PAF's.

Outline

The thesis is divided into three main parts. Following this introductory chapter, *Part I* describes the light adaptation phenomena as seen by different medical sciences. We review and systemize different adaptation and sensitivity change processes that occur in the hu-

man retina. We introduce detailed model of signal flow in the Outer Plexiform Layer used later to describe glare. We also put emphasis on modelling the dazzling glare.

In *Part II* we define an Adaptive Filter and we suggest the application of the filter in a novel opto-electronic image-acquisition system. We define, by numerical modelling of different types of the Transformation Function, the optimal solution for unique image transformation applied to extend the dynamic range or increase the contrast ratio. We further point out the special type of photosensitive materials: photochromes, as a potential solution for implementation of the Adaptive Filter.

In *Part III* details of developing the organic photochromic adaptive filter in polymer environment are described. Manufacturing processes and physical properties of the developed thin films are presented. Results of experiments to determine spectral characteristics of components as well as the whole systems are shown. Finally, a practical example explains the methodology of the procedure developed to measure the transformation function for different photochromic filters.

Conclusions provide a general discussion of the research, summarize the significant ideas presented in the thesis and indicate areas for future work. Logical implementations of the Active Adaptive Filter are indicated as alternatives for the Photochromic Adaptive Filter.

In the *Appendix* a few additional topics are presented. We estimate the measurement errors and errors intrinsic to calculations included in the thesis. We also describe the development of an inorganic thin film photochromic filter and we analyze two specific implementations of the Active Adaptive Filter.

Throughout the thesis the emphasis is on the general analysis and interpretation of experimental results. In fact, only major development steps are presented. We have tried to choose a representative sample to illuminate the pertinent points. We believe that showing the final results gives more information than providing detailed description of a variety of experiments and procedures undertaken. Graphical explanations are used, whenever possible, as one picture is worth a thousand words.

Part I Light adaptation in biological visual systems

| | |
|---|-----------|
| Introduction | 7 |
| The retina – part of the visual system | 7 |
| Adaptation and Sensitivity | 13 |
| Glare | 20 |
| Summary | 31 |

“... it is marvellous in our eyes.”

PSALM 118, Verse 23

Introduction

The human visual system compensates for the poor optical design of the eye by its flexibility and highly advanced signal processing. Nearly all of the external elements of the visual system adjust in response to constantly changing viewing conditions: the lens accommodates; the eyeball moves to bring the high visual acuity portion of the retina into a favorable viewing position; and the retinal neurons change their sensitivity when the mean illumination changes. The set of adjustment mechanisms that respond to change in light conditions are called light adaptation and sensitivity change processes. Before we discuss the light adaptation mechanisms we must explain why the adaptation process is necessary. Why must we wait for our visual system to adjust before we can discern the objects in the darker or lighter place?

In order to be able to operate simultaneously in very dim and very bright light, our system would have to have a very large operating range and good sensitivity. To be able to see large light intensity differences we need a system with a very large operating range. However, as any physical photo-sensor has a finite response range, for the large operating range we have to sacrifice a physical contrast sensitivity. Extending the input domain by decreasing the gain of the intensity-response function degrades the ability of the system to detect important information. For good sensitivity to physical contrast, which translates into high sensitivity to small differences in contrast, we need an intensity-response curve of the visual system that is very steep (high-gain); it then covers only a small range of input intensities (Skrzypek, 1990). Our system can do both things. By using a fairly narrow operating range, and shifting this range to match the average level of illumination, the system achieves good physical contrast sensitivity and a wide operating range. We can see light levels as low as few quanta in the darkness, and as high as trillions of quanta reflected by snow (cf. Goldstein, 1984). Yet we can detect the differences between two objects that differ in an intensity by less than 1 percent (depending on the task). This ability to adapt to the ambient level of illumination is of fundamental importance to vision.

The retina – part of the visual system

Before we start to analyze in detail the adaptation mechanisms of an eye, we have to overview the anatomy and neurophysiology of the vertebrate retina to propose the basis of a

model of how different adaptation mechanisms function, and how signals are processed in the retina.

Transparent parts of the eyeball allow passage of light rays and bring light rays to focus on the light-sensitive retina. The eye produces an image on the retina which transduces the light into an electro-chemical signal. The retina is a very thin (150-300 μm) layer of tissue that lies at the posterior of the eye, it converts light energy into nerve impulses. It is well agreed upon that if we could exactly determine the structure of the retina, most of the unknown elements of the adaptation and processing systems would be revealed (Sjöstrand, 1990). However, the great complexity of the retina and the enormous density of cells, makes it very difficult to identify relationships between component cells. Using very conservative data we can estimate the average cell surface density within the retina: $\rho_s = 227,000$ [cells/mm²]. Figure 1.1 presents the schematic of the human eye.

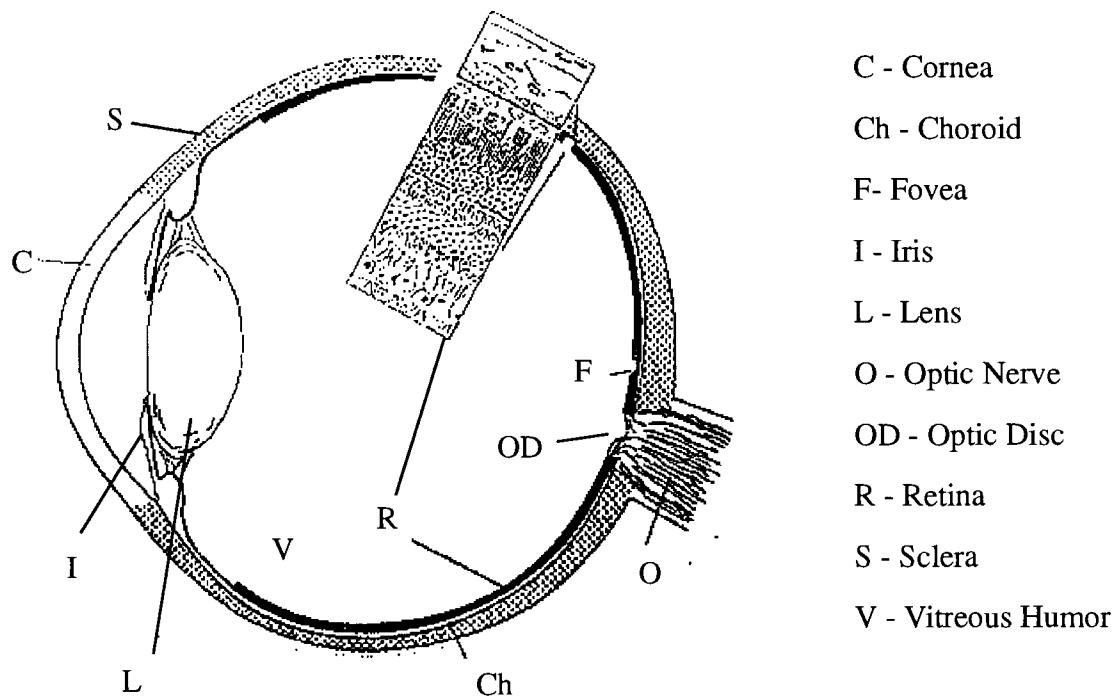


Figure 1.1 Human eye: schematic cross-section

The main function of the retina is to translate light into nerve signals (Hübel, 1988). At the same time, input data are compressed, brightness of the image elements is transformed into contrast information, adaptation mechanisms function to enhance the operating range and the radiant energy recognition process is initiated.

Signal Flow in the Outer Plexiform Layer (OPL)

The retina is made of several layers of six main types of cells. It is a 3-D processing structure, operating in parallel mode, with at least 3 processing layers where signals flow laterally and vertically. Distal (outer layer) retina contains a few groups of highly specialized cells: receptors, bipolar cells and horizontal cells (Figure 1.2). The receptors are rods and

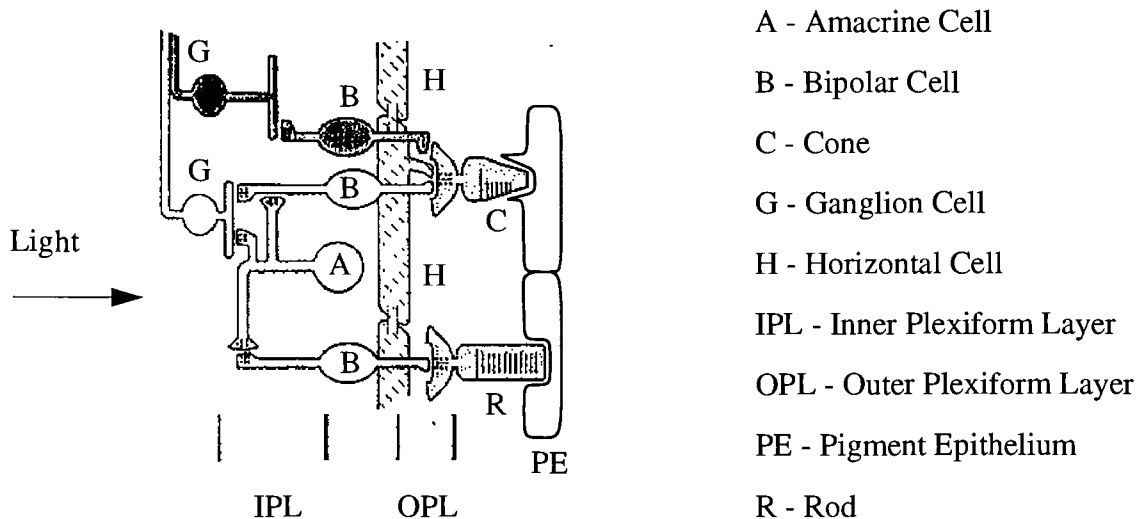


Figure 1.2 Synaptic connections of cells in the peripheral retina

cones – they are specialized to respond to stimulation by radiant energy. They feed the signal into bipolar and horizontal cells. Bipolar cells connect cells in the outer layer with cells in the inner layer, such as amacrine and ganglion cells. Horizontal cells provide feed-forward and feed-back inputs to bipolar cells and photoreceptors, respectively. A book by Polyak (1957) gives an excellent overview of the neural circuitry of the retina.

Light detection by photoreceptors

Only the receptor cells contain photo-pigment and act as transducers, converting light energy into neural signals that are processed by succeeding retinal cells (Held et al., 1976). There are two types of photoreceptors in the retina, rods and cones. They differ in a number of ways. The most important difference is their relative sensitivity: the rod system (which consists of the rod photoreceptors and all the higher order cells in the retina and in the brain to which they communicate) is sensitive to minimal intensities of light, on the

other hand, the cone system requires much higher levels of intensity to function. Rods are primarily designed for the efficient capture, summation, and transmittal of signals involving only a few quanta per rod per second; each rod cell contains 100 million rhodopsin molecules (Schnapf et al., 1987). Under appropriate conditions a single isolated rod in the human retina signals the absorption of the single photon, which activates only one of the rhodopsin molecules in the retina. The detective quantum efficiency has been determined for different target diameters (pulse duration and background luminances), to reach as much as 92% (Jones, 1959). The spectral sensitivity peak for rods is $\lambda=505$ nm. The cone system functions at much higher ambient light levels and has faster response properties. This system is most sensitive to the wavelength of $\lambda=555$ nm. Cones reach a maximum sensitivity steady state as light intensity decreases. It has been found that the sensitivity of rods increases steadily as a person stays in darkness for a prolonged period of time.

The receptors respond to light through a process of bleaching. By utilizing a special shape they are optimized to concentrate and funnel light to increase the probability of light detection. The cones in the foveola presumably compensate for their relative lack of taper by doubling in the total length of their outer segment, with a resultant increase in the probability of photon capture (De Valois, 1988). Photoreceptors may orient themselves perpendicularly to the incident light to increase the quantum efficiency. Another important mechanism observed is coupling between photoreceptors which may increase signal to noise ratio for low light conditions and may reduce saturation effects in high light intensities. After the photon is absorbed, the resulting signal is amplified within the photoreceptor cell up to 100,000 times and is converted to a membrane conductance change. This signal is then transmitted to other cells within the circuitry of the retina.

There are lower and upper limits on the magnitude of the receptors' response. The lower limit is determined by factors such as the quantal nature of the light, or the magnitude of the intrinsic noise (Rose, 1953). The laws of quantum physics impose a firm limit which has been closely approximated by the visual system. Isolated photoreceptor cells can be excited by the single photon.

On the other side of the scale, the intensity-response curve stabilizes, as the upper limit in response is reached, when all of the membrane's active channels are used. This physiological mechanism limits the photoresponse range in isolated rods and cones to about $3 \log_{10}$ units (Normann et al., 1974). The cell is said to be in saturated state, in the sense that it cannot signal further increases in light intensities. However in some cold-blooded vertebrates, but not in mammals, the incremental response returns (Hess et al.,

1990). Photoreceptor adaptational mechanisms help the cell to recover from saturation.

Transmission of the signal to bipolar cells

All of the signals originating in the receptors and arriving at the ganglion cells must pass through the bipolar cells. As such, they constitute the principle relay neurons in the retina and the first relay neuron in the pathway to the brain (Gorden, 1990). Because many bipolar cells (outside of the fovea) contact one photoreceptor cell, when this receptor is stimulated by light it will initiate extra impulses to each of the bipolar cells. This multiplication of the single quantal absorption effect would probably best serve to remove the effect of synaptic noise on the quantal signals arising from the receptors in the centre of the ganglion receptive field (Hess et al., 1990).

Transmission to horizontal cells

Horizontal cells create an extensively coupled 2-D layer across the retina – syncytium (Ammermüller et al., 1993), sometimes called horizontal lattice. They receive synaptic inputs from photoreceptors (Dowling, 1987) and interplexiform cells and they send synaptic inputs to bipolar cells and photoreceptors. Horizontal cells link receptors and bipolar cells by relatively long connections (of the order of 1000 μm) that run parallel to the retinal layer. It is well established that horizontal cells adapt as a group to the light and that they relay the signal over the horizontal cells network in mammals (Lankheet et al., 1993a, b), however the exact location and characteristic of the mechanisms are still unclear. Horizontal cells are part of the indirect visual path.

Feedback Mechanisms

Each photoreceptor contacts both types of second-order cells: bipolar and horizontal. They also contact all of their neighbors. Together they make up an elaborate synaptic network where signal processing takes place. The horizontal cells regulate signal flow from photoreceptors to bipolar cells. They send feedback inputs to photoreceptors. Horizontal cells receive inputs from photoreceptors and form a laterally extended network that feeds inhibition back onto photoreceptor synapses, this inhibition may also be fed forward onto bipolar cell synapses.

Cells of the Proximal Retina

There are several other classes of cells in the proximal (inner layer) retina, including the amacrine, interplexiform and ganglion cells. Amacrine cells form a lateral processing layer similar to horizontal cells, and they provide additional links between bipolar cells and retinal ganglion cells.

The function of the amacrine cells is not fully understood, but they might play a role in feed-back and feed-forward signal processing. The inner layer of cells in the retina contains the retinal ganglion cells, whose processes (i.e. axons) pass across the surface of the retina, collect in a bundle at the optic disc, and leave the eye to form the optic nerve. Spatial summation of the signals from cones by the ganglion cells can increase the gain at the ganglion cell. Another effect would be to improve the signal-to-noise ratio in the ganglion cell junction (compared to its level in a single cone) (Hübner, 1988).

We still lack a good understanding of the functions of such cells as amacrine and interplexiform in the visual pathway. It has been suggested that interplexiform cells may take part in the adaptation mechanisms of the human eye affecting the spread of signals in the horizontal cells network by using dopamine to control the degree of electrical coupling. Interplexiform cells send processes into the outer plexiform layer, where they contact horizontal cells, and into the Inner Plexiform Layer (IPL), where they receive input from the bipolar cells, and/or amacrine cells (Cohen, 1990). By uncoupling horizontal cells (gap junctions) they may control the bipolar receptive field, thus reducing surround inhibition and increasing the transmitted postsynaptic signal.

This mechanism may play a role in increasing the response of the outer layers (dim light stimulates larger response than if inhibitory feedback was stronger). In other words it can enhance the process of dark adaptation.

Amacrine cells occur in many varieties, and may be part of different visual pathways, which are used for different light levels. By taking advantage of different interneuronal circuitry to optimize the performance at different ambient levels of illuminations they may serve to improve the perception.

It has not been proven to exist in the human retina, but lower visual systems have built in mechanisms of adaptation that are controlled by the brain (Barlow, 1993). According to the time of day and light intensity a signal is sent from the brain that affects the region of operation of the retina.

Adaptation and Sensitivity

The overall process of adjustment of the visual system to changing light conditions consists of many separate mechanisms. We divide all of these processes into three categories: habituation, adaptation and sensitivity change processes (Lakowski, 1992).

The brain is involved in habituation processes – one example being the pupillary reflex which controls the total amount of light reaching the retina as a function of background level. It involves a feedback mechanism with a time constant that is considerably slower than those governing light adaptation. The optimal diameter of the pupil, when considering the optical characteristic of the eye, is around 5 mm. Variation in light conditions changes the actual diameter of the pupil; however, with time it returns to that optimal dimension regardless of the existing light intensities level in the environment. Results of experiments show that psychological (emotional) factors can be as important as physical factors (ambient light intensity) in controlling the diameter of the pupil. In lower animals, the nerve cells sending signals from the brain to the retina have been identified. They may be involved in controlling the overall sensitivity of the retina. The importance of the processing of the signal delivered by the eye to the brain is evident when we consider phantom seeing. As Melzack (1992) presents it: “The brain does more than detect and analyze inputs; it generates perceptual experience, Sensory inputs merely modulate that experience; they do not directly cause it”.

From the outset it is convenient to distinguish different phenomena which are all referred to as adaptation, and which may be confusing. As many scientists in different disciplines worked on the problem of adaptation, the terminology is not always very precise. Another confusing factor is the interaction between different mechanisms which adjust simultaneously and on many platforms, making it difficult to segregate them into clearly separated classes. This is especially visible later in this section, when we describe local adaptation mechanism as an example of sensitivity change processes.

Adaptation processes occur in the sense organ, i.e. in the eye. Switching from one family of photoreceptors to another as light conditions change is one example. Adaptation processes require a rather long time to occur. We talk about sensitivity change processes when we discuss different mechanisms that happen on the cellular level. Our ability to adapt to a very wide range of light intensities is made possible, in the first instance, by our photoreceptors. Next, there are also adaptive changes in the retinal network (Leybovic, 1990) and in higher processing levels: habituation processes, the latter of which can be

demonstrated through experiments testing binocular interactions (Hess et al., 1990). In the experiment the adaptation level of one eye is shifted within the scotopic light range. The analogous shift is observed in the covered eye, that was not stimulated.

Adaptation Mechanisms

The adaptation process maintains a constant, or quasi-constant signal sensitivity for the visual system, independent of the input amplitude. We can divide adaptation mechanisms into a few categories: global and local adaptation (with the local being an example of sensitivity change process), slow and rapid, dark and light* adaptation. Another classification divides all the mechanisms into two groups: photo-chemical and non-photo-chemical (neural) mechanisms. We concentrate in our discussion mostly on monochromatic light adaptation.

Global adaptation changes the average sensitivity of the retina. It can be in turn divided into three categories: dark/light, slow and rapid adaptation. The slow adaptation process sets the general operating curve for the whole eye, and once the general operating curve is set, rapid and local adaptation help us deal with variations above and below this general level of adaptation (Goldstein, 1984). To deal with a range of light intensities greater than 3 decades, our visual system employs a rapid adaptation process. In this process the retina shifts its operating curve over a small range within three-tenths of a second after the light level changes; so as our gaze shifts between light areas and darker areas, the operating curve shifts to partially compensate for these changes in illumination.

Local adaptation helps us to deal with images that contain large light differences within the same scene. Dark/light adaptation makes us both diurnal and nocturnal animals. The ability of the visual system to quickly (within seconds) establish a new steady state of visual performance is called light adaptation. The term dark adaptation refers to the recovery of the visual system after exposure to intense illumination. In low light intensities our vision is mostly based on rods, as light intensity increases cones take over. Initial duplicity theory which implied that light-adaptation of the rods is independent from that of the cones has been modified to accommodate the coupling between the photoreceptors (Hess et al., 1990). It has been suggested that coupling between rods and cones can enhance transmission of large signals from the cones under light-adapted conditions (Yang et al., 1987) – it is one example of numerous feed-back and feed-forward mecha-

* Sometimes called background or field adaptation.

nisms that exist within the retinal circuitry.

Many experiments prove that the neural theory of adaptation is a valid one. For example, sensitivity of the rod system recovers, even if the photo-pigment does not regenerate, which clearly indicates that neural mechanism is involved. There are different time courses between photo-pigment regeneration and psychophysical threshold limit. Light adapting a single eye can partially affect the time course of dark adaptation in the other eye.

Dark Adaptation

Dark adaptation is the change in visual processing resulting from the exposure to low intensities of light. Night (scotopic) vision is mediated mainly by the rods as opposed to day (photopic) vision when the rod's system is mostly oversaturated and the cones take over. Dark adaptation occurs when we move from a light place to a darker one and our vision is mediated by rods specialized for operation in extremely low light levels. The visual system adjusts its sensitivity to match the lower light level and several mechanisms are responsible for bringing it about.

The phenomenon of dark adaptation is well known (Goldstein, 1984): when the illumination is changed from light to darkness, it is difficult to see anything at first, but with time, sensitivity increases. When we are dark adapted the rods control our vision and we see in shades of grey. It takes a long time for us to adjust to the darkness, 20-40 minutes (or less) is an often cited period. It has been found that, with a prolonged period of darkness, the sensitivity always increases, approaching the physical limits of individual light quantum needed for photoreceptor excitation. On the other hand, a bright environment slows down the rate at which the eye can dark adapt. This effect is cumulative. A lifeguard, for example, who spends everyday on the beach, does not regain normal nighttime vision even after 24 hours in the dark.

We know about at least two distinct adaptation processes within the rods – multiplicative that is rapid, and subtractive that is slower (Adelson, 1982). At present, it is impossible to say precisely where the adaptation process take place. Some of the effects, but probably not all, may involve the receptors themselves. For a long time it was believed that rods constitute an autonomous system. Recent results show that, as with any other cells within the peripheral retina, rods are interconnected with cones. Suppression of the rod system by the cones was first shown psychophysically by George Wald. This connec-

tion between the two systems can influence the light detection by the rods (Sharpe et al., 1989; Attwell et al., 1987).

The greater sensitivity of rods as compared to cones, can also be explained by the difference in pooling of signals between these two types of photoreceptors. Rods are usually connected in groups of photoreceptors within the receptive field. A group of rods sends signals to the same bipolar cell. As a result of summation of the signals, the response of the bipolar cell can be triggered by lower external light intensities. Another explanation for the increased sensitivity of the scotopic system is a temporal signal summation – that again increases the signal to noise ratio of the system.

As the light intensity reaching the photoreceptors increases, the other type of receptors – cones, start to be active. For a specific range of light intensities, the visual system operates in so called mesopic vision, and with further increase in illumination cones take over the visual process.

Light Adaptation

While the rate of dark adaptation is measured in minutes the rate of light adaptation is very much quicker and is measured in seconds. For any given average light level, the retina is sensitive to approximately three orders of magnitude of light intensities. This operating window is then shifted over a range of 7 decades by a mechanism that responds to the variations in the background light intensity. At any given moment this system provides good discrimination of intensity differences, but we have big difficulties in determining the absolute intensity.

The mechanism behind this adaptation is not known in detail. A pupil, by changing its diameter, can shift the actual operating range over a decade. Photobleaching of pigment in the photoreceptors and interactions between cones, horizontal and bipolar cells is also responsible for adaptation. When we are light adapted, the cones control our vision and we see in color. With all of the differences between dark and light adaptation we have to remember that individual cones are as sensitive as individual rods (Vimal et al., 1989). The minimum number of quanta absorbed per single cone cell for detection is only 5-7. However due to a light absorption by the tissues within the eye, the actual minimum photon number is more than 100 for cones and 80 for rods. Observed differences are derived from experiments performed on the whole system, with all of the adaptation mechanisms in place.

Sensitivity Change Mechanisms

Sensitivity change mechanisms are processes within the photoreceptors or group of retinal cells which contribute to light adaptation. Changes in sensitivity are almost always associated with a change in speed of response. Within the visual system there are two processes, pigment depletion and automatic gain control. In the photopic system much of the gain control occurs within the cone photoreceptors themselves (Boynton et al., 1970).

In contrast, although considerable gain changes occur within the rod photoreceptors, the scotopic system appears to achieve its automatic gain control mainly through post-receptor mechanisms (MacLeod et al., 1989).

Pigment Regeneration

The visual pigment molecule changes shape to start the process of transduction. Following this change the molecule breaks in two. This process is called pigment bleaching because the retina becomes transparent as the molecules break apart. Photo-pigment bleaching, by decreasing the number of molecules available to absorb quanta, would forestall saturation; it seems to do this in the cone visual system.

The reverse process is called pigment regeneration. It is responsible for the increase in retinal sensitivity that occurs during dark adaptation. In rod vision, depletion of pigment molecules is not the main factor of desensitization (Hess et al., 1990); however, there is evidence that rods themselves play a role in the adaptation process (Hood et al., 1995).

Experiments show it takes around 6 minutes for cone pigment to completely regenerate, while rod pigment needs over 30 minutes. It is a well known fact coming from the anthropological studies of native people living for centuries in different climates, that as we go north, where there is more stray light caused by reflection by the snow and the low position of the Sun, the actual photo-pigment concentration in the photoreceptors decreases. It might be connected to excessive light levels in that regions.

People that habituate these areas are also protected by other adaptations; another example is the further restriction of the opening of the eye brought about by relatively narrow, slit-like eye lid openings.

Local adaptation

We use the term local adaptation when we describe the local control of sensitivity over restricted areas of the retina, called the adaptation pool (Hess et al., 1990). When we look steadily at one part of the scene different areas of the retina are exposed to different light intensities – while the fovea is exposed to the intense illumination of the sky, for example an area in the peripheral retina is exposed to dim illumination from the shadows under the bushes. The visual system deals with this problem by the mechanism of local adaptation. Different parts of the retina adapt to different levels of illumination. That is, different parts of the retina can set their operating curves at different places, so that they can operate at different levels of illuminations (Goldstein, 1984).

Local adaptation helps us to deal with variations above and below the general level of adaptation set by the global adaptation process. Changes in background intensity affect the response time and output amplitude of the photoreceptor cells. It is thought that changes in response time may be due to a decreased dependence on temporal summation as the background intensity increases. For example, under dim light, summation of the stimuli leads to a slow response time, while under bright light lack of this summation results in fast response time.

The process of local adaptation may take place within the neural network of the retina and also within the cones themselves. Using interference patterns directly on the retina the hypothesis that local adaptation takes place within the cones themselves has been confirmed (MacLeod et al., 1993). The function of the network processes is to prevent the signals from receptors from exceeding the very limited dynamic range (about 2.0-2.5 \log_{10} units) of the visual neurons, to escape saturation and to continuously use the steepest part of their neuronal stimulus-response function (Hess et al., 1990).

Conclusions

We presented several mechanisms of visual adaptation that can be observed in the biological visual systems. Generally, all processes are most sensitive in their dark-adapted state; light adaptation serves to desensitize a process. That conclusion is later explored when we propose an artificial adaptive visual system. We classified different adaptation mechanisms into groups presented in Table 1.1 and compared them with the existing, or proposed implementations.

Table 1.1 Selected biological adaptation processes compared with equivalent opto-electronic implementation

| Biological phenomena | Possible implementation |
|--|--|
| - switching between different classes of photo-receptors: slower in response and more sensitive class for dim light conditions and less sensitive class with faster response for high ambient illumination (duplicity theory of Schultze – 1866) | <i>Visual system* working in 2 or more modes, with changing light conditions switches from one type of photosensing devices to another (Ward et al., 1993), Another possibility is to control the operation region of single type device</i> |
| - pigment depletion: degree of bleaching elevates threshold | <i>Bacteriorhodopsin-based (Chen et al., 1993) artificial retina‡</i> |
| - variety of feedback mechanisms | <i>Two-layer 3-D structure implementing one feedback mechanism, which results in shifting the operating characteristic of a photoreceptor along the intensity axis (Mahowald et al., 1991)</i> |
| - adaptation pool: local adaptation | <i>System utilizing adaptive filter concept (Implemented in Part III)</i> |
| - logarithmic relationship between intensity and response (Burton, 1973) | <i>Photodetectors with logarithmic rather than linear properties (Etienne-Cummings et al., 1992; Mahowald et al., 1991)</i> |
| - silvery <i>tapetum</i> behind the retina† reflecting light back (may increase blur) | <i>Metal layer beyond the layer of photosensitive devices</i> |
| - response amplitude is reduced as the background of light gets brighter | <i>This phenomena is intrinsic to some electronic architectures (Ward et al., 1993)</i> |
| - pigment epithelium migration between photo-receptors in darkness: rhodopsin regeneration | |
| - signal pooling (spatial summation) in the receptive field: at low light levels it might counteract the effect of signal fluctuations caused by noise, at higher intensities it might prevent overflowing the dynamic range of the neurons | <i>Visual system* working in two modes: for high light intensities each photoreceptor sends a separate signal, for low light conditions signal from a groups of photoreceptors is pooled, to increase sensitivity with resolution lowered</i> |
| - 3-D, parallel detecting and processing structure of the retina | <i>A 3-D architecture for a photosensing and processing system (Johansson et al., 1992; Mathur et al., 1991)</i> |
| - external control of amount of light reaching parts of the retina (pupil diameter, controlling the opening slot made of eyelids, blinking, screening the most sensitive receptors (rods) – retinomotor response) | <i>This method has been utilized starting from first artificial visual systems (Auty et al., 1995) Chopping, that is an equivalent of blinking, has been utilized so far mainly for other purposes. However recently developed systems with flexible exposure time are very similar when the idea is considered (Colorado Video, 1994)</i> |
| - tremor: removes high frequency spatial noise, may protect photodetectors from oversaturating | <i>A scanning CCD transducer used to increase spatial resolution (Ueda et al., 1990)</i> |

* Very complex electronic circuitry as compared with contemporary cameras, low receptor fill factor

† Does not appear in the human retina

‡ New technologies need to be developed to utilize the concept of hybrid bio-electronic system

Table 1.1 Selected biological adaptation processes compared with equivalent opto-electronic implementation

| Biological phenomena | Possible implementation |
|--|--|
| - photosensitivity of the cornea: not confirmed as of today, if exists it might be used by the system to determine average illumination of the external environment, or the level of harmful UV radiation | <i>External sensor determining average illumination – used to control different implemented adaptation processes</i> |
| - response time of the photoreceptors gets faster as the background of light gets brighter (temporal summation and averaging of the signal in low light levels) | <i>This method has been used in photography, some modern CCD systems (Colorado Video, 1994) use a method of on-sensor integration to adjust exposure time to background illumination</i> |
| * Very complex electronic circuitry as compared with contemporary cameras, low receptor fill factor † Does not appear in the human retina ‡ New technologies need to be developed to utilize the concept of hybrid bio-electronic system | |

The human visual system is very complex, various built-in adjusting mechanisms enabling it to operate over a very wide range of light intensities, while simultaneously preserving a high contrast ratio. By mimicking some of the mechanisms of nature, man has built artificial visual system with enhanced capabilities. There are still many poorly understood aspects of the visual process and many ideas yet to be explored. They will deliver principles for design of new artificial image processing systems.

Glare

The glare phenomenon occurs when light intensity exceeds the dynamic range of the visual system for the given adaptation level. The visual system is optimized to detect at any given moment an image of a natural scene with a variation of intensity that usually does not exceed $3 \log_{10}$ units (Rodieck, 1973). Any luminance within the visual field that is sufficiently greater than the luminance to which the eyes are adapted, causes annoyance, discomfort, or loss in visual performance and visibility. The magnitude of the sensation of glare depends upon such factors as the size, position and luminance of source, the number of sources, and the luminance to which the eyes are adapted.

Glare may be evaluated either on the physical characteristics of the source or the functional impairment it creates in acuity or comfort (Potts, 1972). Glare is traditionally divided into disability glare, causing a reduction of visual performance, and discomfort

glare, which is the discomfort caused by glare without any measurable effects on the visual function.

The term “glare” applies to many different conditions. We shall restrict ourselves to glare caused by bright sources at a distance, namely dazzling glare. Dazzling glare is a form of disability glare which is associated with bright lights (sun, headlights, street lights) in the field of view which form images upon peripheral portions of the retina off the line of sight (Nadler et al., 1990).

Neuronal Model of “Dazzling Glare”

Introduction

In the last several years significant progress has been made both in the understanding of early vision in biological systems and in the development of special analog hardware for the implementation of these algorithms. For review see Mathur et al. (1991).

Particularly important for the development of man-made vision systems is an understanding of the role of illumination on the quality of vision and its role in the degradation of the information capacity of the eye. In robotics and remote sensing, illumination varies dramatically in an uncontrolled fashion, thus the results of such studies may have a very important application in improving, for example, low contrast edge detection. One of the features of human vision which has eluded full explanation is dazzling glare.

Image Quality Decrease as a Result of the Glare

The phenomenon of dazzling glare is usually described as reduced visual performance and visibility due to light scattering within the eye. The scattering light model was first proposed by Stiles (1929), then evaluated by Fry and Alpern (1953) and reevaluated (Fry, 1954). It remains a valid hypothesis (Nadler et al., 1990). In the stray light model, particulate non-uniformities (Hemenger, 1992) in the intraocular media act as point sources of light causing light scattering and superimposing a veiling light on the retina (see Figure 1.3b).

A veiling luminance caused by the scatter of light within the eye is superimposed on the retinal image (Abrahamsson, 1986). This stray light will have a contrast-lowering effect on the apparent image of the visual scene, and will thereby decrease the visual ability.

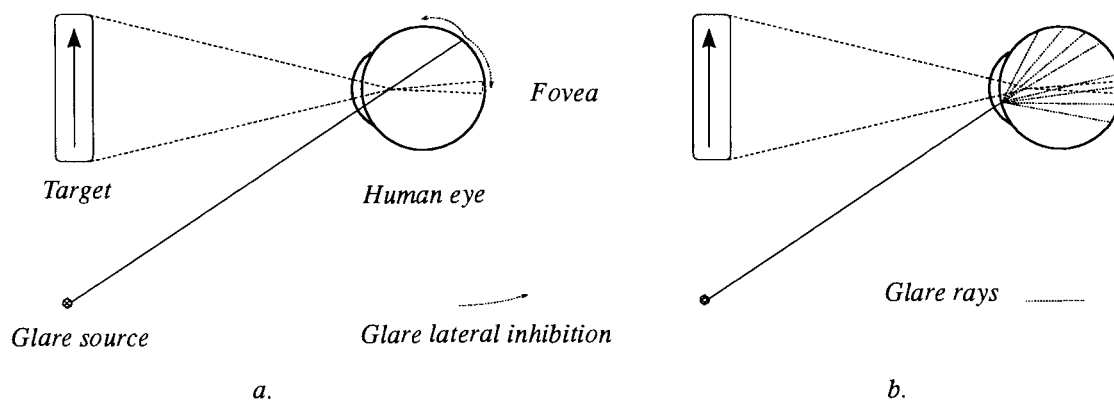


Figure 1.3 Dazzling glare models: a. lateral inhibition in the OPL, b. light scattering

To prove the model, clinicians have made a variety of experiments mimicking cataracts (Nadler et al., 1990). Loss in visual performance caused by glare increases with the age of the person, thereby providing additional support for the “stray-light” model. The reason for this increase has been linked with intensified light scattering in elderly eyes. From the general group of opacities that can cause glare, which includes cornea, lens and vitreous opacities (floaters), most have been ruled out by inversion of an empirical glare function (Hemenger, 1992), except for some rather large refractive-index fluctuations associated with the lens fiber lattice, which extend over distances of tens of micrometers.

This theory, however, does not explain some aspects of glare. First, such phenomena still exist even in perfectly healthy eyes when light scattering within the eye is minimized. Second, increasing background illumination decreases discomfort. Third, according to the recent research (Sloane et al., 1988), the aging of the eye involves not only an optical mechanism (additional scatter centres within the eye) but neurological changes, particularly in the retina (Elliot et al., 1990-1991). Also, only a weak correlation was found between the decrease in low contrast letter acuity and intraocular light scatter for normal subjects and subjects with cataracts (Beckman et al., 1992). To explain these problems we have turned to a neurobiological model of the retina. We believe that optical imperfections of the eye are well compensated for and corrected by the complexity of the retina.

We postulate that a large contribution to the glare phenomena (if not most of it) originates from the spread of lateral inhibition in the retina induced by excessive light localized in the retinal peripheries by the process of neuronal lateral interaction (van den Berg, 1991). The following sections explain the essentials of this model.

Dazzling Glare and Outer Plexiform Layer

The retina is organized as a system of several networks with different electro-chemical parameters. Practically all cells of the peripheral retina of vertebrates are electrically coupled to their neighbors (Leybovic, 1990). These features of the retina control coupling between cells and, as a result, also control a spread of induced signals in a particular network. As far as we know (Buser et al., 1992), we can distinguish between, on the one hand, short-range coupling on the photoreceptor layer involving only the nearest neighbors and, on the other, the coupling between horizontal cells. The latter has a long-range effect and can be used to explain some aspects of the neural global light adaptation of the eye. Horizontal cells receive inputs from the interplexiform cells, which contain and presumably release dopamine (Cohen, 1990). The principal effect of dopamine on the horizontal cells, and as a result on photoreceptors, is a reduction in the light responsiveness of the cell.

In this work we model the propagation of signals in the horizontal cells lattice to apply the implications to a quantitative model of glare. For this model to be valid, the uniformity of the network, i.e. the similarity of the elements and the constant ratio between them, must be preserved. This has been confirmed in monkey retina (Wässle et al., 1989).

In our simplified model we assume that lateral inhibition originates from the image of the light source focused in the peripheral retina. We do not include or differentiate between “ON” and “OFF” signal propagation channels and different types of bipolar and horizontal cells. In our model we neglect the decrease of the sensitivity of the retina in the periphery.

We use psychophysical observations to “dissect” the visual system, and we estimate the density of the connections between horizontal cells using non-invasive techniques.

Horizontal cells are linked together by high-resistance connections (Mead, 1989) called gap junctions, and form an electrically continuous resistive network (syncytium) just below the photoreceptors. The spread of potentials in a resistive network for a simple, one-dimensional case (Figure 1.4), can be described by the following equation (Mead, 1989):

$$V(x) = V_0 \cdot \exp\left(-\frac{x}{\sigma}\right) \quad (\text{Eq. 1.1})$$

Where:

$V(x)$ – photo-electric potential [mV]

x – angular distance from the fovea [arc min]

σ – space constant of the uniform network [arc min]

The space constant describes the effective range of propagation of the generated signal V_0 over the syncytium. The applicability of this kind of equation was experimentally deter-

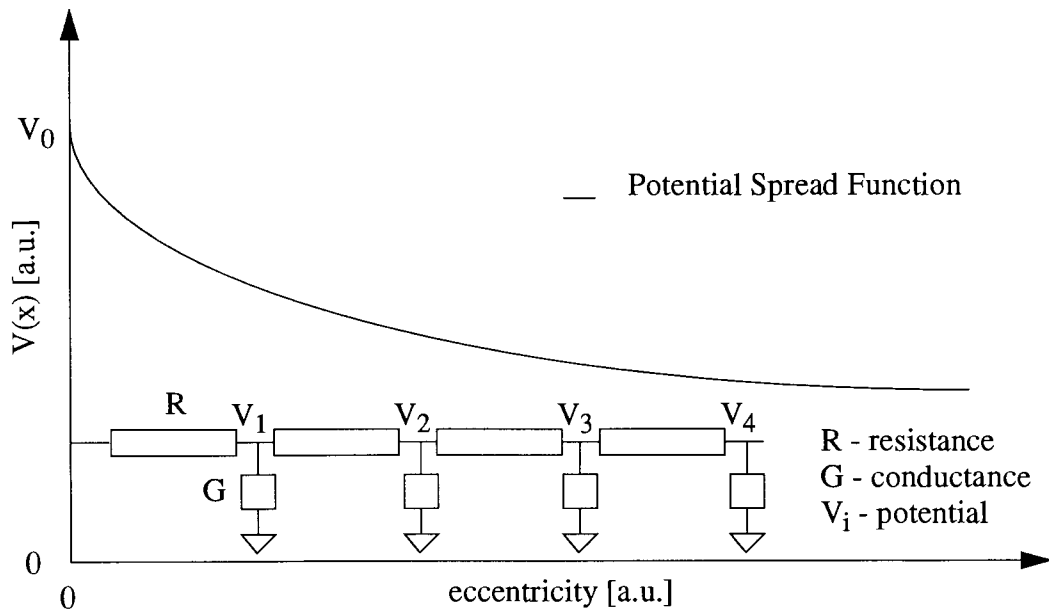


Figure 1.4 Electrical circuit model of one dimensional resistive network

mined for the retinas of turtles by measuring the spread of induced potential in the horizontal cell network (Byzow et al., 1983). By using a long linear light source, a one-dimensional characteristic was obtained, the result of which confirms that coupling between horizontal cells is so extensive that the horizontal cells across the retina act as a functional unit, or syncytium (Leybovic, 1990). Signal spread within this network explains some aspects of the adaptation mechanisms, horizontal cells provide negative feedback to the photoreceptors that are damping incoming signals and feed-forward to neighboring horizontal cells. The final result is a reduction in the contrast ratio of the perceived image.

At large distances, Equation 1.1 also describes two-dimensional cases with a marginal error (cf. Mead, 1989). It indicates that the forward-feed decays exponentially. The neg-

ative feedback damps the signals from photoreceptors, thus the perceived image is in large part independent of the absolute illumination level.

In our opinion the same coupling mechanism is involved in spreading the electro-chemical inhibition induced by glaring light and thus causes the deterioration in our visual performance which we experience as glare. The retina, up to and including bipolar cells, is piece-wise linear (Siminoff, 1991), i.e. at a given steady-state adapting light intensity, the outputs of the cells are linear functions of the physical image. Using an electro-chemical model in which absorption of light results in an electrical potential, we assume that the signal which is sent to the inner plexiform layer is proportional to the difference between the photoreceptor signal and the horizontal cell signal:

$$V_{eff}(x) \propto V_{phot}(x) - V_{hor}^{ave}(x) \quad (\text{Eq. 1.2})$$

Where:

$V_{eff}(x)$ – effective potential at distance x from the fovea

$V_{phot}(x)$ – photoreceptor potential

$V_{hor}^{ave}(x)$ – syncytium potential at a given distance x

Piece-wise linearity, i.e. where output is a linear function of input, of the retina up to the ganglion cell level is a tenet of the present model. The spread of potentials from photoreceptors that are illuminated by the brightest light can affect other photoreceptors thus increasing syncytium potential while decreasing the signal in these photoreceptors. The final result in the case of long-range spreading of the undesired potential in the horizontal cell network* can be a deterioration in visual functions, especially in the fovea. We classify this potential as a contrast-lowering lateral inhibition.

We postulate that dazzling glare is one of the phenomena caused by the above-mentioned mechanism. The images of bright lights in the field, which are formed off the line of direct sight, reduce the sensitivity of the eye for seeing objects in the fovea. The existing model attributes this loss of vision only to the scattering of light within the eyes, which is not sufficient explanation. The degree of disability due to glare can be quantified and the formula of the Glare Constant (GC) (Equation 1.3) has been obtained empirically

* For a comprehensive article presenting models of horizontal cell network see Winslow *et al.* (1991).

(Holladay, 1926):

$$\text{Glare Constant} = \frac{B_s^{1.6} \cdot \omega^{0.8}}{B_b \cdot \Theta^2} \propto \frac{\gamma}{\Theta^2} \quad (\text{Eq. 1.3})$$

Where:

- B_s – luminance of the source
- ω – angular size of the source [arc min]
- B_b – general background luminance
- Θ – distance from the fovea [arc min]
- γ – constant (when sources are time invariant)

Equation 1.3 indicates that disability caused by glare depends mostly on the distance between the fovea and the retinal projection of the glare source (Figure 1.5).

In our model we have assumed that the annular glare source creates a high intensity image on the surface of the peripheral retina. Because the intensity of the glaring light usually exceeds the average range to which cones are adapted, it induces a high potential in the Outer Plexiform Layer which we consider to be neural lateral inhibition.

According to Equation 1.1, the electrical signal in the uniform syncytium is a function of the space constant which depends on the density distribution of elements and their properties. Our retina is anything but uniform (Curcio et al., 1990a) and we have to assume a generally non-uniform distribution of horizontal cells. Then, when we substitute the parametric $\sigma(x)$ for constant σ , Equation 1.1 becomes:

$$V(x) = V_0 \cdot \exp\left(-\frac{x}{\sigma(x)}\right) \quad (\text{Eq. 1.4})$$

Where:

- $V(x)$ – photo-electric potential
- x – angular distance from the fovea [arc min]
- $\sigma(x)$ – space parameter [arc min]

Comparing Equations 1.3 & 1.4, we find that the best match for $\sigma(x)$ is a linear function,

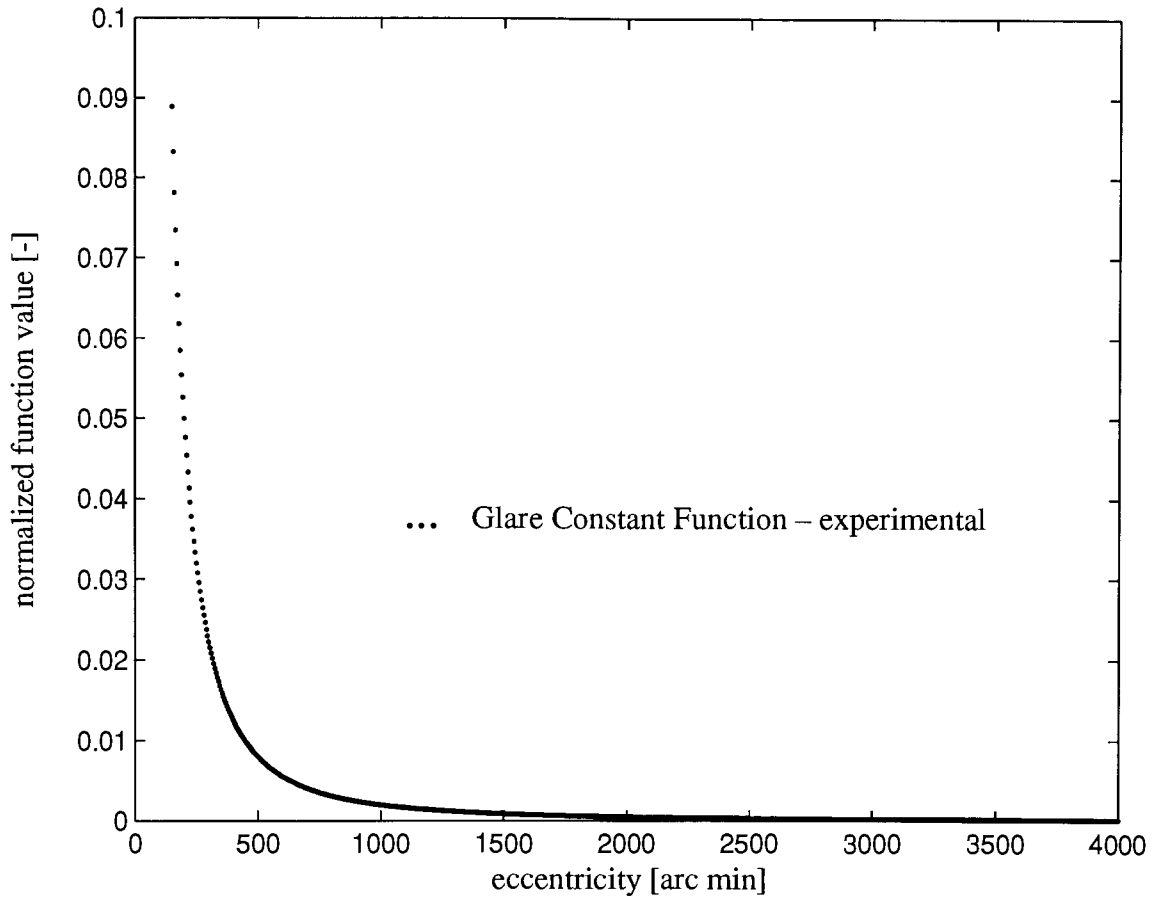


Figure 1.5 Experimental glare function vs. angular distance from the glare source derived from Equation 1.3

thus:

$$V(x) = V_0 \cdot \exp\left(-\frac{x}{a + b \cdot x}\right) \quad (\text{Eq. 1.5})$$

Where:

a, b – constants

With $a = 46$ and $b = 0.112$, there is a significant similarity between the two curves described by Equations 1.3 & 1.5 (see Figures 1.5 & 1.6). Substituting those values into Equation 1.5, we can estimate the range of $\sigma(x)$ in the human retina as falling between $330 \mu\text{m}$ close to the fovea and $2650 \mu\text{m}$ at the periphery. In comparison, for turtles $\sigma(x)$ varies between 135 and $600 \mu\text{m}$ (Byzow et al., 1983). As extremely hazardous as it is to

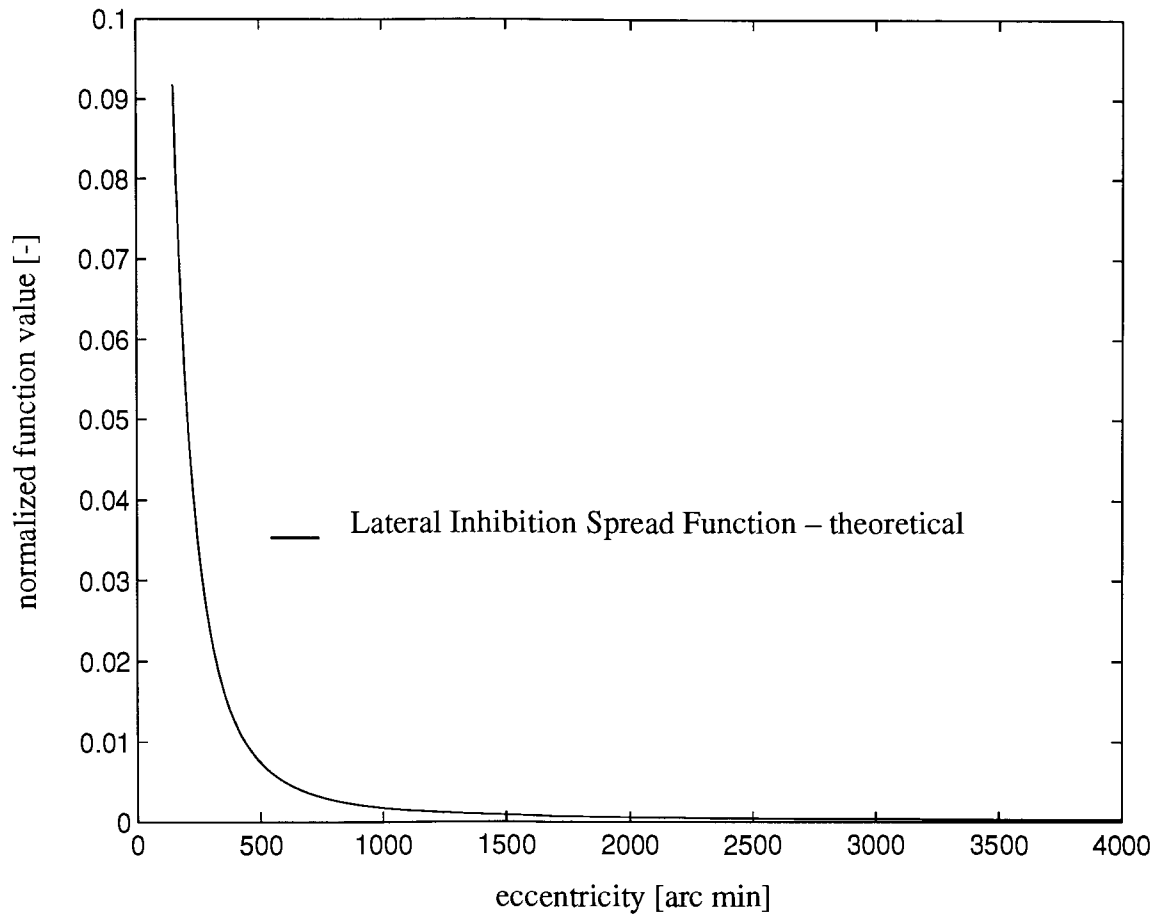


Figure 1.6 Normalized lateral inhibition spread function calculated from Equation 1.5 with $a = 46$ and $b = 0.112$

compare retinas in these two species, this is the only data available at present.

Estimation of Horizontal Cell Connection Density Distribution

Using Equation 1.5, we predict spatial density of the horizontal cell in OPL. Assuming a one-dimensional case of a uniform discrete resistive network, one can show that:

$$\rho \propto \sigma^{-1} \quad (\text{Eq. 1.6})$$

Where:

ρ – density of resistive elements of network

σ – network space constant

This formula results from a comparison of inhibition potential attenuation in networks with different space constants. For a non-uniform distribution we introduce the average density of elements in the range (0, x):

$$\rho_{ave} \propto \frac{\int_0^x \rho_{loc}(x) dx}{\int_0^x dx} \quad (\text{Eq. 1.7})$$

Where:

- ρ_{ave} – average density of elements
- $\rho_{loc}(x)$ – local density of elements

On the other hand, average density ρ_{ave} corresponds to the density of uniform network with a space constant equal to:

$$\sigma_{ave}(x) = c \cdot x + d \quad (\text{Eq. 1.8})$$

Where:

- $\sigma_{ave}(x)$ – space parameter defined for distances falling in the range (0,x)
- c, d – constants
- x – angular distance from the fovea [arc min]

This formula enables us to estimate the local spatial density of horizontal cell connection. Combining Equations 1.6, 1.7 & 1.8 we get:

$$\rho_{loc} \propto \frac{d}{(c \cdot x + d)^2} \quad (\text{Eq. 1.9})$$

Where:

- $\rho_{loc}(x)$ – local density of elements
- x – distance from glare projection to fovea [arc min]

Our model predicts that the density of horizontal cell connection in OPL will decrease as

$1/x^2$ with distance from the fovea (Figure 1.7). In the same figure we marked experimental

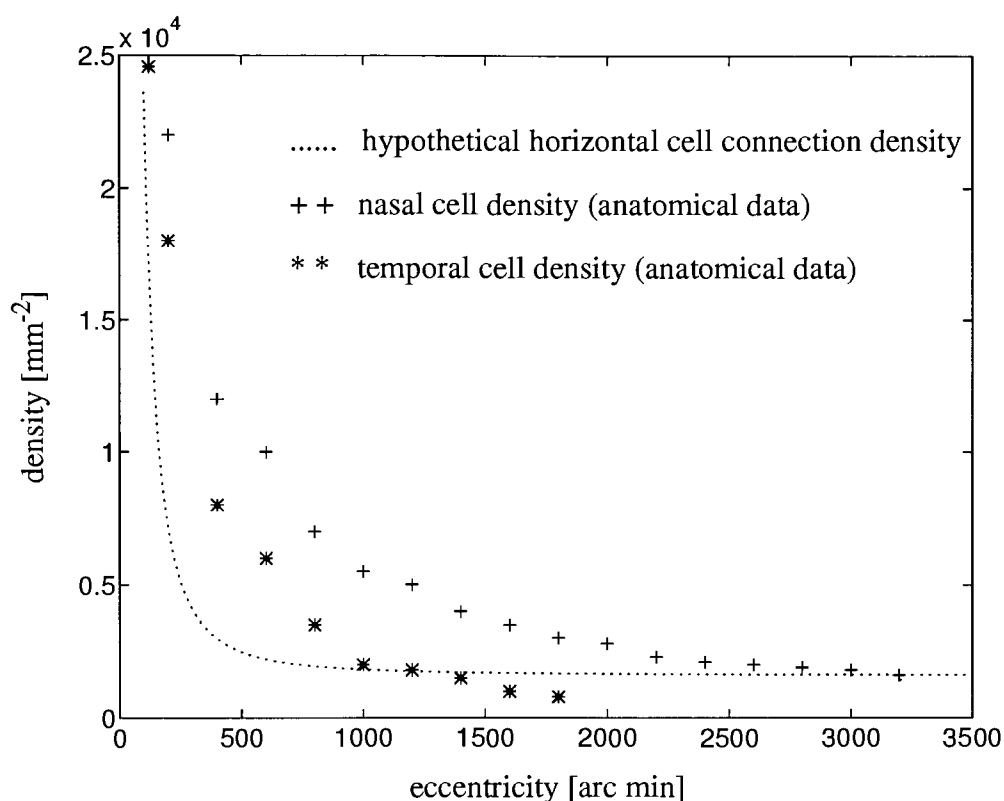


Figure 1.7 Horizontal cells and horizontal cell connection density distribution

data taken from the monkey retina (*Macaca fascicularis*), adapted from Röhrenbeck et al. (1989). Under the assumption that this specimen has very similar anatomy to that of man, we can compare the anatomical data from the monkey with the psychophysical observation from humans. The visual system of the macaque monkey is similar to that of humans with respect to psychophysics, spectral responsivity (Crook et al., 1987) and visual pathway anatomy (Röhrenbeck et al., 1989). Therefore a modelling of the human retina can be based on experimental data from primates as well as psychophysical data from humans.

The profound decline in density predicted by the model is plausible in view of our knowledge of cone and ganglion cells density (Curcio et al., 1990b, Nerger et al., 1991), and some partial estimation of horizontal cells density (Krebs et al., 1991). We do realize however, that we still lack a good knowledge of the structure of the human retina and at this moment we don't even know exactly how many types of the horizontal cells exist on the retina (Kolb et al., 1994).

Conclusions

Retinal cell biology is still very descriptive. As more information is acquired, new properties of the biochemical processes will become evident. A complete visual science would require formal connection between vision psychophysics and neurophysiology of the retina. By analyzing the model of dazzling glare based on the lateral inhibition within the horizontal cell network, we might to a small extent develop those connections. Our model is different from the existing model in terms of the mechanism responsible for a loss of vision in the phenomena of glare. In this model of glare, lateral inhibition, the neurophysiology of the retina is the main glare factor rather than simple scattering of light. Of course, these two processes can coexist and even add to the increased vision deterioration caused by dazzling glare. Based on our hypothesis we predict the distribution of horizontal cell connection in the human retina and the approximate values of the space constant.

Many questions remain concerning the nature of the phenomena that account for dazzling glare. A primary reason for investigating glare is to analyze hypothetical distribution of horizontal cell connection by combining psychophysical results with physical models.

The presented work will be very useful in designing the next generation of opto-electronic artificial retinas. For example, designers of artificial retinas based on the resistive nets concept will face an image deterioration problem due to excessive illumination, that is equivalent to dazzling glare.

Summary

In this part we described different adaptation and sensitivity change mechanisms that allow biological visual systems to effectively act over a very wide range of light intensities. We are still a long way from being able to explain all of the mechanisms that are responsible for changes in different adaptation processes; however, partial conclusions can be drawn and the results applied in human-made vision systems. Some of those mechanisms are used to enhance the capabilities of artificial image acquiring systems, such as video cameras. Devices that intimately associate a photosensitive image acquiring layer with processing facilities are called "smart retinas". As compared to ordinary cameras, smart retinas play an important role in optical information processing by providing the means to

achieve fast, low power consuming systems, that may adjust autonomously to expand their capabilities.

One of the simplest solutions is to use photodetectors that produce a signal that is proportional to the logarithm of the incident intensity, similar to the camera-film system. The next step is to use photodetectors that can operate in different modes, with a different operating range for each mode, or to use a photodetector with a controlling system which changes the operating curve according to the light intensity. This change of operating curve can be implemented electronically or optically (Wysokinski, 1994). Another possible implementation can use spatial summation. At high light levels each photodetector signal would be detected individually. At low light levels a high resolution would be lost but sensitivity would be increased by using spatial summation principle. Signals from a group of photodetectors will be pooled to reach a level that can be manipulated by post-processing circuitry. Yet another solution possible with an artificial vision system is to control the exposure time of a single frame. Controlling adaptation is a very important part of the visual system as adaptation in turn controls other properties, such as the perception of contrast.

We also further develop in this part a neuro-biological model to explain glare phenomenon. The glare controversy is very old and still has not been resolved. Wright refers to it in the 1920's (Dawson et al., 1984), mentioning stray light and lateral inhibition as sources of glare. A decade ago, the concept of using "spurious electronic noise" in the retinal system to interpret glare was explored by Rawicz (1991).

Our static model, developed in 1992, is based on assumptions about vertebrate horizontal cell coupling and it thereby makes predictions about horizontal cell connection density distribution in the human retina. Using a well established model for transmission of signals in horizontal cell networks, a spread function is derived that fits the glare constant function. This fit requires a non-uniform distribution of horizontal cell connection. We predict a decline in the density of horizontal cell connection from the fovea as $1/x^2$ (where x is the distance from the fovea).

In the next part of this thesis we present the concept of an adaptive filter – a device which preprocesses spatially the light intensity distribution of the image before it is detected by the photosensitive array. Applying this filter in an opto-electronic system, which unites a charge-coupled-device (CCD) camera with an adaptive filter, expands the operating range of the systems and mimics some of the adaptation mechanisms (adaptation pool) one can find in the biological vision system.

Part II Adaptive Filter: the concept

| | |
|-------------------------------------|-----------|
| Introduction | 34 |
| The concept | 34 |
| Transformation Function (TF) | 37 |
| Modelling | 39 |
| Summary | 48 |

“The retina, after being acted upon by light or darkness, is found to be in two different states, which are entirely opposed to each other.”

Johann Wolfgang von Goethe: **Theory of Colours**

Introduction

The idea of photodetector dynamic range modification by means of an Adaptive Filter (AF) stems from the analysis of processes found in the human visual system. Human photoreceptors, part of the visual system that is characterized by a very wide light dynamic range, are very sensitive to extremely weak sources of light. It is well established that they are sensitive enough to detect a few photons, and with more light coming in, the sensitivity of the visual system decreases due to a variety of adaptation mechanisms* that transform the observed image for better perception. Another result of image processing existing in our eye is the minimization of a glare.

Generally, we can divide biological adaptation mechanisms into two types: global and local. Global adaptation changes the average sensitivity of the whole retina. Local adaptation describes the process of sensitivity change over parts of the retina – the adaptive pools. We propose to apply the adaptive filter combined with an extremely sensitive photodetector array to implement local and/or global adaptation in a novel image acquiring system. The implementation of the adaptive filter in the camera would improve the picture quality, as compared to ordinary video cameras which have limited dynamic range (e.g. the span between the brightest and dimmest light detected without distortions). Very sensitive cameras produce high quality pictures in dim light, their limited dynamic range reduces the quality of the image at high light levels, due to overloading of the photodetectors. The adaptive filter would prevent the photo-sensor array from overloading, thus extending the dynamic range of the whole system.

In this part, we model image transformation functions similar to the local adaptation mechanism of human eye.

The concept

A globally adapting filter is uniformly transparent across the surface. The application of this kind of filter would be to globally change the average intensity of illumination on the photoreceptor array plane. Such an attenuation process is equivalent to the change of the effective aperture of the entrance lens, for keeping the average light intensity at the focal

* See *Part I* of the thesis.

plane constant. However, it differs from the actual change of the aperture when we consider the image quality. The global adaptive filter, unlike the opto-mechanical device (the aperture), does not change the depth of focus and sharpness of the detected image (Ray, 1979).

A locally adapting filter is a type of filter that can change its light transmittance in response to temporal and spatial light intensity variation. This filter, on the one hand, can be used in conditions where large spatial and temporal differences in light intensity in the image occur to extend and shift the dynamic range of the filter/photodetector system. On the other hand, its application can be foreseen to change the characteristic of the operation of the filter/photodetector system in a given light intensity region to enhance/stretch the contrast within the scene. Particularly difficult light situations, such as a brightly lit subject that stands out against a dark background, or backlit subjects, that can not be properly detected with standard cameras, might be very successfully recorded with the system utilizing the local adaptive filter. This system would have a wider dynamic range and would render the entire range of light intensities with little distortion. The darkroom procedure called “burning in” (Goldstein, 1984) is essentially similar. It is used by photographers to increase darkness, and as a result the contrast ratio of the lighter areas within the picture. In this process the underexposed parts within the picture are darkened by exposing them to extra light during the printing process. As a result pictures with a very large range of intensities in the scene are produced. The same picture would be obtained if the film could locally adapt like the eye does, to compensate for very high or very low light intensities in parts of a scene.

In this work we model a variety of adaptive filters and we later test Photochromic Adaptive Filters (PAF), that can perform similar types of tasks*. Photochromic materials are a special kind of photosensitive materials, that reversibly change their light transmission in proportion to incident light intensity.

In our model of the locally adapting filter, a thin layer filter is placed in the focal plane of an optical system on top of a photosensitive array (Figure 2.1). More intensely illuminated parts of the focused image produce a proportional darkening of the filter, blocking a fraction of the light. It results in the negative, neutral-grey image of the scene within the filter. This phenomenon is called local adaptation. With an increase of average light intensity, the increased average absorbance of the filter limits the light reaching photodetec-

* See Part III of the thesis.

tors, thus mimicking global adaptation. Global adaptation can also be achieved by substituting an ordinary clear lens with a lens that can lower its transmittance in proportion to the ambient light level. A globally adapting filter, that has space uniform transparency can shift the operating range of photodetectors, much as a variable diaphragm does.

The adaptive filter can act both locally and globally. Depending on the location of the adaptive filter in the optical system and a method of controlling the filter (see Figure 2.1),

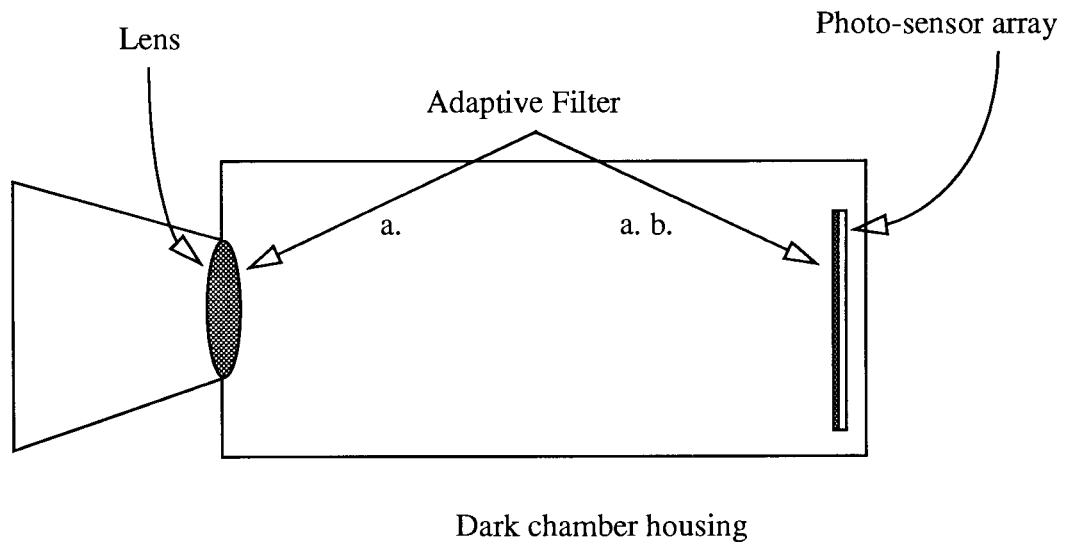


Figure 2.1 Utilization of the adaptive filter in a. global and b. local operating mode

the two functions can either be separated or used jointly.

The adaptive filter can be implemented in a number of ways. For parallel image processing electrically or optically controlled Two Dimensional (2-D) Spatial Light Modulators (SLM) are used most often. Two Dimensional SLM's have been very succinctly described (Neff et al., 1990), as: "devices which can modulate one of the properties of an optical wavefront (amplitude, phase or polarization), as a function of two spatial dimensions and time, in response to information bearing control signals (either optical or electrical)". The Adaptive Filter (AF) utilization is schematically shown in Figure 2.2. The passive and active methods of controlling filter properties are presented.

Active control is achieved by a feed-back loop through a CPU, where the detected image is analyzed and the adaptive filter state is adjusted accordingly to specified parameters. For that purpose, Liquid Crystal Displays (LCD's) and Digital Micromirror Devices* (DMD's) are very well suited. Another possibility is to use a passive system which inde-

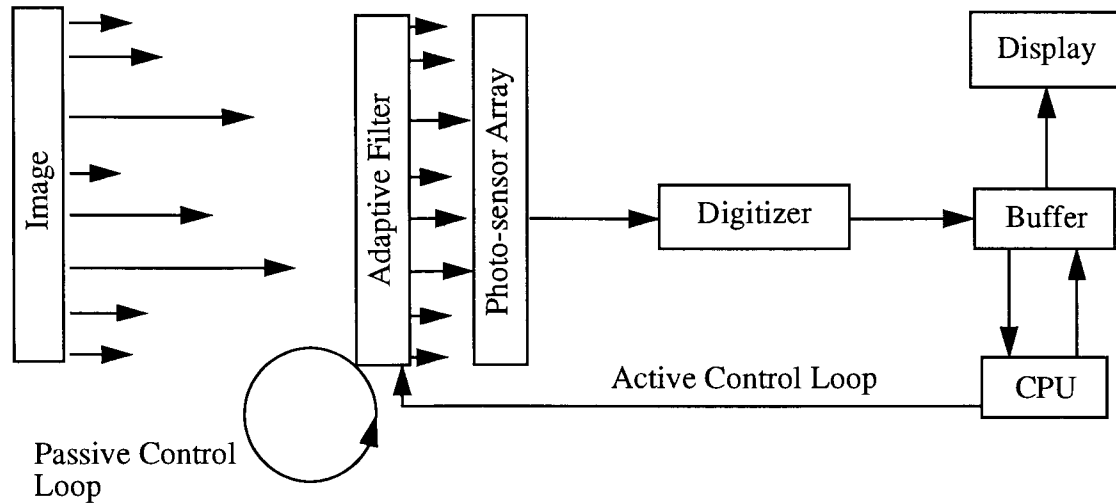


Figure 2.2 Block diagram of the image processing system utilizing active and passive types of the Adaptive Filter

pendently adjusts to changing light intensity. It can be made using photo-sensitive materials, like photochromes which undergo reversible photo-chemical reactions when excited by irradiation. As a result, their absorption spectrum in VIS range changes. Either way, as a final result of the use of the adaptive filter, image parameters such as brightness and contrast are changed, to match them to the dynamic range and sensitivity of the photo-sensor array.

Transformation Function (TF)

The type of image conversion performed by the adaptive filter is strongly related to the shape of the transformation function. The Transformation Function, sometimes called a transfer function, describes the relationship between an input quantity (x axis) and an output quantity (y axis) Such a relation is characterized by a number of parameters:

1. Sensitivity
2. Stability and Repeatability
3. Accuracy and Precision
4. Response Speed

* See *Appendix* of the thesis.

Sensitivity tells us what change in the output can be expected for a given change in input quantity. Stability is determined by the constancy of the sensitivity over time. Accuracy determines the maximum error in the output quantity and response speed describes the delay between the input and output change.

Some of these parameters can be directly determined from the shape of the Transformation Function, one example being the sensitivity which is related to the slope of the tan-

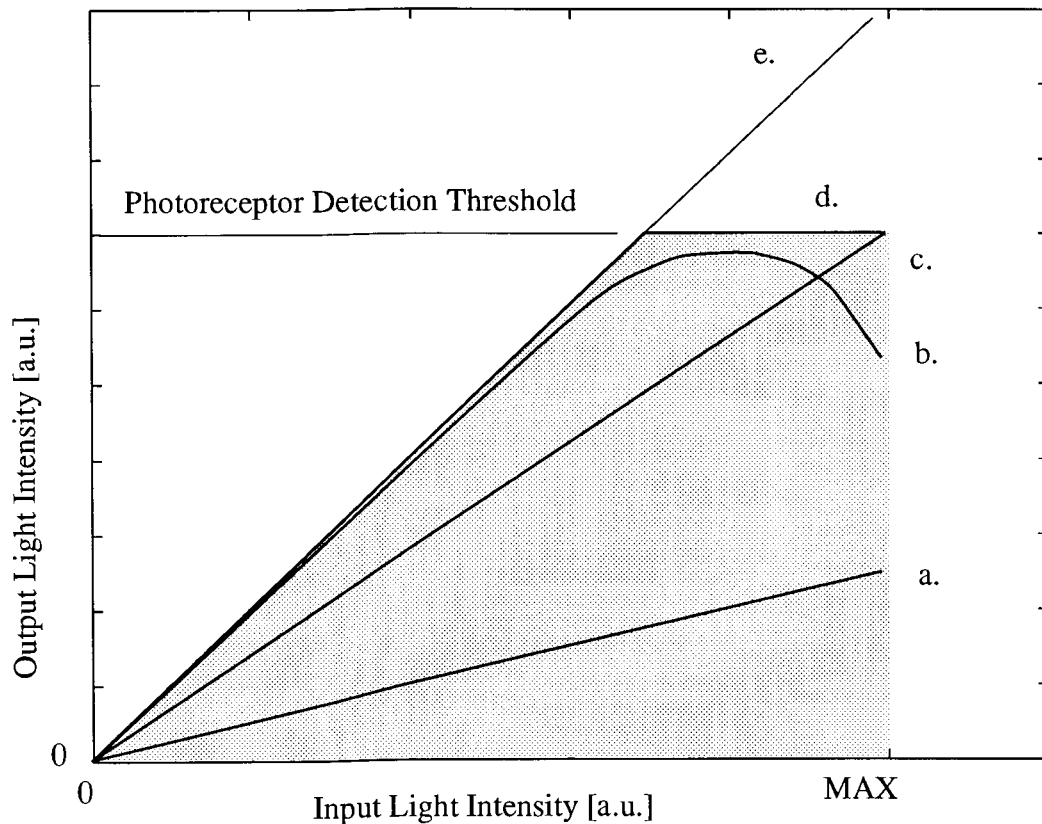


Figure 2.3 Selected image transformation types:
 a. proportional reconstruction
 b. nonlinear reconstruction
 c. optimal proportional reconstruction
 d. proportional reconstruction with part of the image saturated
 e. exact reconstruction

gent. Others can be deduced from the temporal changes of the TF. For image transformation, the TF relates the input and output light flux which passes through a transforming device – the Adaptive Filter.

Modelling

Figure 2.3 presents different shapes of the Transformation Function and explains differences between them in image reconstruction. The shaded area corresponds to the operating space, where image transformation and detection take place. Within this area a few basic types of transformation function are presented:

- Curve a. corresponds to the case where the proportional detection process uses only part of the dynamic range of sensors, so that image light intensity distribution is very compressed, and sensitivity is low.
- Curve b. shows a nonlinear Transformation Function. Nonlinear function may be very important in enhancing contrast within the specific range of light intensities. They can be used to change contrast from normal to high-contrast to enhance the contrast of a scene having a small range of intensities (Goldstein, 1984), such as might occur in a picture taken in a dimly lit room. By compressing in a unique form the high intensity region this function can also be used to widen the dynamic range. However, if this function is not unique, as is the case in Figure 2.3, then we observe specific image deficiencies like artifacts (Figure 2.6).
- Curve c. is the optimal case. In this example we utilize maximum dynamic range of the sensors, and we have proportionality between input and output parameters.
- Curve d. shows the proportional transformation curve in case where external light intensities exceed the dynamic range of operation of the sensors. As a result parts of the image will be saturated, with all the image details within that parts lost.
- Curve e. is an exact reconstruction line. It means that input and output light intensities are identical, and no change within the system occurs.

Modelling Image Transformation by Different Transformation Functions

In this part we model the image transformation by different global and local adaptive filters. We treat the modelling as a fast and flexible approach for testing different hypotheses. Only a few special cases of the transformation function are presented and tested to visualize the potential image quality improvements after the adaptation process took place.

The spatial distribution of light intensity after passing through an adaptive filter is described by the gray-level Transformation Function (TF) of the system. The transforma-

tion function correlates the light intensity of the original image to the corresponding light intensity of the transformed image for each picture element (pel) with coordinates (i,j):

$$I_{i,j}(I_{i,j}^0) = TF(I_{i,j}^0) \quad (\text{Eq. 2.1})$$

Where:

$I_{i,j}^0$ – intensity of light entering the filter

$I_{i,j}$ – light intensity distribution after the transformation process

On the other hand, we can express this relation using basic optics equation:

$$I_{i,j}(I_{i,j}^0) = I_{i,j}^0 \cdot T_{i,j}(I_{i,j}^0) \quad (\text{Eq. 2.2})$$

Where:

$T(I_{i,j}^0)$ – transmittance of the filter at a given location

This equation can be rewritten as:

$$T_{i,j}(I_{i,j}^0) = \exp(-\alpha(I_{i,j}^0) \cdot d) \quad (\text{Eq. 2.3})$$

Where:

d – thickness of the filter

$\alpha(I_{i,j}^0)$ – absorption coefficient of the filter at a given location

Assuming different transmittance functions, one can model filters that alter the images in a specific manner. In our modelling we assumed the following:

1. Filter has uniform thickness and is homogenous.
2. The spectral transmittance of the filter does not depend on the light intensity and it closely follows the characteristic of the neutral-grey filter for visible light.
3. To preserve uniqueness of the image, we seek transmittance of the filter as a continuous, decreasing function of the light intensity.
4. Normalization requires that the transmittance of the filter is less or equal to 1.

Substituting these conditions in Equation 2.1 leads to the system of differential inequalities:

$$\left\{ \begin{array}{l} \frac{\partial I_{i,j}(I_{i,j}^0)}{\partial I_{i,j}^0} > 0 \\ \frac{\partial^2}{\partial (I_{i,j}^0)^2} I_{i,j}(I_{i,j}^0) \leq 0 \end{array} \right. \quad (\text{Eq. 2.4})$$

There is a class of solutions of Equation 2.4 for transmittance in the form:

$$T_{i,j}(I_{i,j}^0) = \frac{\text{const}_1 - \text{const}_2 \cdot I_{i,j}^0}{\text{const}_3 + \text{const}_4 \cdot I_{i,j}^0} \quad \therefore \quad (\text{Eq. 2.5})$$

Values of constants in Equation 2.5 dictate the form of the changes in the transmission.

There also exist other solutions of Equation 2.4. For the case of exponential dependence of transmittance on incident light intensity we get:

$$I(I_{i,j}^0) = \exp(-\mu \cdot I_{i,j}^0) \cdot I_{i,j}^0 \quad (\text{Eq. 2.6})$$

Where:

μ – constant

In that case, from Equations 2.1 & 2.3 we find that absorption coefficient α , is a linear function of light intensity.

Discussion of a few special cases of adaptive filters

In this section we analyze the adaptive filter/photosensitive detector array system for use in image acquisition. We investigate adaptive filter models with different transmittance characteristic and their possible applications.

Within the broad class of particular solutions of Equation 2.5 we discuss below a few examples that represent the most interesting variants. The starting image for use in our model is the highly illuminated image that would be too bright for a proportional detec-

tion by a very sensitive camera – see Figures 2.4a & 2.5a. Maximum light intensity within the image (on the focal plane) is two times above the photoreceptor detection threshold. As a result, the image acquired by the camera shows regions that are oversaturated. After the simulated adaptation process the maximum light intensity is reduced by half, which corresponds to the change of Optical Density of the Adaptive Filter: $\Delta OD=0.3$.

To illustrate how some particular filters transform the image, we convert them into a gray scale element matrix. On each element of this matrix analytical computation is made in MATLAB[®] mathtool using a 2-D transformation algorithm. Finally, the transformed matrix is converted back into the form used for display or to get a hard copy of the picture.

Model 1. Taking $const_{2,4} = 0$ corresponds to an ordinary proportional filter, i.e. all transformations made by the filter are linearly proportional to the light intensity. The transmittance and absorption coefficients are in that case constant and TF is linearly increasing. Figure 2.4* shows simulated transformation of the image by the global adaptive filter that halves the light intensity. In the oversaturated picture we can not determine the border between the forest in the background and the sky. It is difficult to recognize the contours of the buildings. These tasks are very easy to perform after the modelled adaptation process took place (Figure 2.4b).

Model 2. Taking $const_2 < 0$ and $const_3 < const_4$ corresponds to the type of filter that slightly compresses highly illuminated part of the image, maintaining the more or less linear character of Equation 2.1. We use this model to test the image transformation of the local adaptive filter made of inorganic photochromic material. Transmittance and TF are in that case polynomial ratio functions of light intensity. We can observe how this type of filter modulates highly saturated image (Figure 2.5a) into the form that contains much more details (Figure 2.5b). Transmittance of the filter is expressed as:

$$T_{i,j}(I_{i,j}^0) = \frac{0.6 \cdot (100 + 0.8 \cdot I_{i,j}^0)}{100 + I_{i,j}^0} \quad (\text{Eq. 2.7})$$

* The picture “Trees” used for the simulation has been taken from British Telecom (BT) image database.

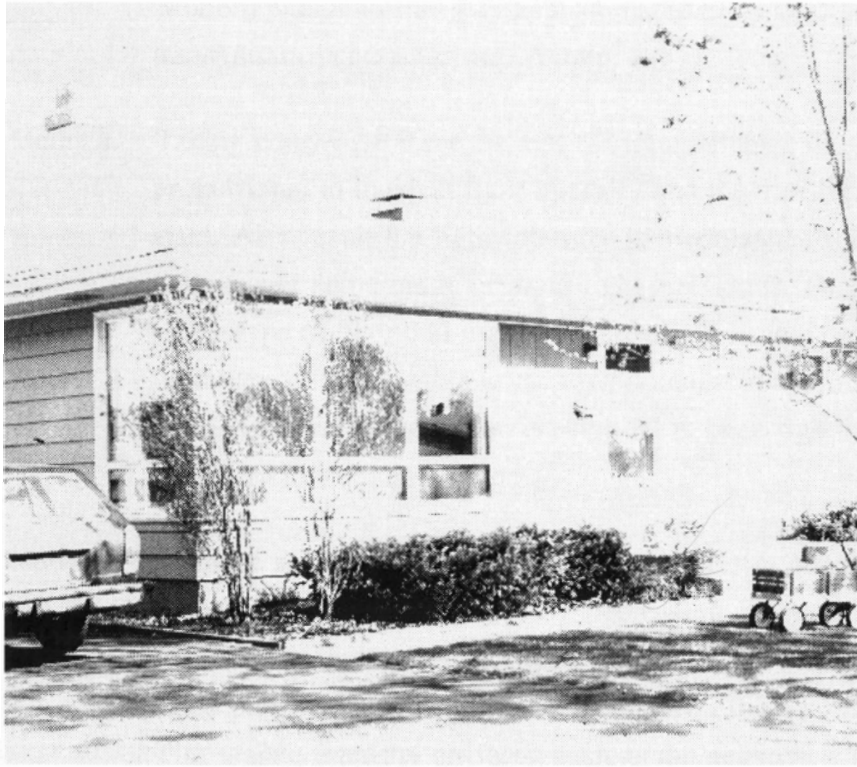


a.



b.

Figure 2.4 Global adaptation modelling – “Model 1”, a. initial (overexposed) image, b. transformed image (the forest in the background clearly visible)



a.



b.

Figure 2.5 Local adaptation modelling – “Model 2”, a. initial (overexposed) image, b. transformed image (many more details are clearly visible)

Modern photochromic glasses manufactured by Corning Inc. have this type of transmittance characteristic (Araujo, 1987).

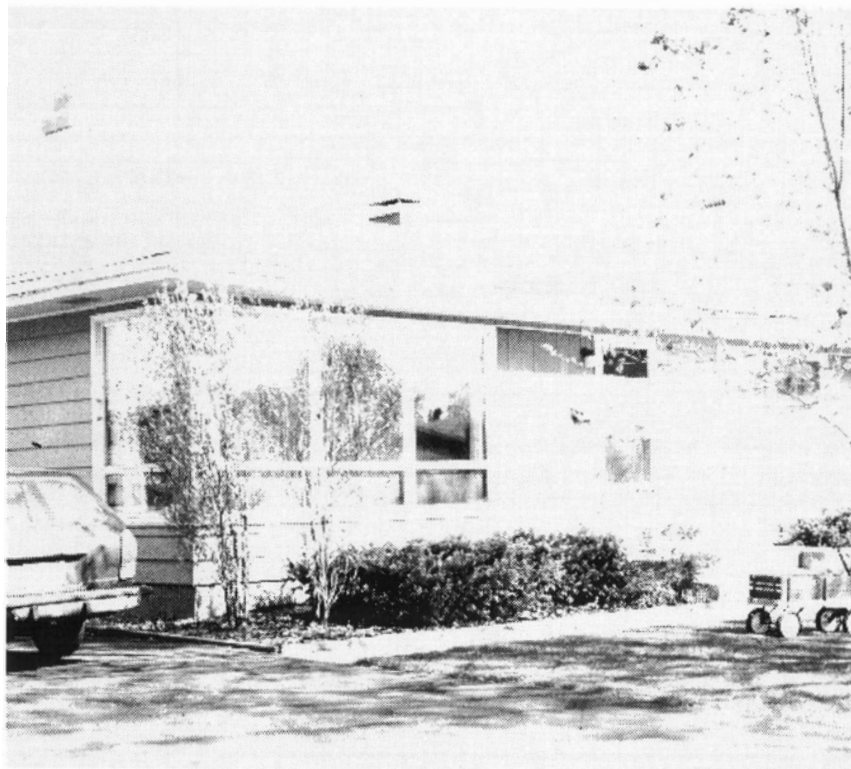
Model 3. Taking $\text{const}_{2,3} = 0$ means that the transmittance of such a filter is inversely proportional to incident light intensity and the transformation function is constant. As a result the light intensity is modulated so that we get the constant output over some range of input light intensities. This is potentially an interesting type of filter that together with a light source becomes a uniform planar light source that is stable in the time domain. For example, such a light source giving uniform illumination is essential to back-lighting of a recorded picture with very low contrast ratio.

Model 4. Another special case is when $\text{const}_1 = \text{const}_3$, $\text{const}_2 > 0$ and $\text{const}_4 = 0$. Transmittance is then a linearly decreasing function and the transformation function is parabolic. In this case, the filter highly compresses the most illuminated part of the image. Figure 2.6b shows the results of this transformation with visible intensity artifacts, such as the negative image of the most illuminated part within the scene as the resulting image has lost the preservation of gray levels because the transformation function is not monotonically increasing. However this type of transformation can be useful for specific tasks, such as observing the hot air flow from the chimney against the sky background. Transmittance of this filter is:

$$T_{i,j}(I_{i,j}^0) = \frac{500 - I_{i,j}^0}{246} \quad (\text{Eq. 2.8})$$

In the above examples we specified a few cases of different filters that transform the image. One type can be used for enhancing the contrast in the image for low and medium values of illuminance (Model 4), another for enhancing contrast in darker part of the image – Model 2. Figure 2.7 shows the shape of the transformation functions that were used to model the image transformation.

The use of photochromic glasses, which are closely characterized by Models 2 & 1 has been suggested for attenuation of the light flux in the brightest portion of the picture for controlling an automated welding system (Tunimanova et al., 1991).



a.



b.

Figure 2.6 Local adaptation modelling – “Model 4”, a. initial (overexposed) image, b. transformed image (note the hot air above the chimney, the license plate)

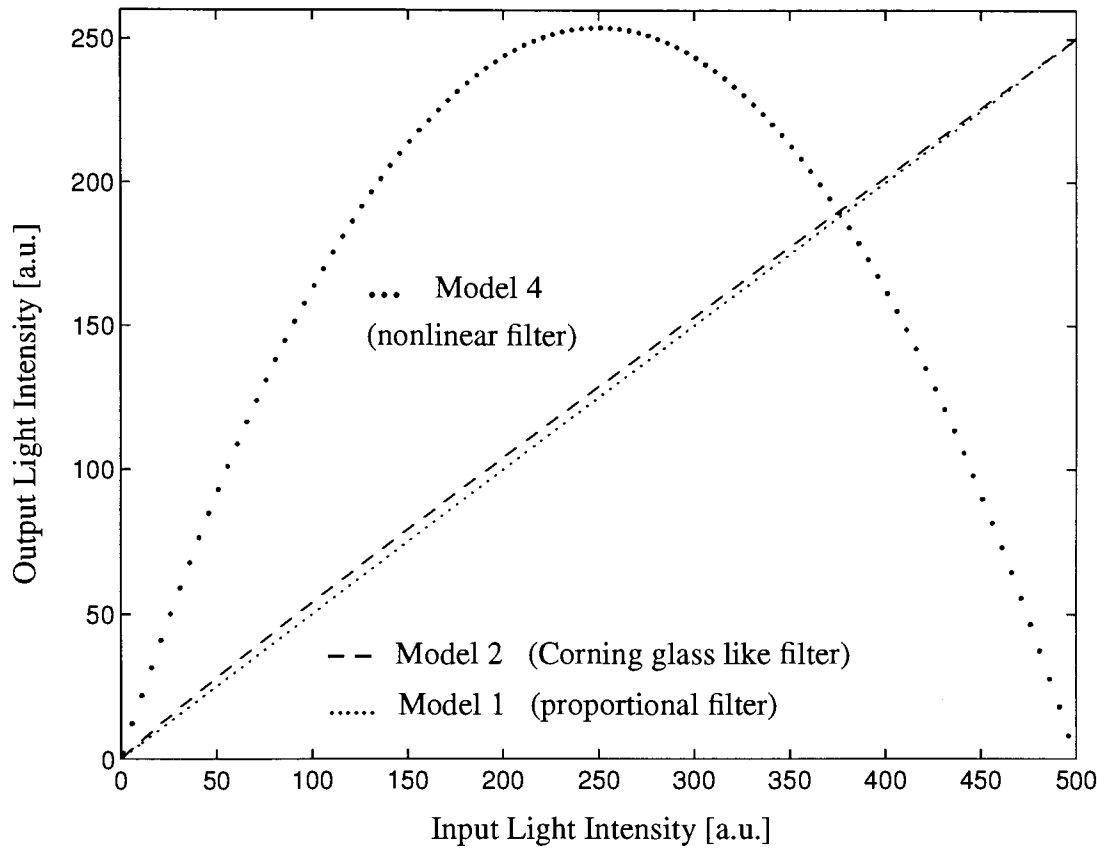


Figure 2.7 Investigated transformation functions

By compressing the highly illuminated part of the image it is possible to transform the image so that it can be acquired by a camera without saturating any part of the photosensitive array. It is a partial equivalent of the mechanism called local adaptation of the human visual system. The local adaptation enables us to see light sources, without losing details in the darker part of image. In that sense it widens the dynamic range of the camera.

This modelling shows that including an adaptive filter in form of a 2-D spatial light modulator improves quality of the image. Some of the modelling results were confirmed by simple experiments using ophthalmic photochromic lenses (Wysokinski et al., 1995a). Part III of the thesis describes details regarding development and testing of the custom-made photochromic filters.

Summary

The numerical modelling confirms that it is feasible to use adaptive filters as spatial light modulators. An adaptive filter/detector array system having linear and nonlinear characteristics can be used to implement specific types of image transformation. For example, the adaptive filter/detector array system can operate over a wider dynamic range of light intensities than the detector array alone.

The modelled transformation of the image can be implemented with both passive and active types of filters. The active type gives us more freedom to adjust for different illumination conditions – this type of image processing can be performed with Liquid Crystal Display Spatial Light Modulators (LCD SLM's) (Efron et.al., 1989). The passive type can be implemented with photochromic filters. The photochromic system is different from that using LCD SLM because it does not require an external electrical power supply and it is self-adjusting.

Presently available types of photochromic materials allow construction of only a limited variety of filters, especially the ones described as “Model 1 & 2”. These types of filters can be used to take a picture that includes a light source such as plasma, Sun or another UV-radiating source within the frame. New types of photochromic filters need to be developed and fabricated in order to construct new types of cameras for specific uses. Such uses could include those with a very bright non-UV light source within the frame, those requiring contrast stretching of some part of the image, or achieving image uniformity, or reflex reduction, or optical system requiring self-protection against destructive light intensity levels in the image.

At the present stage of development, photochromic materials are still relatively slow, particularly for most real time visual processes. Another limiting factor is sensitivity mostly to highly energetic UV radiation. However, there is much research aimed at developing new photochromic agents, sensitive to visible light and responding much faster. The main advantages of using these materials are parallel image processing, very good resolution, automatic local adjustment to different absolute light intensity levels and no additional energy consumption.

Part III Photochromic Adaptive Filter

| | |
|--|-----------|
| Introduction | 50 |
| Photochromic Systems | 50 |
| Development of a Photochromic Adaptive Filter | 55 |
| Photochromic Filter – Implementation | 73 |
| Determination of the Transformation Function | 83 |
| Summary | 88 |

**PAF – a device that manipulates and controls
light intensity by means of photo-sensitive
material**

Introduction

Although the first documented observation of the reversible change of color of the painted gate was as early as XIX century (Phipson, 1881), the photochromism initially received a limited attention. Only recently this area is rapidly expanding and the research in the field has shown steady growth. Many new compounds were prepared, both organic and inorganic. Many scientific advances were made including mechanisms explaining different photochromic processes and structures. Some classes of photochromic materials are subject of particularly active research and development programs in industrial laboratories because of their potential usefulness in a variety of applications, many others still await practical applications due to limitations like sensitivity, fatigue, stability.

However we have just begun to understand some photochromic processes; others that have been proposed are subjects of debate by researchers in the field. There are quite a few problems which remain to be solved, like lack of stability of organic photochromic materials to environmental factors, before they can be widely applied in practical applications.

Another problem is the scattered information of the knowledge available in present. Information about photochromic materials exists mainly in technical reports and circulates among the college of workers in the field (Brown, 1971). There has been little information about photochromic materials published in the primary scientific literature, so there is a high probability of multiple attempts to challenge the same task by different research groups without knowing about others.

A promising future exists for photochromic materials in many fields, such as information processing and display devices. We postulate the use of these materials as a photonic component: a thin layer photochromic filter, in opto-electronic systems for analog image parameter like brightness and contrast, processing. Following sections describe the research done in this field and present results of the application of the photochromic filter.

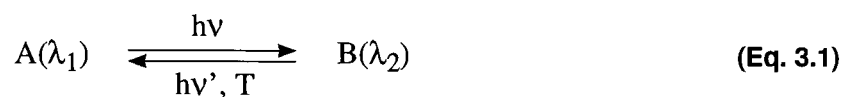
Photochromic Systems

General classification of photochromic systems divides them into two groups: organic and inorganic. We designed, prepared and tested several compositions in both groups. A section in the *Appendix* of the thesis summarizes the work done with inorganic compounds.

In the following sections we concentrate on research done investigating organic photochromic systems to enhance capabilities of image acquisition systems.

Photochromic systems – general description

Photochromism is defined (Brown, 1971) as a reversible transformation of a single chemical species between two states, whose absorption spectra are recognizably different, brought about, in at least one direction, by electromagnetic radiation (Equation 3.1):



Species A is transformed into higher-energy form B as a result of light irradiation (Horspool, 1995). The reverse reaction to A usually occurs as a spontaneous thermal process, but may also be light-induced.

The term used to describe the reversible coloration “photochromism” is made of two parts: photo (light) and chrom (color). Recently developed materials may show change in the spectral properties beyond that of the sensitivity range of the human eye, so there is no visible change in the color. Nonetheless they are described as photochromes. When embedded in glass or plastic photochromic agents adjust the global or local transmittance of an optical component. As the illumination energy is removed, the system reverts to its initial state.

Inorganic photochromic systems*

The types of inorganic solids that exhibit photochromic phenomena almost always involve materials having a large energy band gap (3-12 eV) so that, in the unactivated state, they have negligible optical absorption in the visible region of the spectrum (Brown, 1971).

The optical excitation leads to the formation of metastable centers which absorb light in the visible region, giving rise to the characteristic color. This photochromic system is based on an electron transfer/redox reaction. The system can return to its original ground state either by optical excitation within the color-center band or by heating the

* For more information see *Appendix*.

band to elevated temperature. The most popular example of such systems are alkali halides photochromic glasses – the first major photochromic commercial product.

Organic photochromic systems

Photochromic reactions are always attended by rearrangement of chemical bonds. Organic materials are activated almost exclusively by ultraviolet light within the wavelength range of 200-400 nm (Dürr et al., 1990).

The organic photochromic systems can be classified into several main groups according to the nature of the photochemically induced primary step. It includes: heterolytic cleavage, homolytic cleavage, *cis-trans* isomerism and tautomerism (Brown, 1971).

If a bond breaks in such a way that both electrons remain with one fragment, the mechanism is called heterolytic cleavage and results in ions. When each fragment gets one electron, free radicals are formed and such reactions are said to take place by homolytic or free-radicals mechanisms (March, 1985). *Cis* and *trans* isomers are compounds that have the same sequence of bonds but differ in the arrangement of their atoms in space. They can be interconverted only by breaking bonds (Vollhardt, 1987). The rapid change of the molecule (faster than 10^3 times per second) between two structures is called valence tautomerism.

In our work we investigate organic photochromes that belong to two families: indolinospirothoxazines and pyrans. They are representatives of the group characterized by

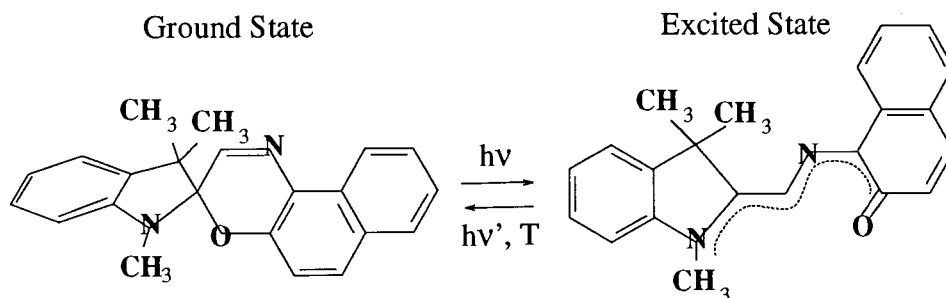


Figure 3.1 Heterolytic bond cleavage mechanism in spiroxazine “N”

photochromic process involving heterolytic bond cleavage.

Spiroxazines were discovered to be photochromic in 1961 but only in 1980' they re-

ceived a broader interest (Dürr et al., 1990) as they are very photostable. In the lower-energy, colorless state they consist of two halves of heterocyclic fused rings connected at the tetrahedral sp^3 carbon. Those two parts are electronically isolated from each other because of the orthogonality of the π -electron wave functions in both parts.

Typical photochromic reaction responsible for coloration of spirooxazine is shown in Figure 3.1 (McArdle, 1992). Irradiation of the colorless spiro-compound leads to cleavage of the single covalent $C_{\text{spiro}}-O$ bond to give the open-chain molecule, that is structurally different from the ground state.

Photoactivated photochromic system undergoes very fast ring opening to the colored form with a good quantum yield ($\phi_R = 0.2$ to 0.8 , (Horspool, 1995)) in solution as in films. Open-colored species of the photochromic have merocyanine like structures which is characterized by shift of the UV absorption in the visible region. A π -electron cloud can extend now from the indoline part to the oxazine part of the molecule. The first electronic transition of such a molecule occurs in the visible part of the spectrum, thus appearing colored. This open colored form can exist in few stereoisomeric forms, what results in broad absorption peak.

Bleaching process may be either thermal or photochemical, and its higher energy content is, in most cases, the driving force (Malatesta et al., 1992). The color fades thermally very rapidly to regenerate the original molecule. The photochemical back-reaction is, however, very slow. This class of photochromes shows high long-term photostability what makes it the best photochromic organic systems used today.

By analyzing distribution of the covalent electrons in both energy states and structures, we deduced similar schematic for representative of another investigated type of photochrome: naphthopyran (Figure 3.2). Photochromism of pyrans was discovered only

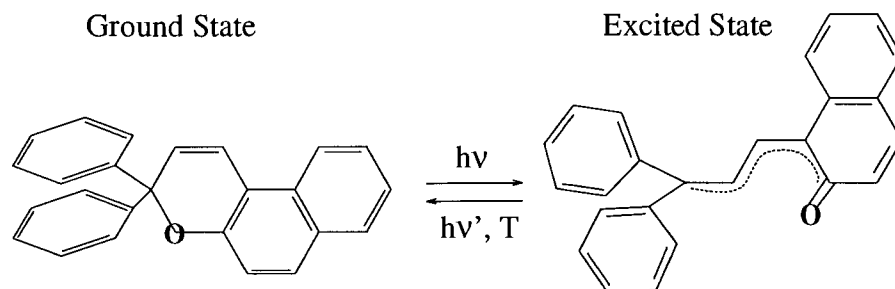


Figure 3.2 Heterolytic bond cleavage mechanism in naphthopyran “Y”

in 1952 (Dürr et al., 1990). Photosensitive pyrans continue to arise a strong interest in connection with their application in various fields such as: non-silver high resolution photography, optical devices and holographic systems. Pyrans are less fatigue resistant or fatigue free than the structurally related oxazines. Long irradiation can lead to photodegradation products. Atmospheric oxygen facilitates this photodegradation by radical processes.

Applications of photochromic systems

The inherent properties of photochromic systems make them suitable for use in many different areas (Horspool, 1995):

1. Control and measurement of radiation intensity
2. Visual contrast effect
3. Solar energy conversion
4. Information imaging and storage (Irie, 1994)
5. Optoelectronic circuits (Hornak, 1992)
6. Image processing (Krongauz et al., 1995)
7. Optical computing and signal processing (Lessard et al., 1992)
8. Integrated optics (McArdle, 1992)

Photochromic compounds have also potential practical application in such field as photolithography, where they can be used as a reversible photoresist. Spiropyrans may be used in the colored form in processes of non-silver photography as catalyst of an amplification phenomenon. They may also be used as light controlled regulators of various physico-chemical processes. Photochromic films and glasses have apparent use as wrappers and containers for photosensitive products (Dürr et al., 1990).

In this work we postulate using photochromic systems for optical image transformation in the optoelectronic systems. This image transformation is achieved by means of adaptive filter* made of photochromes. Those systems mimic in particular conditions the adaptation mechanisms that can be found in the biological vision systems. Input image is transformed by spatial light modulator in a predetermined manner to adjust output light intensity range to the dynamic range of detecting system.

Figure 3.3 presents a block-diagram of the photochromic processing system. The

* The general idea of utilizing the adaptive filter is presented in *Part II* of the thesis. *Figure 2.1* shows implementation of the Photochromic Adaptive Filter.

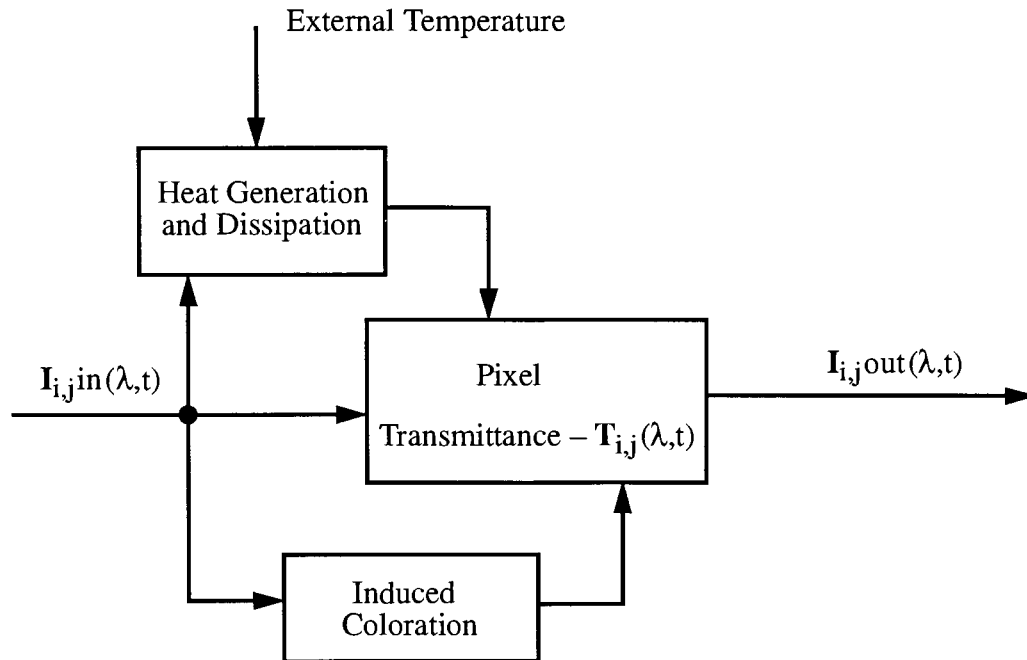


Figure 3.3 Block diagram of an optic-optic light modulator unit

state of the system (transmittance) is determined by input – incident light and temperature. Transmitted light intensity is the output.

Development of a Photochromic Adaptive Filter (PAF)

We developed the photochromic filter consisting of a polymeric thin film with embedded photochromes. There are several important points we considered while developing thin layer filter using polymers as a matrix. Polymer adhesion to substrate interface is a very important factor in the construction of PAF. Good adhesion is required not only at low temperatures, but also after exposures of up to several hours at higher temperatures (200-400°C), e.g. during thermal treatment and also during normal operation conditions of the system.

Polymeric planarization is affected by many parameters, including polymer solution properties (polymer molecular weight, solution compositions, and viscosity), spin-coat processing parameters (dispense volume and speed, and final spin speed), film shrinkage

and thermal flow during curing, and feature size (step height and pitch).

Higher photochromic concentration translates into higher photochromic response (ΔOD) values attainable, but one has to avoid aggregation effects which can adversely influence kinetic behavior as well as the spectral characteristic of the media. These are important aspects of designing thin layer filter that were considered and tested through the experimentations.

Polymeric matrices

In process of experimentation we tested several different polymeric matrices in which we embedded different photochromes. Our aim was to obtain a stable system, with high photochromic concentration and good optical qualities. We tested several most common polymers, which are characterized in Table 3.1. All materials were of the highest grade

Table 3.1 Product names and acronyms of investigated polymers

| Polymer | Abbr. | Solvent* | Notes/Supplier |
|-------------------------------------|-------|---------------------------------------|--|
| Poly(Methyl Methacrylate) (acrylic) | PMMA | MEK MMA TRI | Difficult to spin and to dissolve. Good layer stability. Obtained layer is brittle. <i>Polysciences USA</i> |
| Poly(Styrene) | PS | ΦCl ΦMe ΦMe_2 | Solvents are harmful, difficult to use. Spinning relatively easy. Cracking observed. <i>Aldrich Chemical USA</i> |
| Poly(Vinyl-Alcohol) | PVA | H ₂ O | Bad adhesion to glass. <i>Polysciences USA</i> |
| Poly(Carbonate) | PC | CHN | Difficulty with dissolution. <i>Aldrich Chemical USA</i> |
| Butyl Methyl Methacrylate Copolymer | B-725 | TRI TRI + BCS TRI + CHN | Good layers obtained. <i>Polyvinyl Chemical Industries – Div. of Beatrice Chem. Co. Inc. Wilmington, MA. USA</i> |

* See Table 3.2 for details

available and were used without any further purification.

The following Table 3.2 explains abbreviation used for the solvents. Solvents used had to be both compatible with the polymeric matrices and able to solve our photochromic

materials. The solubility of spiropyrans is rather poor in alcohols and aliphatic hydrocar-

Table 3.2 Solvents used in trial experiments

| Solvent | Abbr. | Notes – adapted from Merck* |
|---------------------|------------------|---|
| Methyl Ethyl Ketone | MEK | Flammable, volatile, acetone-like odor |
| Methyl Methacrylate | MMA | Very distinct smell, severe skin and mucus sensitizer, may act as strong irritant |
| Water | H ₂ O | The most universal solvent known |
| Trichloroethylene | TRI | Nonflammable, odor resembling that of chloroform Caution: can cause narcotic effects |
| Toluene | ΦMe | Flammable, Caution: narcotic in high concentrations |
| Xylene | ΦMe ₂ | Flammable, less toxic than benzene |
| Chlorobenzene | ΦCl | Faint, not unpleasant odor |
| Butyl Cellosolve® | BCS | Low volatility |
| Cyclohexanone | CHN | Oily liquid, Caution: poses health hazard |

* Budavari, S., Ed. *The Merck Index*, 11-th edition, Merck & CO. Inc., 1989.

bons, rather good in aromatic hydrocarbons, and intermediate in ethers, ketones, and esters (Brown, 1971).

Photochromes

Table 3.3 presents structures, names and abbreviations of the photochromes used in the present study.

Table 3.3 Structure and conventional names of investigated photochromes

| Abbreviations/Supplier | Chemical structure and full name |
|---|---|
| Photochrome “R” – Red (Red PNO) “2nd Story Concepts” Inc. Canton, OH, USA | <p>The chemical structure shows a spirocyclic system. One ring is an indoline derivative with three methyl groups (CH₃) attached to the carbon atom at the spiro center. The other ring is a naphthoxazine derivative with a piperidine ring attached to the naphthalene system.</p> |
| | 6'-Piperidino-1,3,3-trimethylspiro[indoline-2,3'-[3H]naphth[2,1-b][1,4]oxazine] |

Table 3.3 Structure and conventional names of investigated photochromes

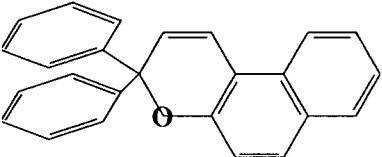
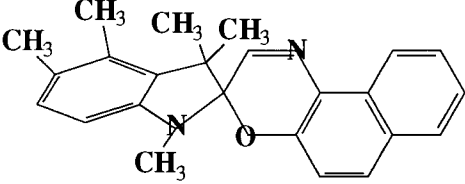
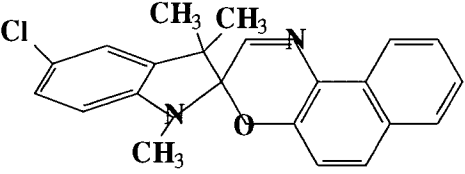
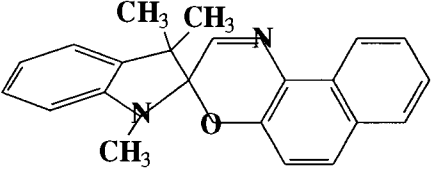
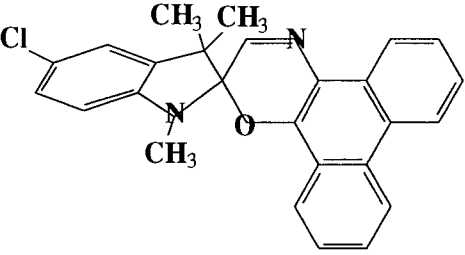
| Abbreviations/Supplier | Chemical structure and full name |
|--|--|
| Photochrome "Y" – Yellow Photo Yellow <i>"2nd Story Concepts" Inc.</i> <i>Canton, OH. USA</i> |  3,3-Diphenyl-3H-naphtho[2,1-b]pyran |
| Photochrome "B" – Blue Blue D <i>"2nd Story Concepts" Inc.</i> <i>Canton, OH. USA</i> |  1,3,3,4,5,-Pentamethylspiro[indoline-2,3'-[3H]naphth[2,1-b][1,4]oxazine] |
| Photochrome "Cl-N" <i>Aldrich Chemical USA</i> |  5-Chloro-1,3-dihydro-1,3,3-trimethylspiro[2H-indole-2,3'-[3H]naphth-[2,1-b][1,4]oxazine] |
| Photochrome "N" – NOSI I <i>Aldrich Chemical USA</i> |  1,3-Dihydro-1,3,3-trimethylspiro[2H-indole-2,3'-[3H]naphth[2,1-b][1,4]oxazine] |
| Photochrome "Cl-P" <i>Aldrich Chemical USA</i> |  5-Chloro-1,3-dihydro-1,3,3-trimethylspiro[2H-indole-2,3'-[3H]phenanthr-[9,10-b][1,4]oxazine] |

Table 3.3 Structure and conventional names of investigated photochromes

| Abbreviations/Supplier | Chemical structure and full name |
|---|---|
| Photochrome "P" Aldrich Chemical USA | <p>The chemical structure shows a spirocyclic system. On the left is a 2H-indole ring system with a nitrogen atom at the bottom. On the right is a phenanthrene ring system with an oxazine ring fused to it. The two ring systems are connected at a spiro carbon atom. This spiro carbon is also bonded to three methyl groups (CH₃), one on the indole ring and two on the phenanthrene ring. The oxazine ring contains an oxygen atom and a nitrogen atom.</p> |
| 1,3-Dihydro-1,3,3-trimethylspiro[2H-indole-2,3'-[3H]phenanthr[9,10-b]-[1,4]oxazine] | |

Design and fabrication

After series of trial tests we zeroed in on one particular type of host matrix: copolymer B-725, which gave us the most satisfactory results. The final version of Photochromic Adaptive Filters were prepared by means of a spin-coating technique from the mixture of Butyl Methyl Methacrylate Copolymer (B-725) solution, and photochromic substances (Wysokinski et al., 1996b).

The glass substrate was high quality, flat sheet. Before polymer deposition the glass was chemically cleaned, washed with DI water, spin-dried and put in the oven. For a trial series we used smaller (75x50x1^{*} mm) and (50.8x50.8x0.508[†] mm) substrates, and for preparing filters used for image transformation we used bigger (110x110x2.3[‡] mm) sheets of glass, some of them were earlier sand-blasted on one side to create a translucent screen.

Desired thickness of the filter was obtained by varying concentration of the copolymer and conditions of the spinning process. The overall thickness of the layer may vary by 1-2 μm across the surface, however, the surface was free of local deformations.

Specific percentages of different photochromes were added to achieve custom transmittance through visible region. Table 3.4 presents typical parameters of the solution and spinning procedure used to fabricate the final version of the thin film using B-725 copolymer. Such thin-films deposited in the glass substrate were used for testing image transformation.

* Fisherbrand Microscope Slides (#12-550C): $n_D=1.52$.

† Corning glass (#7059): $n_D=1.53$.

‡ Agfa-Gevaert Millimask glass: $n_D=1.51$.

Table 3.4 Typical photochrome-polymer solution formulation

| | Polym. conc. C_{wt} [%] | Solvent conc. C_{wt} [%] | Phot. conc. C_{wt} [%] | Spinning conditions speed [rpm] : time[s] | Film Thickn. d [μ m] |
|-----------|------------------------------|-------------------------------|-----------------------------|--|------------------------------|
| NN series | 25.5 | 72 | 2.5 | 500 : 30 | 19.0 |

Table 3.5 presents specific parameters for samples that are presented in the thesis. Links to

Table 3.5 Sample composition

| Sample Abbrev. | Polym. Matrix | Film Thick. ^o d [μ m] | Thin Film density ρ_s [mg/cm ²] | Photoch. [‡] used in fabrication | Total Phot. Concentr. C_{wt} [%] | Refr. Ind. of matrix n_D [-] | Notes / Links to Other Data Presented |
|----------------|---------------|--|---|--|---------------------------------------|-----------------------------------|--|
| PL #1 | B-725 | 5.7 [†] | 0.74 | | 0 | 1.52 | All "PL" and "N" series samples were deposited on the Corning glass substrate. |
| PL #3 | B-725 | 6.0 [†] | | | 0 | 1.52 | |
| PL #4 | B-725 | 6.4 [†] | 0.65 | | 0 | 1.50 | |
| PL #5 | B-725 | 4.0 | | R+Y+B | 10 | 1.51 | |
| PL #6 | B-725 | 5.5 | | R+Y+B | 10 | 1.51 | |
| PL #20 | B-725 | 6.0 [†] | 0.70 | Yell | 8 | 1.51 | F. 3.5,9,15, T. 3.6,8 |
| PL #21 | B-725 | 5.2 | | Red | 6 | 1.51 | F. 3.4 |
| PL #24/26 | B-725 | 6.0 [†] | | Blue | 6 | 1.46 | T. 3.6 |
| PL #27 | B-725 | 5.8 [†] | | N | 6 | 1.46 | |
| PL #28 | B-725 | 3.4 | | N | 6 | 1.46 | T. 3.6 |
| PL #31 | B-725 | 5.3 | | P | 6 | 1.49 | F. 3.5, T. 3.6,8 |
| PL #32 | B-725 | 5.7 [†] | 0.65 | P | 6 | 1.49 | |
| N #2 | B-725 | 6.8 | | CI-P | 6 | 1.52 | |
| N #3 | B-725 | 5.5 [†] | | CI-P | 6 | 1.50 | T. 3.6 |
| N #5 | B-725 | 6.9 [†] | | CI-N | 6 | 1.50 | T. 3.6 |
| N #8 | B-725 | 7.4 | | CI-P | 6 | 1.50 | F. 3.5, T. 3.8 |
| N #9 | B-725 | 5.6 | 0.78 | Red | 12.8 | 1.49 | F. 3.5,6,16 T. 3.6,8 |
| N #18 | B-725 | 28.4 [†] | | | 0 | 1.49 | |
| N #22 | B-725 | 16.3 | | R + CI-P | 20 | 1.50 | F. 3.4 |
| NN #2 | B-725 | 18.9 | | CI-P | 8 | 1.49 | F. 3.25 |
| NN #3 | B-725 | 19.2 | 2.72 | Yell | 10 | 1.50 | F. 3.20 |
| NN #4 | B-725 | 19.1 | | CI-P + P | 12 | 1.51 | F. 3.19 |
| NN #6 | B-725 | 19.2 | 2.72 | Yell | 9 | 1.50 | F. 3.18 |

* Determined using DEKTAK II A profilometer, unless indicated otherwise

† Calculated using spectral data (see Section: "Thickness estimation ...")

‡ See Table 3.3 for details

Abbreviations used:

** F. a.a – Figure a.a

T. a.a – Table a.a

Table 3.5 Sample composition

| Sample Abbrev. | Polym. Matrix | Film Thic. ^o d [μm] | Thin Film density ρ _s [mg/cm ²] | Photoch. [‡] used in fabrication | Total Phot. Concentr. C _{wt} [%] | Refr. Ind. of matrix n _D [-] | Notes / Links to Other Data Presented |
|--|---------------|--------------------------------|--|---|---|---|---|
| NN #7 | B-725 | 19.0 | 1.29 | Red | 5 | 1.49 | F. 3.17 |
| NN #9 | B-725 | 19.3 | | P+Cl-P+Y | 12 | 1.51 | F. 3.21-24 |
| PMMA #12 | PMMA | 25.0 | | | 0 | 1.49 | |
| PVA | PVA | 3.9 | | | 0 | 1.52 | |
| * Determined using DEKTAK II A profilometer, unless indicated otherwise † Calculated using spectral data (see Section: "Thickness estimation ...") ‡ See Table 3.3 for details | | | | | | | Abbreviations used: ** F. a.a – Figure a.a T. a.a – Table a.a |

other tables and figures which present data for a particular sample are also shown in the table.

Preparation and characterization of the samples consist of several steps:

1. Substrate cleaning and preparation
2. Polymer dissolution
3. Photochrome dissolution
4. Solution mixing
5. Spin-coating
6. Heat treatment
7. Quality control
8. Thickness and weight determination
9. Spectral properties determination

Average time of preparation of one series of samples is 2 days.

Spectral properties of photochromic filters

For different photochrome-polymeric matrix systems spectral characteristic has been taken with the Beckman DU[®] series 600 spectro-photometer. It is a single beam, high accuracy ($\Delta\lambda = 0.5$ nm) and quick response time ($\Delta t = 0.05$ s) measuring system. Data collection rate is 20 sampling/second.

We tested simple systems with a single photochromic species embedded in B-725 matrix. Using Beckman monochromator it is possible to set the scan speed so the entire visible spectrum is scanned in less than 10 seconds, thus we could get spectral characteris-

tic with little deformation due to discoloration process. To avoid as much as possible re-coloration of the samples by measurement procedure, we carried out transmittance measurements towards the most energetic part of the spectrum. To obtain repeatable and comparable spectral characteristic data we designed a stringent procedure of taking the measurements. To collect the absolute transmission spectra all samples were irradiated with 200W HBO lamp from a distance of 50 cm, for a period of 1 minute.

Table 3.6 shows both absolute and relative transmittance curves. For those measurements we irradiated samples with a 200W HBO lamp for 3 minutes from a distance of 50 cm. Next we took 10 readouts separated by two-minute interval. In between measure-

Table 3.6 Spectral and temporal properties of photochromic filters

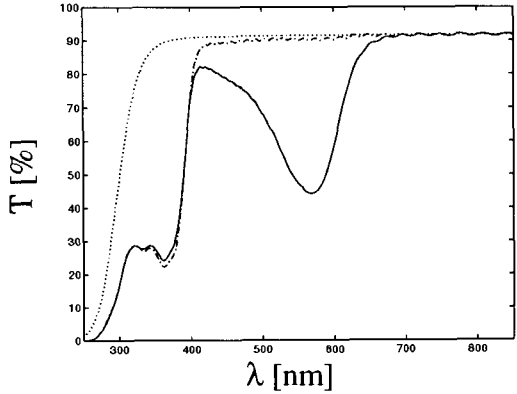
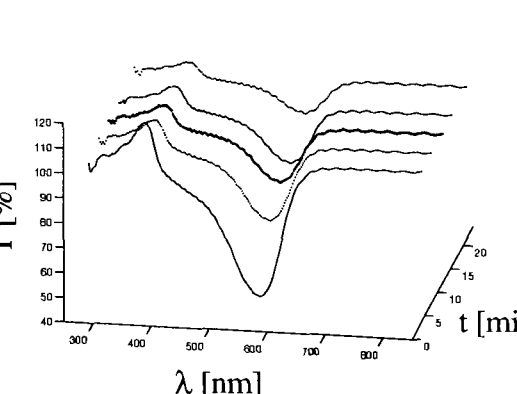
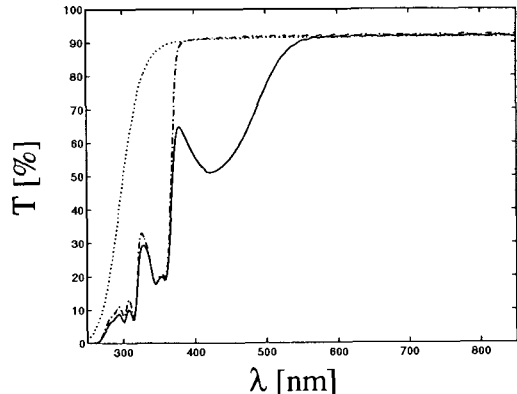
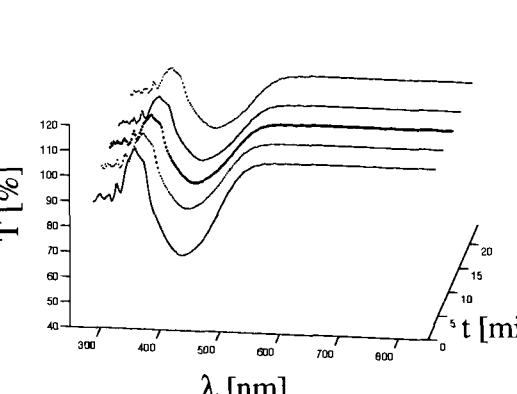
| Absolute transmission spectra* | Reaction [‡] spectrum, recorded in transmittance |
|---|---|
| <p>Red PNO, N #9[†]</p>  | <p>Time relation 3-D</p>  |
| <p>Photo Yellow, PL #20[†]</p>  | <p>Time relation 3-D</p>  |
| <p>* ... Substrate - - - Unexposed — Exposed [†] Photochrome type, Sample acronym (See Table 3.5)</p> | <p>[‡] Exposed sample relative to unexposed one.</p> |

Table 3.6 Spectral and temporal properties of photochromic filters

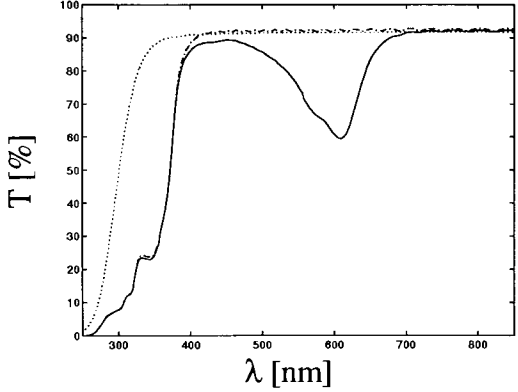
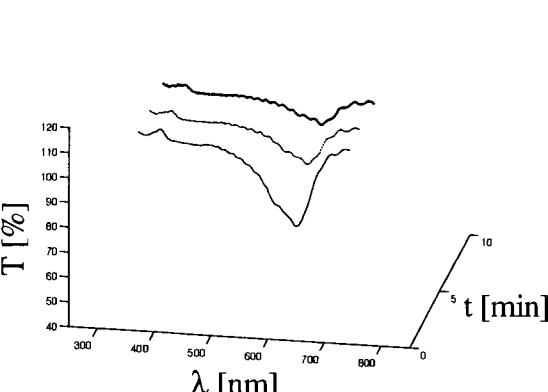
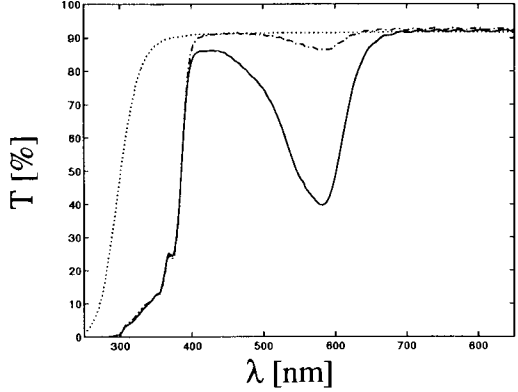
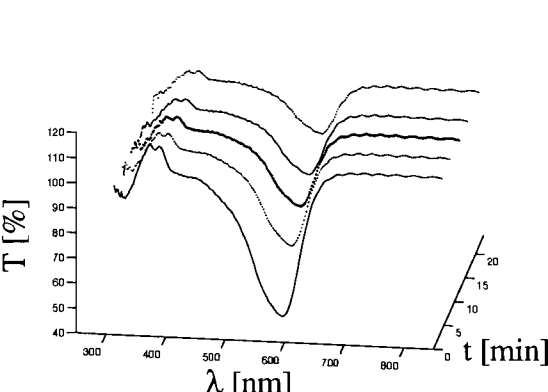
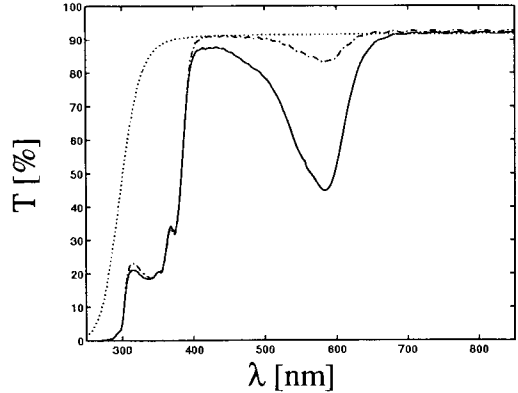
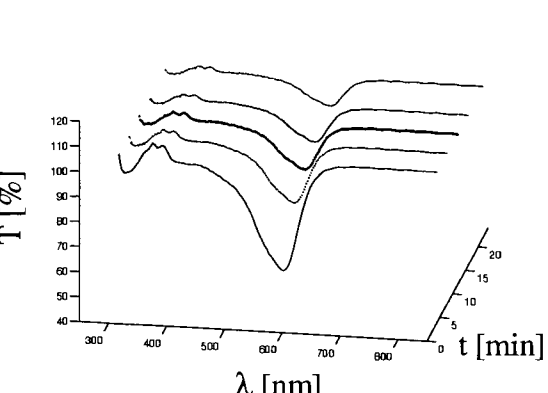
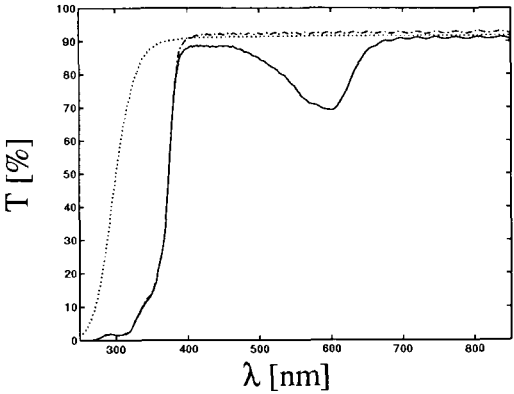
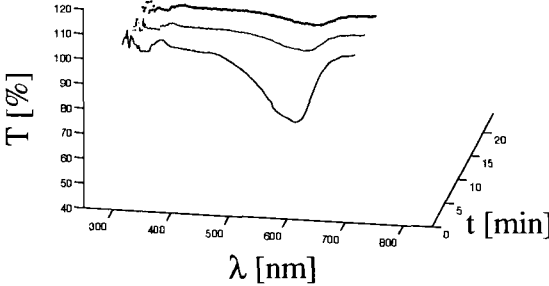
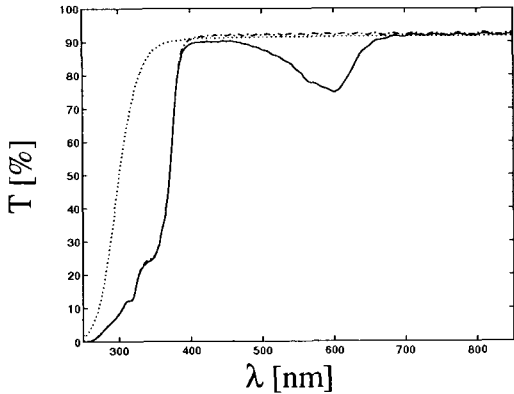
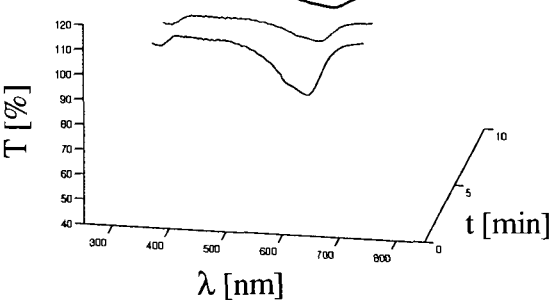
| Absolute transmission spectra* | Reaction‡ spectrum, recorded in transmittance |
|---|---|
| <p>Blue D, PL #26†</p>  | <p>Time relation 3-D</p>  |
| <p>Photochrome CI-P, N #3†</p>  | <p>Time relation 3-D</p>  |
| <p>Photochrome P, PL #31†</p>  | <p>Time relation 3-D</p>  |
| <p>* ... Substrate --- Unexposed — Exposed † Photochrome type, Sample acronym (See Table 3.5)</p> | <p>‡ Exposed sample relative to unexposed one.</p> |

Table 3.6 Spectral and temporal properties of photochromic filters

| Absolute transmission spectra* | Reaction† spectrum, recorded in transmittance |
|--|--|
| <p>Photochrome Cl-N, N #5†</p>  | <p>Time relation 3-D</p>  |
| <p>Photochrome N, PL #28†</p>  | <p>Time relation 3-D</p>  |
| <p>* ... Substrate -- Unexposed — Exposed † Photochrome type, Sample acronym (See Table 3.5)</p> | <p>‡ Exposed sample relative to unexposed one.</p> |

ments samples were kept in darkness, to minimize the change of coloration by light. The relative characteristics were taken by measuring the transmittance of the activated sample relative to the unactivated one. This type of measurements shows more precisely the difference between the activated and unactivated sample – the effect of photochromic reaction of the material. 100% level on Y axis corresponds to no change in the transmittance during the activation process.

We also designed, developed and tested multi-component systems which consisted of a few different photochromic species embedded in polymeric matrix (Figure 3.4). We aimed at getting a system with as much uniform absorbance characteristic in the visible

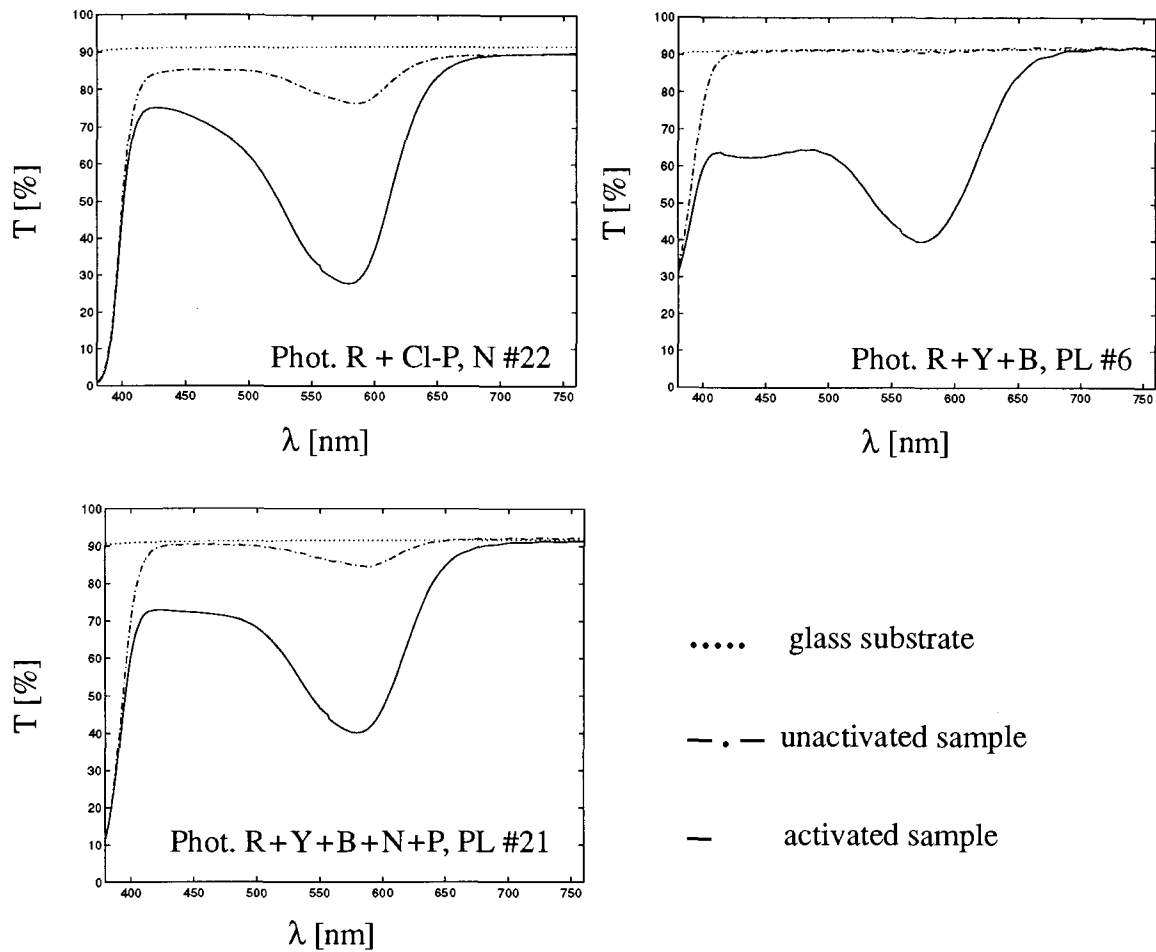


Figure 3.4 Spectral properties of multi-component photochromic systems

spectrum as possible, to make an equivalent of neutral-density filter. As can be seen, it is possible to attain a grey-like filter by choosing different concentration of the photochromic materials with different spectral properties. However as of today we lack photochromes which absorbs in long wavelength which limits the usable range of grey filter.

Table 3.7 presents maxima of the absorption peaks of different photochromes tested. We also included in the table data collected by other researchers.

In other experiment we determined the approximate value of time constant of the photochromic systems. For that measurements we irradiated the samples with 200W HBO lamp for 3 minutes from a distance of 50 cm. Next we measured the Optical Density (OD) of the sample, in the pre-determined peak of absorption. We continued this measurement

Table 3.7 Spectral parameters for different photochromic systems

| Polymer | B-725 | PS | OTHER RESEARCHERS DATA |
|---|-------------------------|-----------------------|---|
| Photochrome(s) | λ_{\max}^* [nm] | λ_{\max} [nm] | |
| Red PNO | 568/572, 568, 570 | 562 | λ_{\max} : 560 [†] , 565, 578, 590 [‡] [nm] ϵ_{\max} : 32 [†] [$10^{-3}\text{dm}^{-3}\text{mol}^{-1}\text{cm}^{-1}$] |
| Yellow | 422/424 | 428 | λ_{\max} : 432 [‡] [nm] |
| Blue – D | 608/610 | 604 | λ_{\max} : 595 [†] , 615 [‡] [nm] |
| Phot CI-P | 580 | --- | |
| Phot P | 582/585 | 584 | |
| Phot CI-N | 600 | --- | |
| Phot N | 600, 602 | 596 | λ_{\max} : 592 [nm] ϵ_{\max} : 31 [†] [$10^{-3}\text{dm}^{-3}\text{mol}^{-1}\text{cm}^{-1}$] |
| Red + Yellow | 572 | 564 | |
| R + Y + B | 578 | 572 | |
| Transitions** | --- | --- | λ_{\max} : 492, 616 [nm] |
| * Absorption peak spread for fabricated samples | | | † In toluene |
| ** “Transitions” plastic photochromic lenses | | | ‡ In ethanol |

for 10 minutes, with the interval of 2 seconds between measurement points (Figure 3.5).

Table 3.8 presents calculated approximate values of time quasi-constant (τ), that were calculated from data from Figure 3.5.

Table 3.8 Calculated values of time constant – first approximation

| Photochrome & Sample Abbr. | P PL #31 | Y PL #20 | CI-P N #8 | Red N #9 |
|----------------------------|----------|----------|-----------|----------|
| Time Constant τ [s] | 78 | 120 | 126 | 174 |

Because the discoloration process is not a simple exponential function of time, time constants depend on the initial conditions in addition to the ambient temperature of the sample and light conditions.

Thin film thickness estimation

Amorphous polymers are usually very highly transparent in visible light. Typical examples of this group of materials are poly(methyl methacrylate), poly(carbonate), poly(vinyl

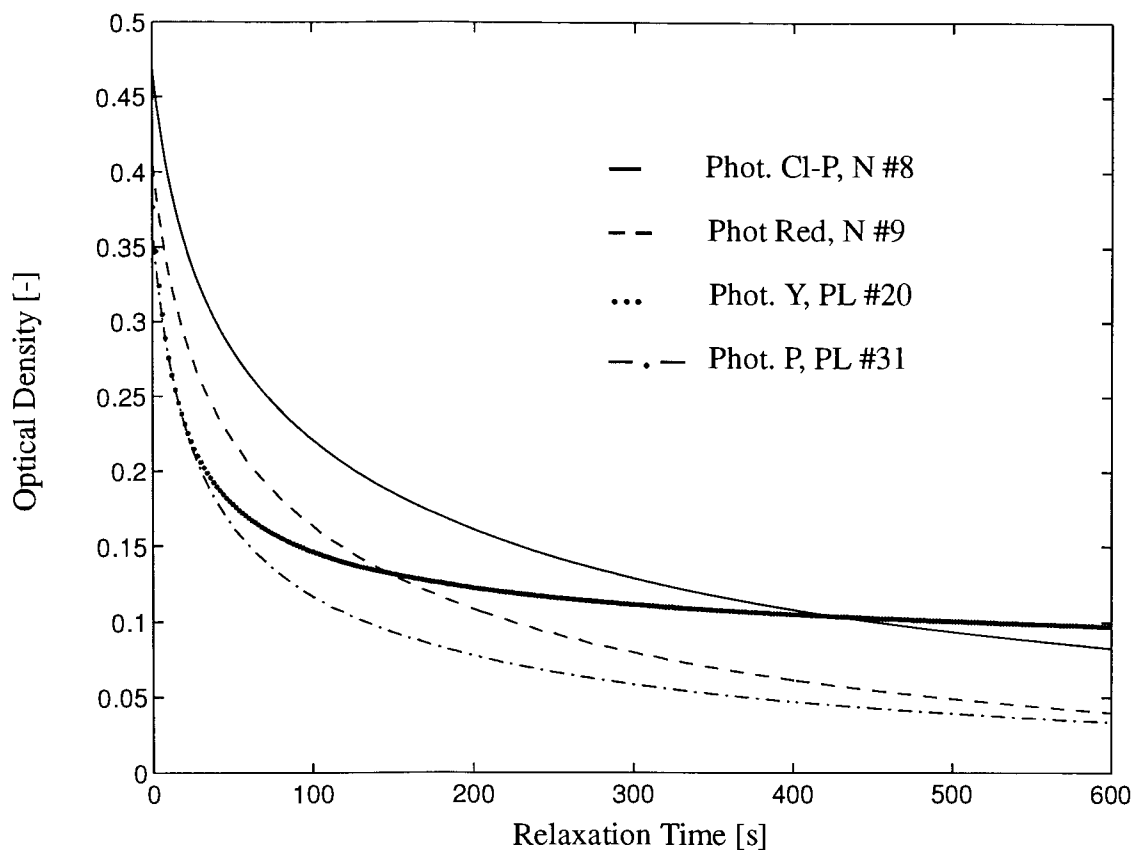


Figure 3.5 Kinetic properties – thermal decay of the colored forms of samples

alcohol). These materials transmit visible light almost perfectly: up to 92% transmittance is possible.

A light beam entering a piece of transparent material from the vacuum is reflected and refracted at the surface (Figure 3.7). The index of refraction (n_λ), is defined in Equation 3.2:

$$n_\lambda = \frac{\sin(\alpha)}{\sin(\beta)} \quad (\text{Eq. 3.2})$$

Where: α – the angle of incidence and β – the angle of refraction.

Reflection and interference of the light adds an additional periodic component to an external transmittance of the filter. This can be seen in Figure 3.6. The graph shows spectral characteristic data for a bare substrate and a system of substrate and polymeric thin

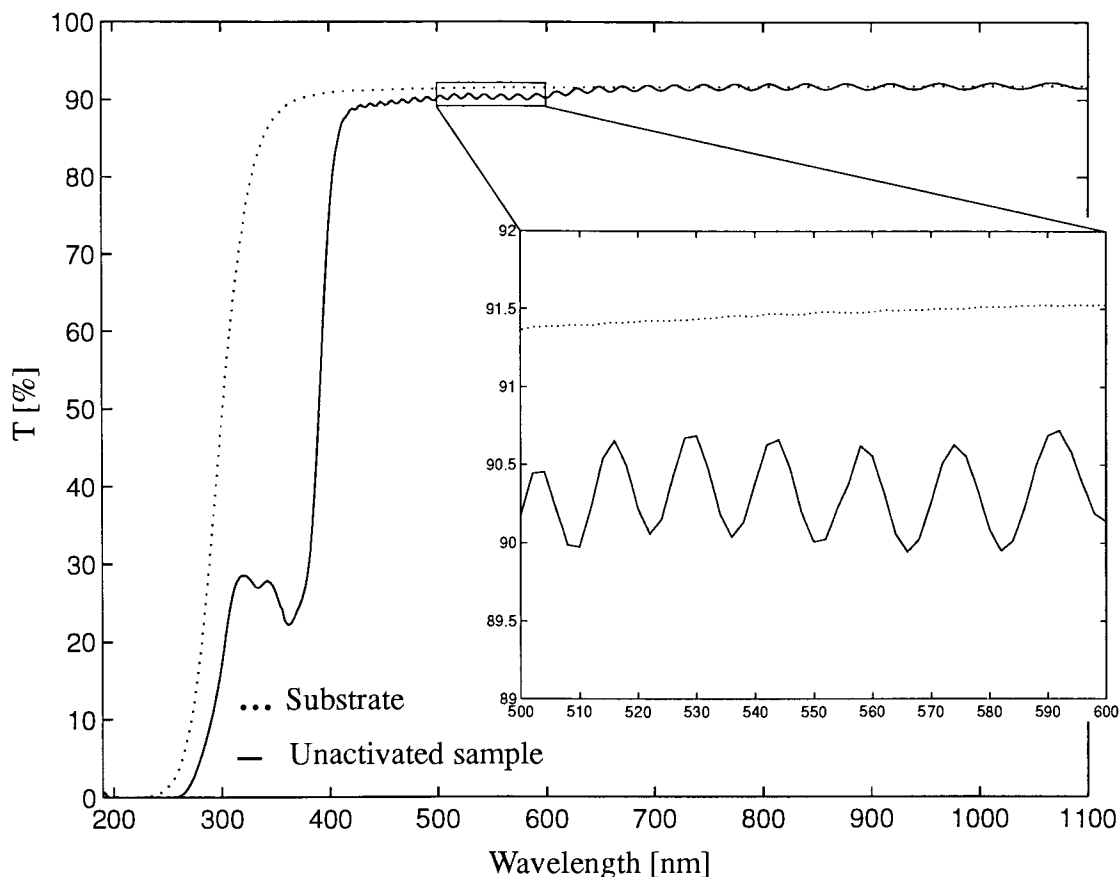
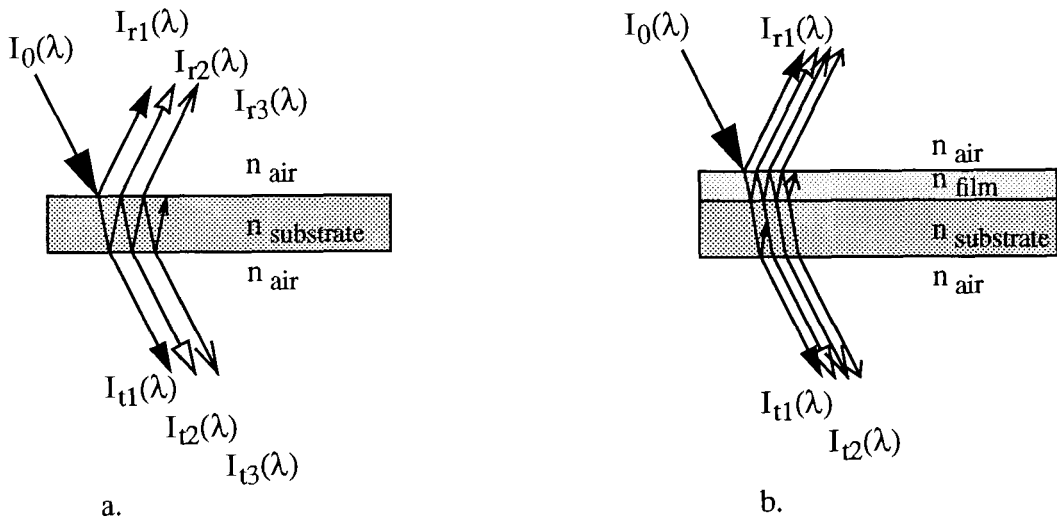


Figure 3.6 Spectral transmittance for bare glass plate and a plate coated with thin film: Red photochrome in B-725 matrix, N #9

film obtained using single beam, DU-600 Beckman spectrometer.

The superimposed sinusoidal component of the signal is a result of a difference of the optical paths between the beam that propagates through the layers and beam that is reflected on the polymer-substrate and polymer-air interface. Figure 3.7 gives a schematic representation of the reflected and transmitted intensities resulting from an incident beam of intensity I_0 , falling a. on a thick plate and b. on the sample consisting of the thick plate and additional thin layer on the top of it. In case b. not all the reflections from the substrate-air interface are shown to make this picture more clear. The weight of the arrow indicates a decrease in the magnitude of the light intensity for higher order reflections.

If the two waves are coherent, when they combine interference occurs. When two waves are 180° out of phase destructive interference occurs – that corresponds to local minima on the graph. Because the refractive index of the polymer is less than those of the



Not to scale

Figure 3.7 Reflectance and transmittance of a. a thick substrate, and b. system of the substrate and a thin layer

glass substrate, light reflected at polymer-substrate surface is retarded at 180° – or $\lambda/2$ (Figure 3.8).

By combining the proper Fresnel equation we get the expression for the reflectance:

$$r = \frac{I_r}{I_0} = \frac{\sin^2(\alpha - \beta)}{2 \cdot \sin^2(\alpha + \beta)} + \frac{\tan^2(\alpha - \beta)}{2 \cdot \tan^2(\alpha + \beta)} \tag{Eq. 3.3}$$

Where:

r – reflectance

I_0 – incident light intensity

I_r – reflected light intensity

α – the angle of incidence and β – the angle of refraction.

At normal incidence where $\alpha = \beta = 0$, the reflection at the interface is given by:

$$r = \frac{I_r}{I_0} = \left(\frac{n_2 - n_1}{n_2 + n_1} \right)^2 \tag{Eq. 3.4}$$

Where:

r – reflectance

n_i – index of refraction

For the infinite numbers of reflections of monochromatic light a system of equations can be derived (Equation 3.5). This calculation assumes that the thin layer is not an absorbing material.

$$\begin{cases} I_r = I_0 r + I_0 (1-r)^2 r + I_0 (1-r)^2 r^3 + \dots \\ I_t = I_0 (1-r)^2 + I_0 (1-r)^2 r^2 + I_0 (1-r)^2 r^4 + \dots \end{cases} \quad \text{(Eq. 3.5)}$$

Where:

I_0 – incident light intensity

I_r – reflected light intensity

I_t – transmitted light intensity

r – reflectance

By taking into consideration limited sensitivity of the instrument used for measurements we can restrict calculations to two terms of the series. Using that approximation we can now calculate special cases of destructive and constructive interference. Average trans-

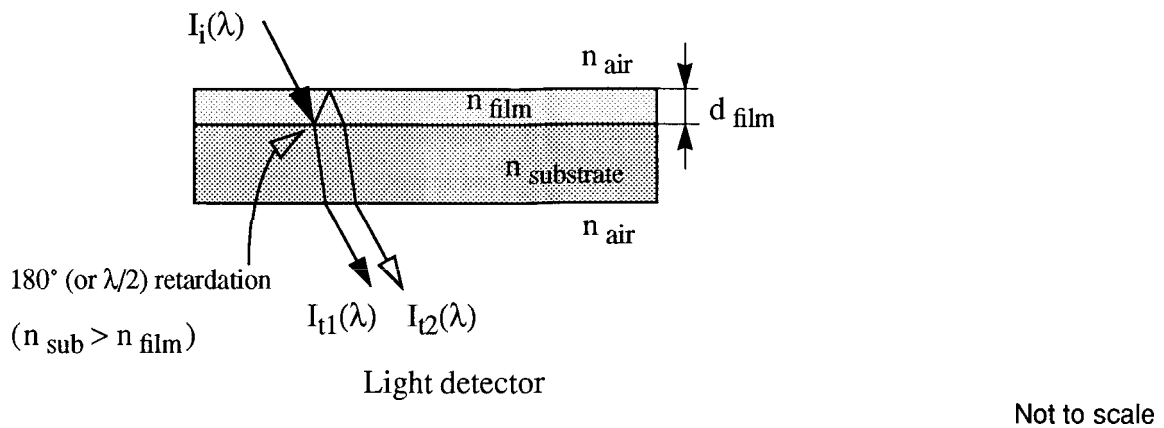


Figure 3.8 Interference phenomena in a thin film

mittance of the system shown in Figure 3.8 can be simplified by the following expressions:

$$\left\{ \begin{array}{l} T = \frac{I_{transmitted}}{I_{incident}} \\ T = \frac{I_0(1-r)^2 + I_0(1-r)^2r^2}{I_0} = (1-r)^2 + (1-r)^2r^2 \end{array} \right. \quad (\text{Eq. 3.6})$$

On top of that we have to include periodic modulation due to before-mentioned interference phenomenon. Altogether there is a total difference of $2n_{film}d + \lambda/2$ in optical path length between the two interfering coherent light beams. If the phases of $I_{t1}(\lambda)$ and $I_{t2}(\lambda)$ differ by 180° destructive interference occurs, the following conditions must be fulfilled:

$$n_\lambda \cdot d = \frac{m \cdot \lambda}{2} \quad (\text{Eq. 3.7})$$

Where:

$$m - \text{integer (} m = 0, 1, 2, \dots \text{)}$$

Using Abbe Refractometer – Model 2WA, we measured the refractive index for different coatings, the value of which are summarized in Table 3.5. From Figure 3.9 we found values of λ_{min} for several subsequent minima. It is important, that those minima are as close to wavelength $\lambda_D = 589.3$ nm as possible. The refractive indexes are measured for this specific sodium spectral line wavelength and commonly marked as n_D (Crawford, 1968).

The refractive index depends on the wavelength. The overall change of the refractive index across the several interference minima (e.g. 50 nm), is below the measurement error, therefore we did not include this change in Equation 3.7.

Next we calculated reciprocal value of wavelength ($1/\lambda$), and we plotted previously chosen points on the x-y plain, where x axis corresponds to integer m, and y corresponds to value of $1/\lambda$ [nm^{-1}]. By testing different sets of m value we eventually got a set of points that together with axis origin (0,0) form a line. This constitutes a graphical solution of the problem. Now we can find the wavelength value corresponding to the minimum and related value for m. Substituting for λ and m into Equation 3.5 yields the thickness of the film.

This method utilized a side results of measurement of spectral absorption of the film and gave very accurate results, with the maximum measurement error less than ± 0.05 μm . The results were then compared to those obtained with profilometer (Dektak IIA Surface

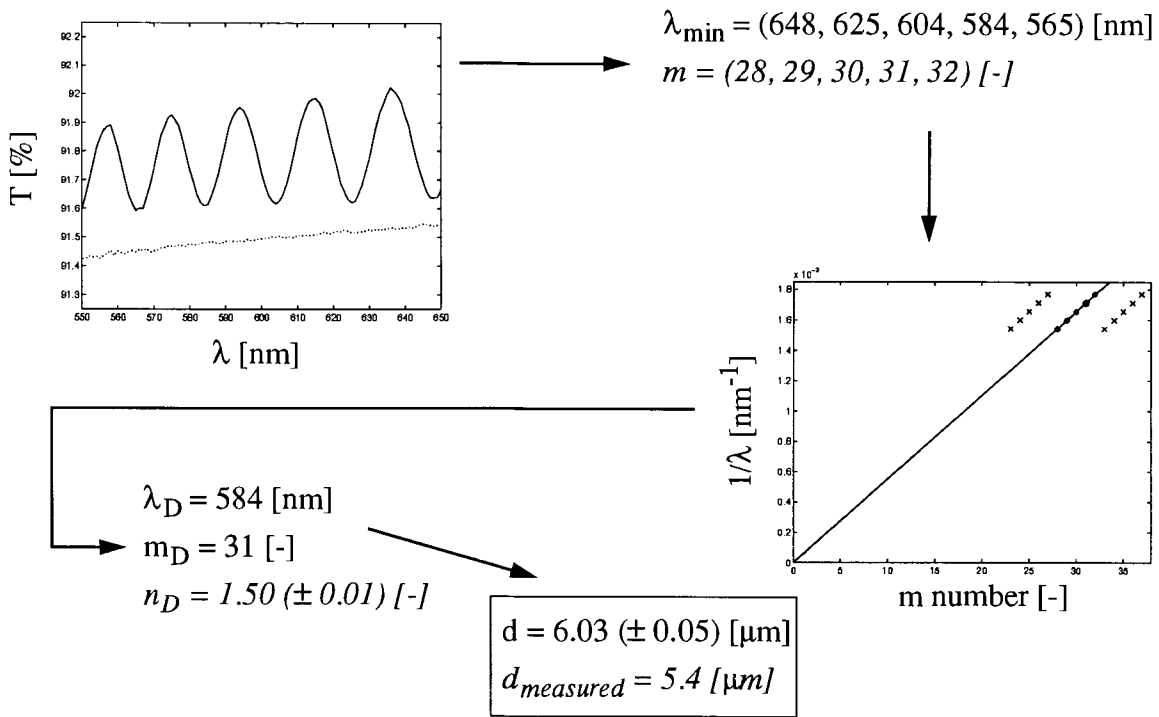


Figure 3.9 Graphical method of estimating thin film thickness:
Yellow photochrome in B-725 matrix, PL #20

Profile Measuring System – by Precision Research Instruments, Inc.). By comparing the calculated thickness with the one measured with the profilometer, we found the offset of the profilometer used for the measurements: $\Delta d = -1.0 \mu\text{m}$.

The difference between these two methods of measurements is that our method is non-destructive for the samples prepared using spin-coating technique. The data comes together with data of absorption spectra, so no extra measurement steps are necessary. This method is very resistant to a noise. Even for a very small amplitude of the sinusoid exact thickness of the film can be calculated.

And by analyzing positions, regularity and values of the minima we can also estimate other parameters of the surface, such as roughness and external transmittance. Combining absorption spectra with thickness of the thin film, we can roughly predict the refractive index.

Photochromic Filter – Implementation

Developing of the test bench

Utilizing standard video camera and frame-grabber attached to the Sun work-station we developed a system for testing parameters of the photochromic filters and for checking the PAF influence on the quality of the image.

Our standard test bench is shown in Figure 3.10. It is used to test local adaptation

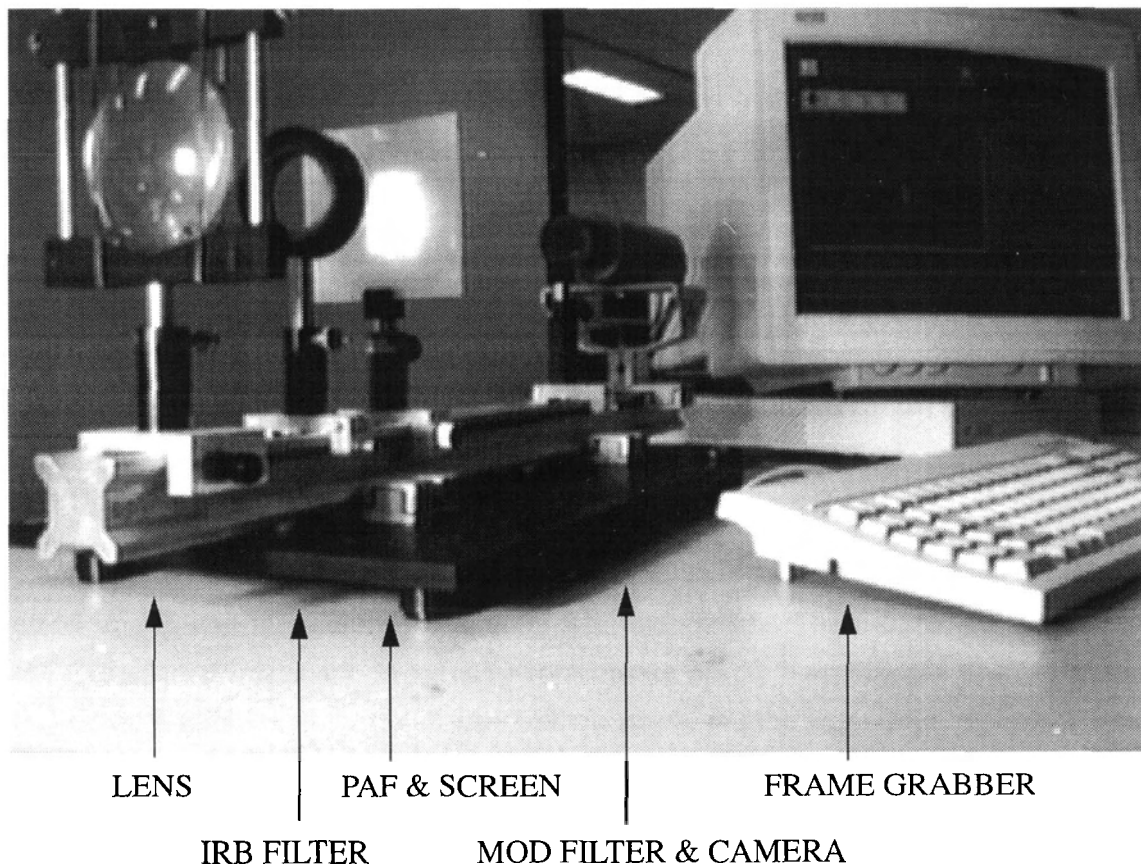


Figure 3.10 Experimental set-up for testing photochromic filter (for clarity, housing has been removed; spectral properties presented in: T. 3.6 & F. 3.12)

mode of the filter. Modification of this set-up is used to determine properties of the photochromic filter, such as the transformation function.

Figure 3.11 shows a schematic drawing of the same test bench. Image is focused through

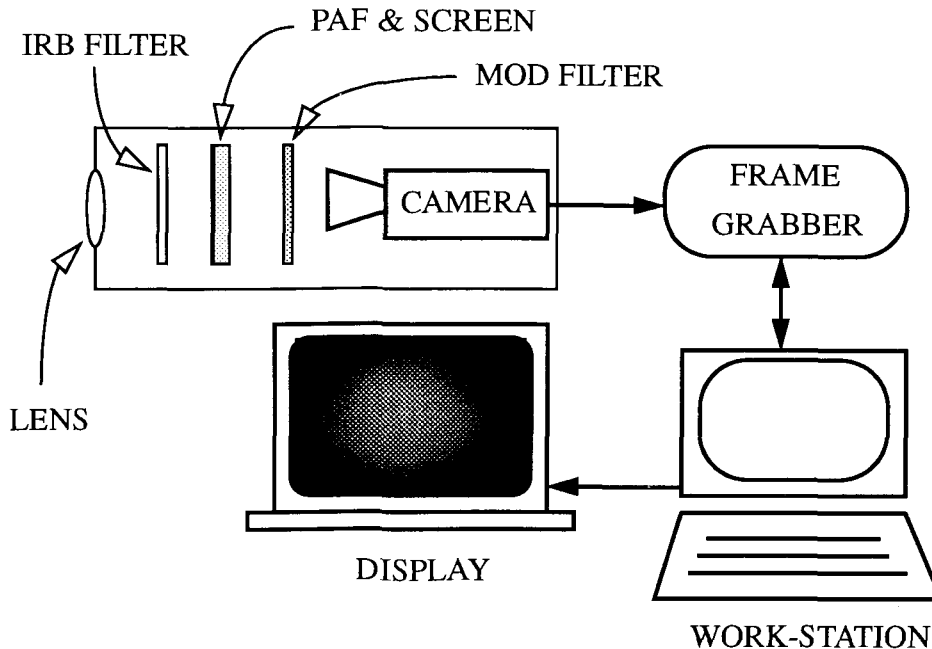


Figure 3.11 Block diagram of the experimental set-up for testing local adaptation

a positive quartz or fused silica lens on a thin photochromic filter placed on the glass substrate, with the translucent screen on the other side. This screen is used to view the processed image, and the picture is recorded with the camera. The translucent screen was used to focus the image and to partially compensate for the light lost due to a big difference in the f-numbers of the small lens in the camera and the large-diameter quartz lens. Any high spatial resolution B/W camera with known relation between light intensity and output voltage (linear function being most common) can be used. We use the 8 bit, 1810 series COHU camera.

In some experiments Infra-Red Blocking filter (IRB) is used to restrict heating of the filter that reverts coloration. For that application we use Oriel IR Blocking colored glass filter #59050.

For each prepared photochromic filter specific interference filter or color glass filter is used as a Modification Filter (MOD) to restrict analyzed spectrum to the region of sensitivity of the photochromic filter (see Figure 3.12 and Table 3.5). We use a broad-band fil-

ter with the peak of the transmittance close to the sensitivity maximum of the human eye in photopic vision $V_\lambda = 550$ nm. The filter we use had maximum transmittance peak at $\lambda_{\max} = 536$ nm.

Figure 3.12 shows spectral characteristic of those modification filters that were used

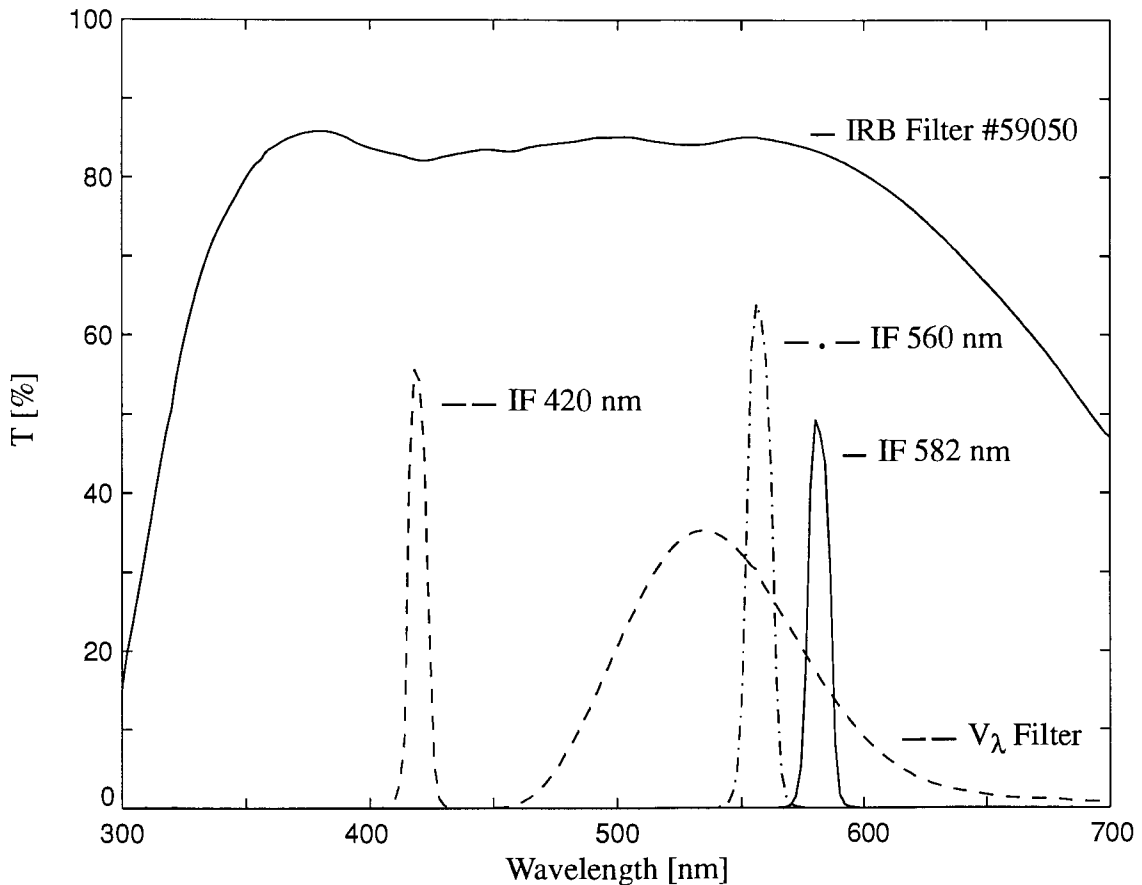


Figure 3.12 Transmittance of Modification and IRB Filters

in experiments presented in the next part of this thesis. Characteristic of the infra-red blocking filter in the visible part of the spectrum is also included. Cut-off wavelengths for the lenses used in the experiments were 180 nm.

In experiments testing global mode of adaptation of the filter a simpler version of the test bench is used shown in Figure 3.13. In this case we use a photochromic filter deposit-

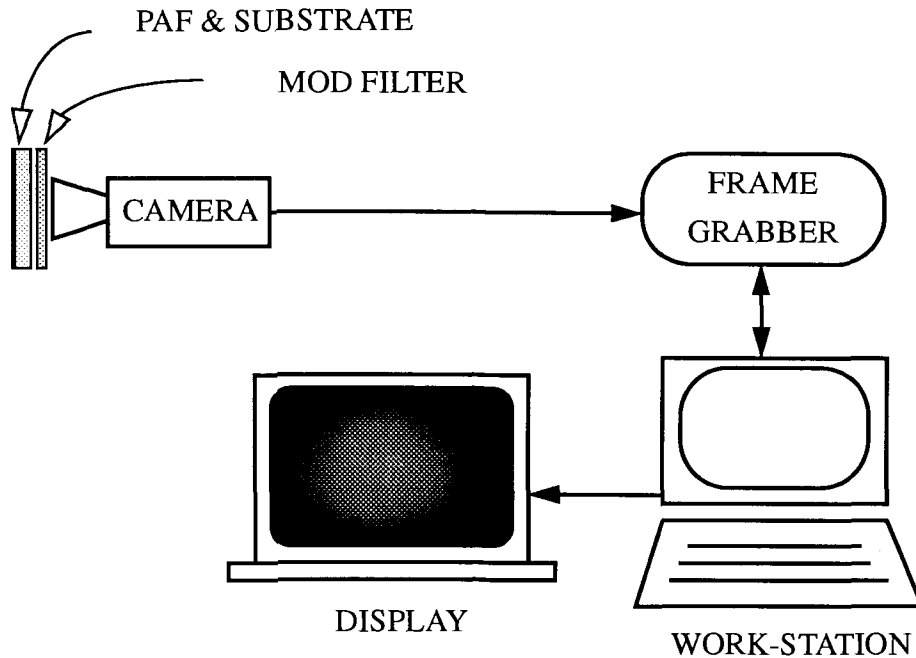


Figure 3.13 Block diagram of the experimental set-up for testing global adaptation

ed on the glass substrate.

Experimentation

In order to investigate local changes in the transmittance of Photochromic Adaptive Filter (PAF) due to radiant intensity from sample images, we used constructed test stand (Figure 3.10). The pictures of the image focused on a translucent screen just behind the PAF were taken with a “COHU” RGB, 8 bit, CCD camera. In the experiments a high pressure mercury arc (100W & 200W) lamps, a halogen (300W & 500W) lamps and Sun-like (300W) lamp were used. The light intensity of the halogen lamp was controlled using autotransformer.

Figure 3.14 shows in a simplified way the particular steps made during experiments. Initial images that have dynamic range beyond that of photodetector devices are shaped by the adaptive filter.

In some experiments we added one additional step – image normalization. We did it by increasing the diaphragm of the camera, thus allowing more light to pass through the optical system and be detected by the photosensitive array.

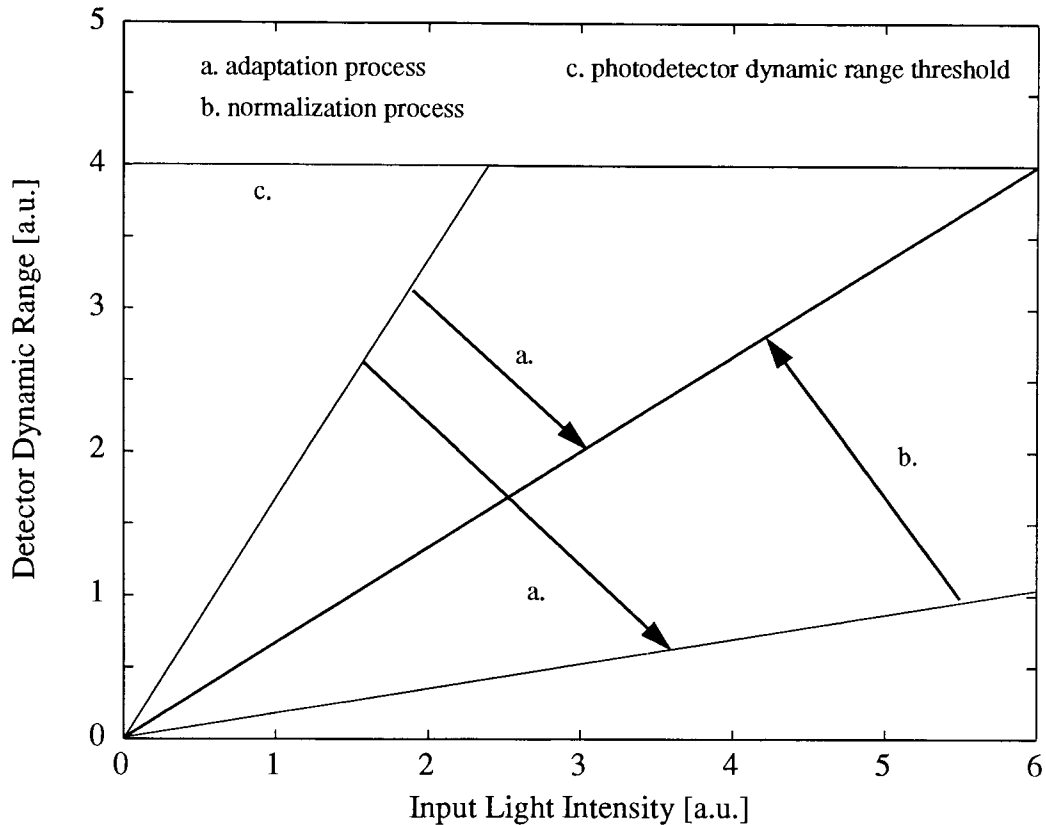


Figure 3.14 Experimentally observed image transformation types

Typical image quality improvements*

Using developed test bench we performed several types of experiments to determine some important properties of the developed filters. For each tested photochromic filter a specific modification filter was used to restrict analyzed spectrum to the region of sensitivity of the photochromic filter.

First, we tested the photochromic filter applied in the global mode of adaptation. We took a picture of a relatively dark object – vehicle licence plate, against very bright background, in this case high pressure mercury lamp (left center part in the picture, Figures 3.15 & 3.16). After filter adaptation took place, more details of the image are visible, blooming (defined as a localized charge overflow) around the light source is reduced and

* In the following pages we present pictures in the gray-scale format. Color version of the original pictures can be found at: <http://fas.sfu.ca/ensc/people/GradStudents/tomasz/personal/tomasz.html>, or at: <http://fas.sfu.ca/ensc/people/Alumni/tomasz/personal/tomasz.html>.



a.



b.

Figure 3.15 Image quality improvement a. before and b. after global adaptation: Yellow photochrome in B-725 matrix, PL #20; MOD – 420 nm



a.



b.

Figure 3.16 Image quality improvement a. before and b. after global adaptation: Red photochrome in B-725 matrix, N #9; MOD – 560 nm

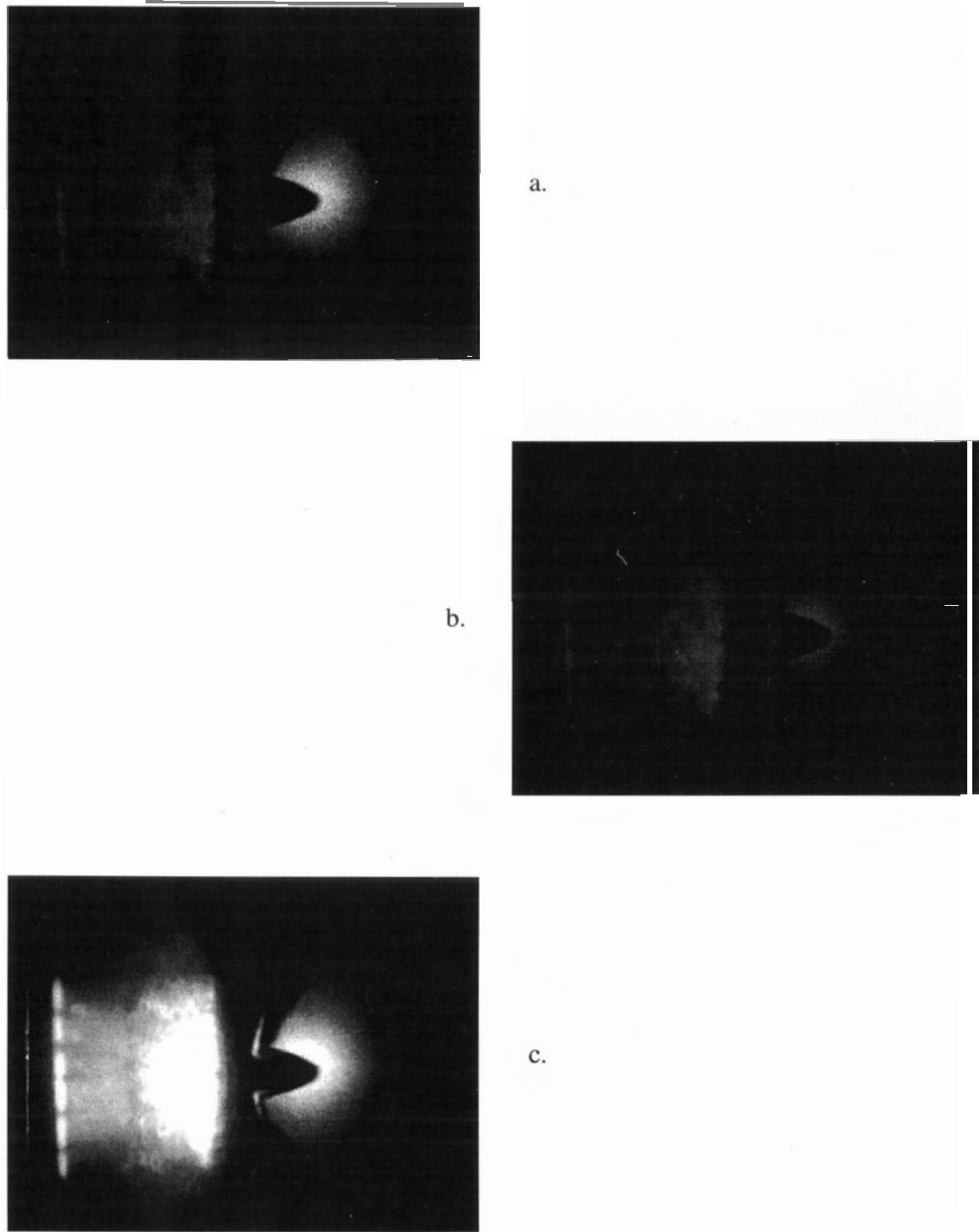


Figure 3.17 Picture taken a. before adaptation, b. after adaptation and c. after normalization: Red photochrome in B-725 matrix, NN #7; MOD – 560

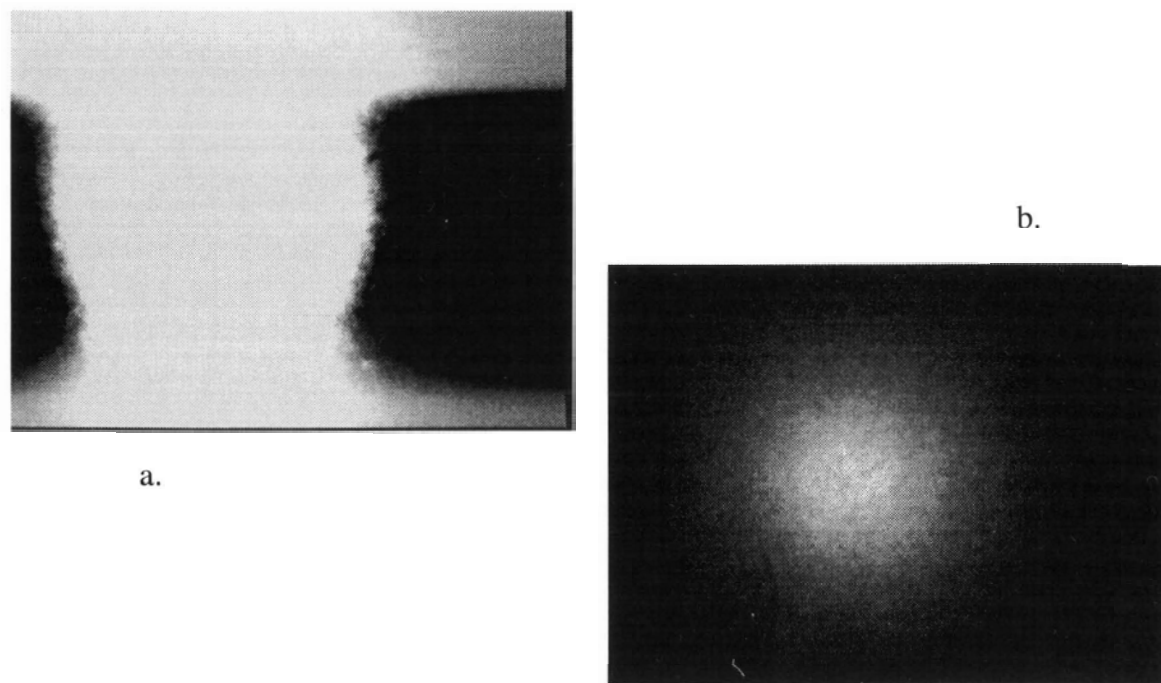


Figure 3.18 Image quality improvement a. before and b. after local adaptation: Yellow photochrome in B-725 matrix, NN #6; MOD – 420 nm

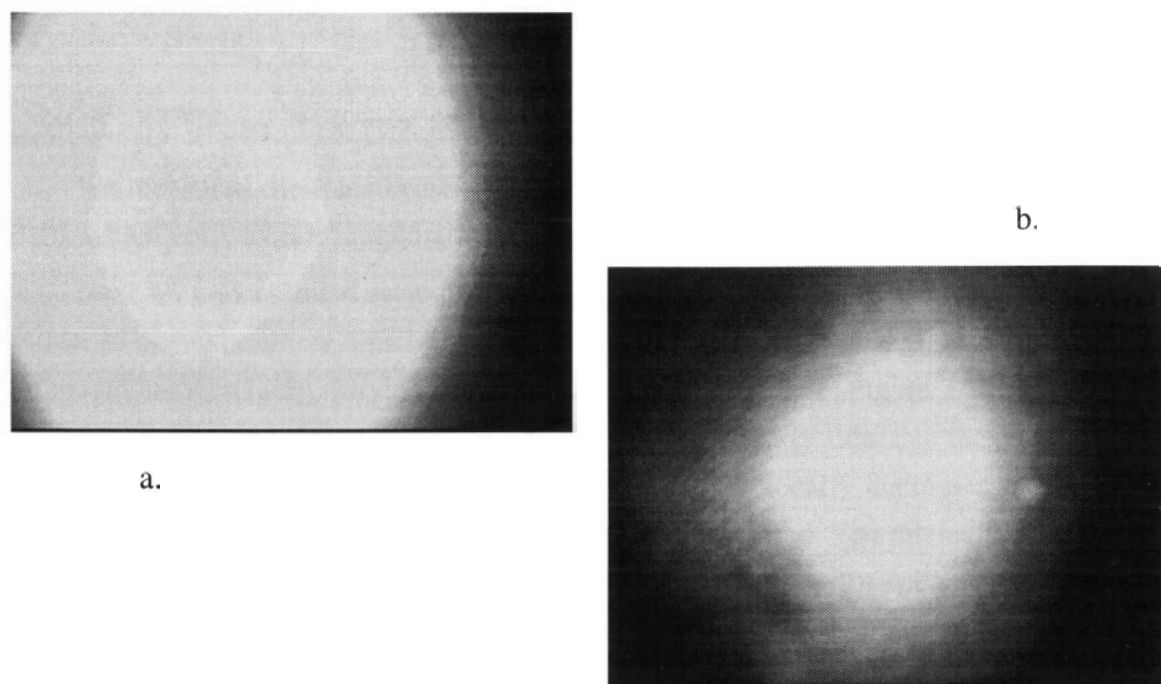


Figure 3.19 Image quality improvement a. before and b. after local adaptation: CI-P & P photochromes in B-725 matrix, NN #4; MOD – 582 nm

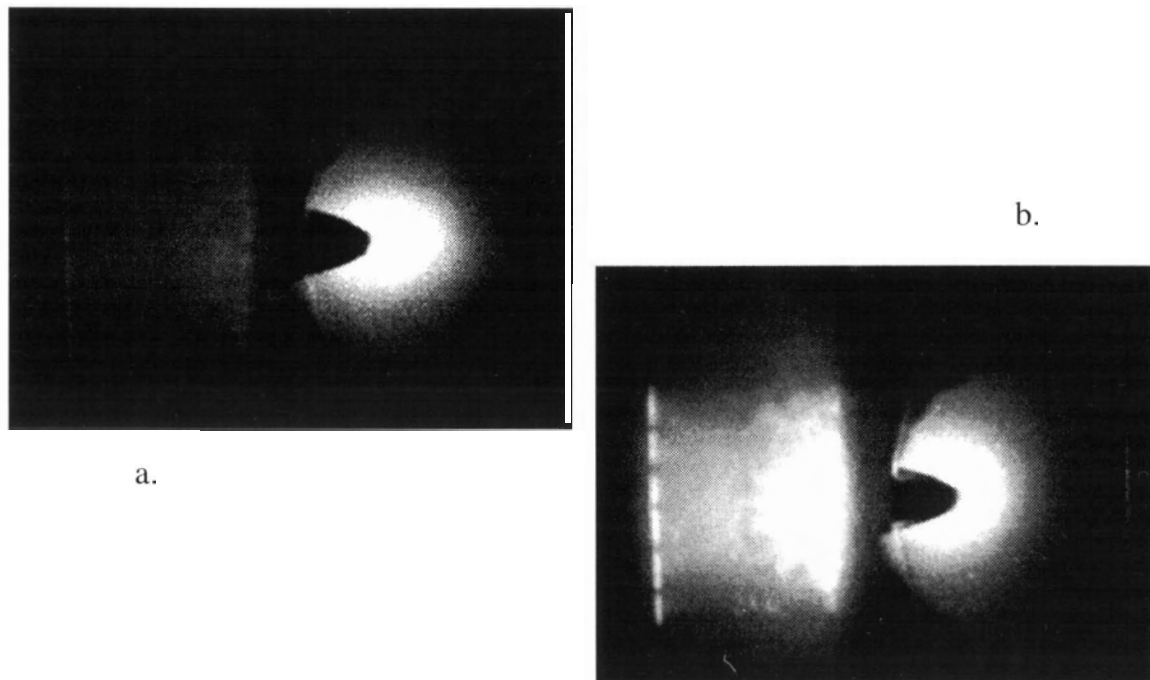


Figure 3.20 Image quality improvement a. before and b. after local adaptation: Yellow photochrome in B-725 matrix, NN #3; MOD – 420 nm

contrast ratio of part of the picture is increased as well.

We measured the transformation function of the photochromic filter used in Figure 3.16, which corresponds to theoretical curve of TF used in “Model 1” of Part II*.

Next we concentrated on experiments testing photochromic filter in local adaptation mode. In one experiment a picture was taken of two different light sources – mercury arc lamp and halogen lamp, varying in light intensity over 1 decade (Figure 3.17 & 3.20). The image of more intense mercury arc lamp (on the right), nearly saturates the camera. With time, focused image of the high intensity mercury lamp locally decreases the transmittance of the filter, due to the UV radiation emitted by this lamp. The intensity of the image of the second lamp stays at the same level, as this lamp’s image does not cause any changes to the filter. Figure 3.17b shows the picture taken after a few seconds. Both lamps have their brightness nearly at the same level as light from the mercury lamp is filtered out. At that point we opened the diaphragm of the camera wider and took one more picture. This

* Next section of the thesis describe the methodology of this measurements.

procedure corresponds to the image normalization, shown in Figure 3.14, to match the image with the operating range of the camera.

By comparing Figures 3.17a & 3.17c, and Figures 3.20a & 3.20b, we concluded that image was transformed by PAF in such a way, that only part of the spatial distribution of image light intensity was compressed – we can say that local adaptation of the PAF occurs. As a result this local adaptation process allowed us to get picture that contains more visible details of the other part of the image*. In the same time no part of the picture is over-saturated, thus negative effects like blooming are suppressed.

In another test we took a picture of a supersaturated image of the mercury lamp (Figures 3.18a & 3.19a). In the picture taken with the fully translucent filter many image defects are easily noticeable. We can observe blooming (charge spill) due to excess charge of electrons in the lamp image. However once filter adaptation took place, the image quality radically improved (Figures 3.18b & 3.19b). Blooming is largely reduced and interesting details appear that were not visible before.

In summary, experiments have shown that application of the photochromic filter in image acquisition improves the quality of the image and extends the dynamic range of the visual system.

Determination of the Transformation Function of PAF

We developed a simple, fast and accurate procedure for measuring a Transformation Function (TF) of a Photochromic Adaptive Filter (PAF). Photochromic filters, whose spectral transmittance depends on previous and immediate radiant exposure and other environmental conditions, require special methods of spectrophotometry to determine their properties.

This section (see also Wysokinski et al., 1996a) describes easy to implement method of characterizing the luminous transmittance as a function of light intensity. Transformation functions of sample filters for different sources of radiation and varied light intensity are evaluated. The measuring system can also be used for fast determination of spatially and spectrally uniform light sources with a UV spectral component.

* For results of the initial tests performed with commercially available photochromic lenses see (Wysokinski et al., 1995b).

Introduction

Photochromic systems reversibly change their light transmission in proportion to incident illumination (Brown, 1971). Because transmittance of photochromic materials changes rapidly with changing light conditions, and depends on many other environmental factors, it is difficult to accurately determine the optical characteristics of such systems using conventional methods (Ross et al., 1991). This implies the need for different, reliable methods of measurements, which determine properties of potential devices into new areas of applications – like photonics, example being development of all optical computers (Birge, 1995).

In this section of the thesis we describe a method for evaluating the transmittance and the transformation function (input/output relationship) of a photochromic system. Modification of the measuring techniques allows to evaluate a transmittance for a specific range of wavelength.

Experimental

Instruments

Transformation Function is determined by analyzing the lamp image. Figure 3.10 shows a typical set-up used for measurement of the shape of the transformation function. The method requires a small (point like) light source stable in the time domain with a UV component in the emission spectrum. A short arc mercury lamp (HBO 200W) and a Sun-like lamp (300W) were used as light source. The image of the lamp was focused on a screen through a quartz or fused silica lens and a picture was recorded with a camera. Any high spatial resolution B/W camera with known relation between light intensity and output voltage (linear function being most common) can be used.

An Infra Red Blocking (IRB) filter was used to restrict heating of the photochromic filter and to minimize fading. Interference filters, or color glass filters were used as Modification filters (MOD). Interference filters were used to limit response of the PAF to a specific narrow range of wavelength. Color glass filters were used to weight light intensity spectrum accordingly to the sensitivity of human eye adapted to daylight (V_λ curve) or night vision.

Fabrication

PAF filters were prepared by spin-coating of a glass substrate with a solution of Butyl Methyl Methacrylate Copolymer, containing photochromic substances*. The glass substrate (110x110x2.3 mm) was earlier sand-blasted on one side to create a translucent screen. Desired thickness of the photochromic filter (~20 μm) was obtained by varying concentration of the copolymer and conditions of the spinning process. Specific percentage of different photochromes are added to achieve custom transmittance through visible region.

Transformation Function

The Transformation Function, also called Transfer Function describes an image transformation. The photochromic filter acts as an operator on input image. PAF may be used as a globally adapting filter with space uniform transmittance – as in ophthalmic lenses. They can also be applied as locally adaptive filters used as optical memory, or for image processing (Pham et al., 1995).

How a given type of TF can control image transformation is described in Part II of the thesis and was published (Wysokinski et al., 1995a). Both linear and non-linear cases of TF were treated and a modification of the original image by the filter is presented.

Figure 3.21 shows the cross-section of a 3-D visualization of the lamp image. Cropped part of the section was used to calculate the Transformation Function. One curve shows section of the image in the faded state. Another curve was taken from the lamp image after exposing the filter for 30 seconds to a 200W mercury lamp. Due to an adaptation of the filter the distribution of light intensity had changed and was lower as compared to an image obtained with non-adapted filter.

Results and Discussion

We calculated the transfer function based on the data from Figure 3.21. In the cropped part there are 160 measurement points. The transformation function which relates the input and output light flux is plotted in Figure 3.22. For the average (0.1-1.9 mW/mm^2) light intensities ratio this function is linear what corresponds to direct proportion between num-

* See section: “*Development of a Photochromic Adaptive Filter (PAF)*” and article (Wysokinski et al., 1996b).

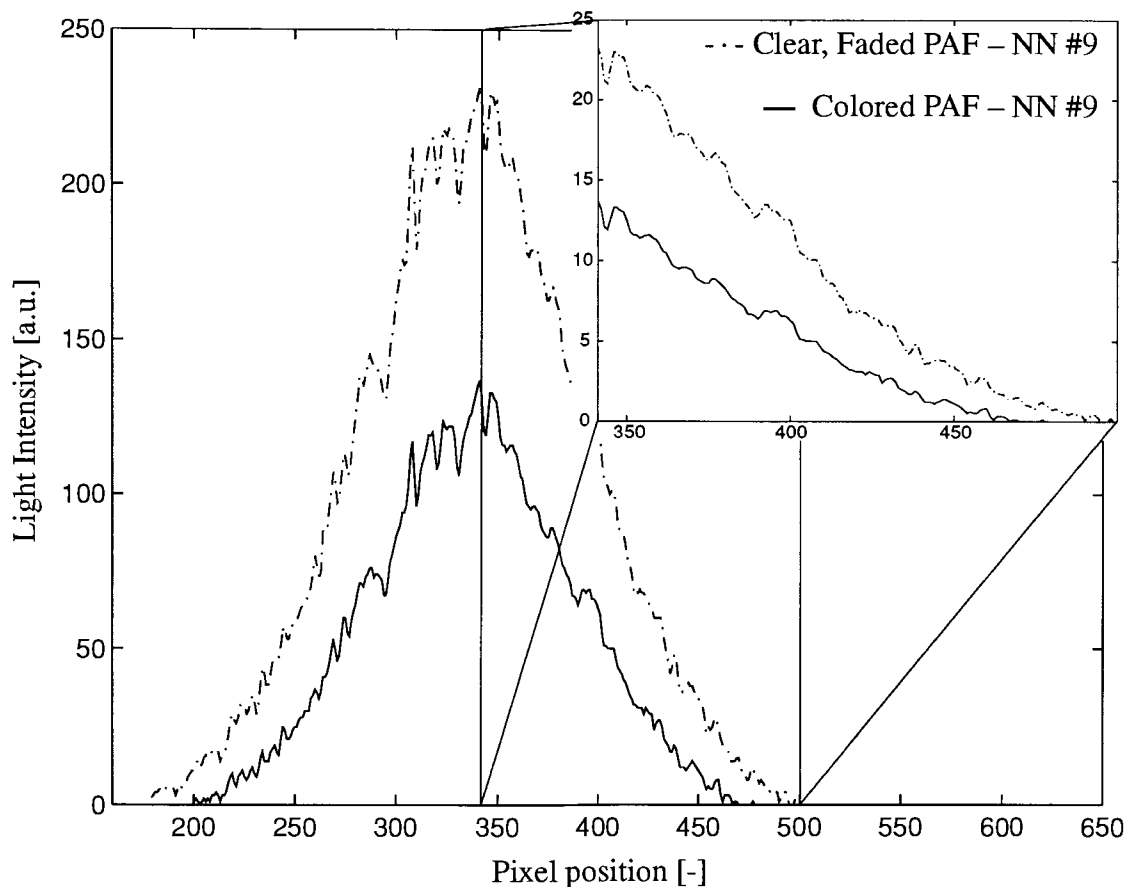


Figure 3.21 Cross section of the image of the light source

ber of activated molecules and amount of light. The transformation function does not start from the axis origin, due to optical losses and threshold characteristic of the CCD camera.

For high light intensity we noticed a small deviation of TF from linearity as a result of saturation of the photochromes in the upper energy state which corresponds to depletion of available molecules in the lower state.

Next, we calculated the ratio of the incident input to output light intensities, results are shown in Figure 3.23. We see that as light intensity increases, the coloration of the filter decreases due to increased discoloration process, speeded up by heat.

Next we calculated Optical Density (OD) (see Figure 3.24) of this filter, for given

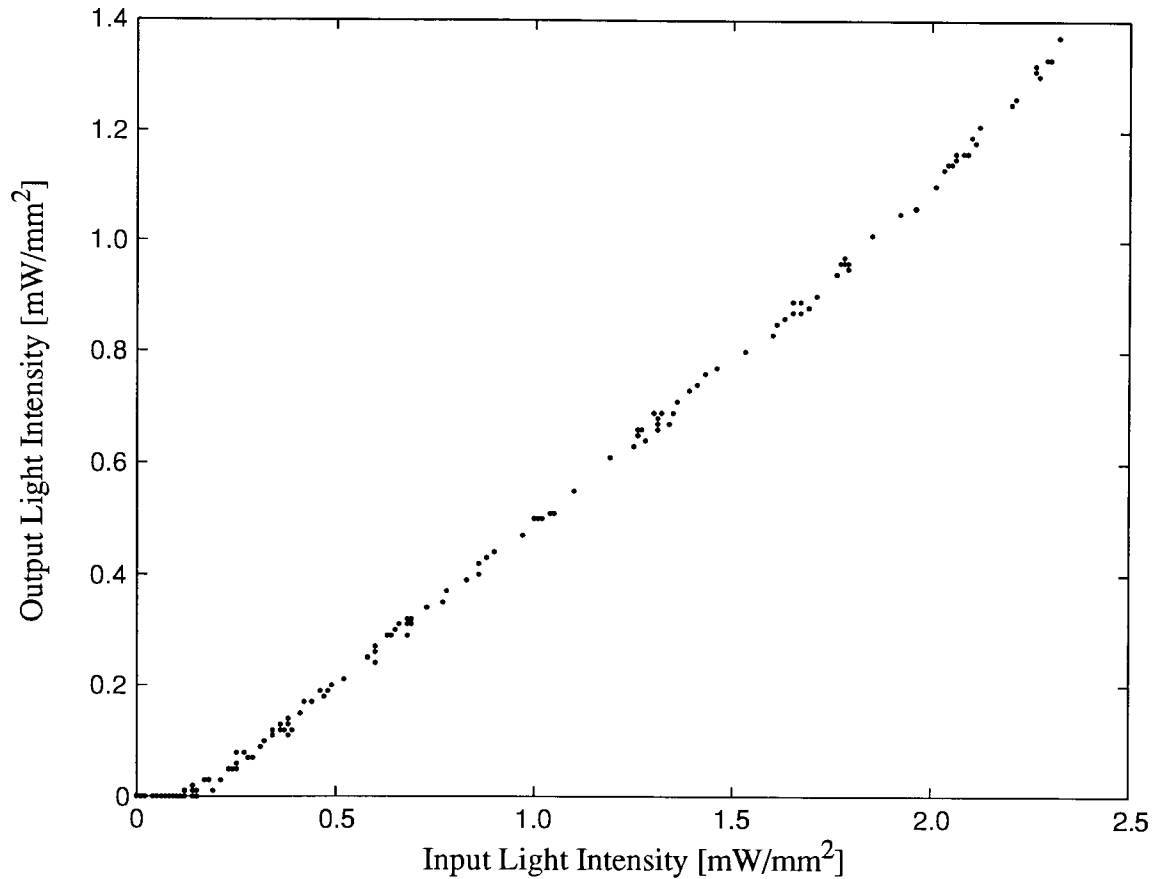


Figure 3.22 Transformation Function of a photochromic filter, calculated from data in inset in Figure 3.21

light intensities:

$$OD = \log_{10} \frac{I_{in}}{I_{out}} \quad [-] \quad (\text{Eq. 3.8})$$

Similarly to I_{in}/I_{out} ratio, Optical Density decreases at high light intensities. We calculated OD for results of other experiments performed. The highest optical response value found, was $\Delta OD=0.8$. In all of the above experiments we used a 200W mercury lamp. The photochromic film was exposed to the whole emission spectrum of the lamp, minus absorption by the quartz lens.

By comparing two series of measurements for the same photochromic system in dif-

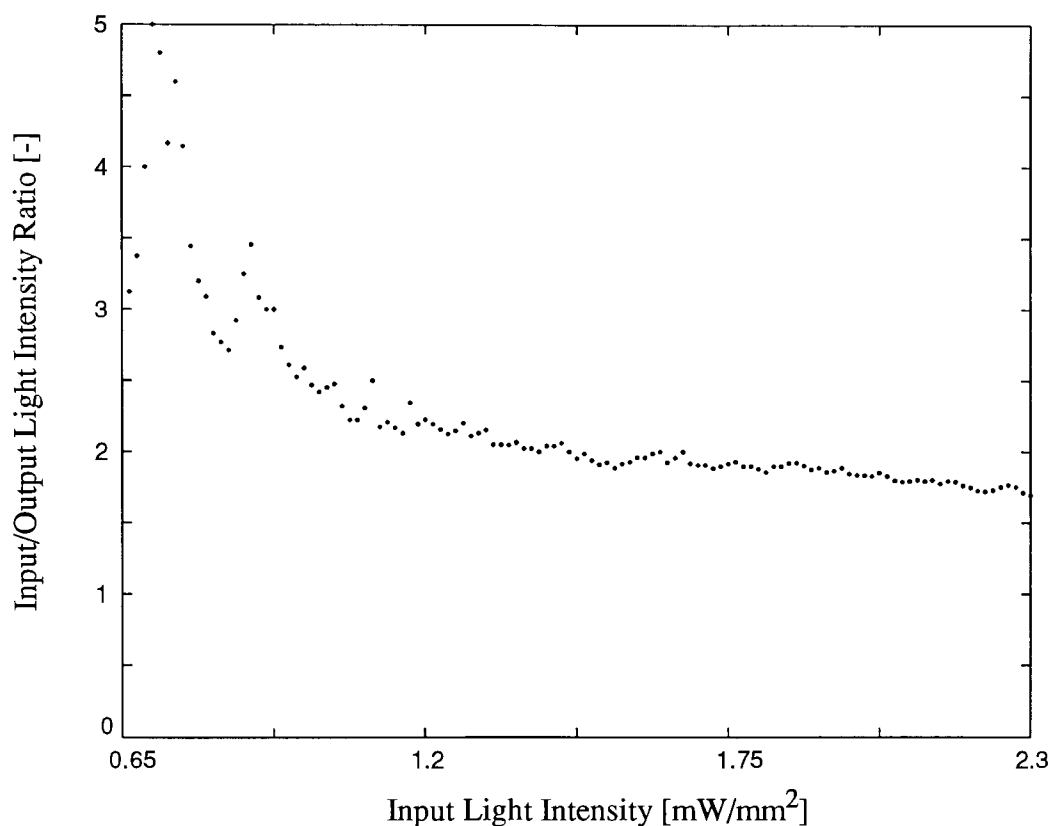


Figure 3.23 Reciprocal transmittance as a function of light intensity, calculated from Figure 3.21

ferent positions, non-uniformities in surface concentration of photochromes can be detected.

By analyzing two transformation functions for two different light sources we can very quickly evaluate spectral and spatial non-uniformities of the light source. For example by comparing shape of curves in Figure 3.25 we see that lamp visualized in sub-figure b. has a very non-uniform component of UV spectrum in the high intensity region.

Summary

In this part of the thesis, research project leading to the development and applications of Photochromic Adaptive Filters has been described. We designed and fabricated a series of

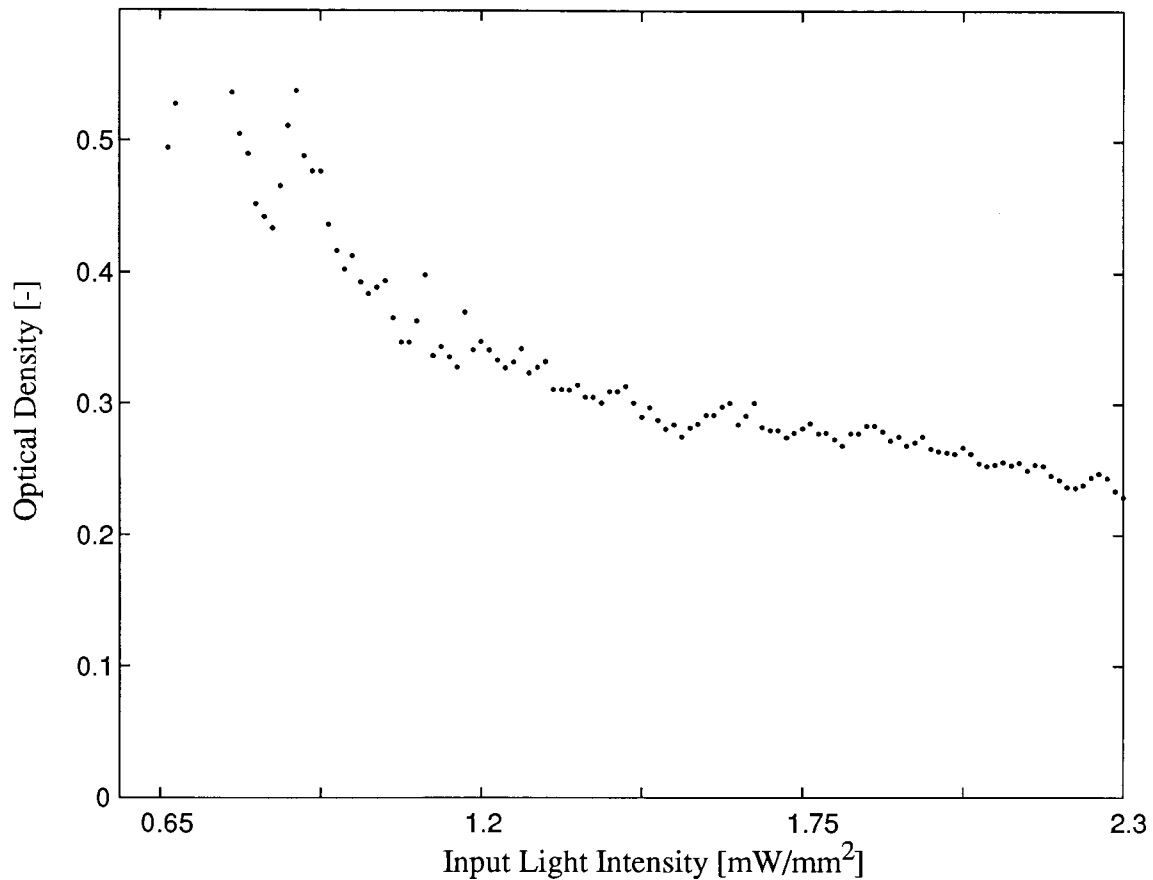


Figure 3.24 Optical Density of the filter as a function of light intensity, calculated from Figure 3.21

thin films made of polymers and photochromic materials. We successfully applied the developed filters in opto-electronic system which unites CCD camera with photochromic filter to create an adaptive camera. This system is capable of operating in wider range of light intensities. By using adaptive filter we extended the dynamic range of operation, and as a result we increased contrast ratio and minimized blooming and flare. We also presented results of experiments to determine the spectral characteristic of the filters.

Photochromic filters are likely to find numerous applications in the newly developed areas of photonics (Wysokinski et al., 1995; Fischou, 1994; Yeh, 1994; McArdle, 1992, Cathey et al., 1992), in which exact determination of the Transformation Function is an essential part of characterization of the response of the system. If photochromic filters are composed of a few elements that have different dynamic and static characteristics, it

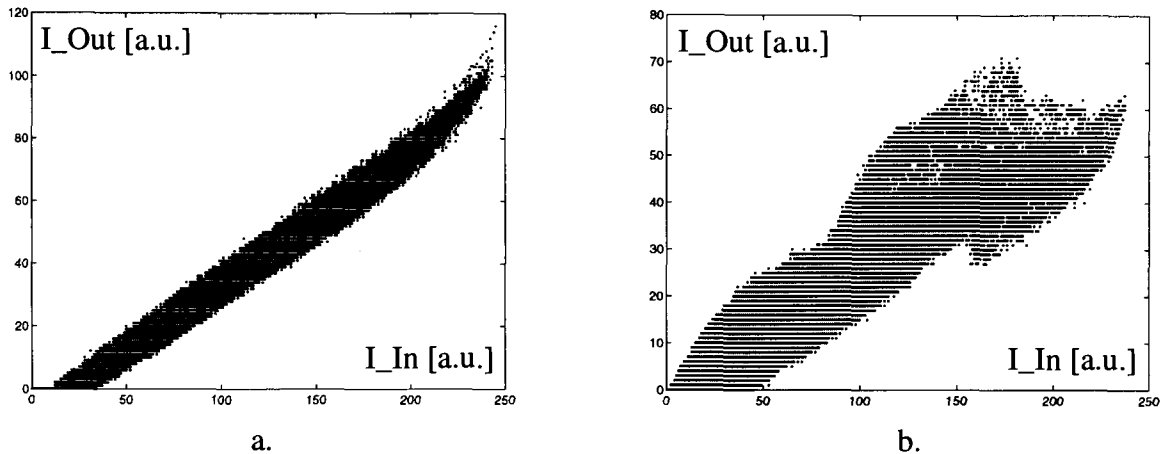


Figure 3.25 Transformation function for a. spectrally and spatially uniform (point-like) and b. non-uniform light sources, NN #2

would be very time consuming to obtain full characteristic of those devices using conventional methods. In the last section we described easy to implement and versatile method for measuring the transformation function of the Photochromic Adaptive Filter (Wysocki et al., 1996a). This function describes the relation between the input and output light intensity of a light beam passing through the filter. The method allows for quick measurements using only two pictures of the light source. Choosing Sun-like illumination and V_{λ} filter one can obtain response to the changing transmission of photochromic filter similar to that of the human eye.

Expansion of this method gave us values of the Optical Density of the photochromic filter as a function of light intensity, in the spectrum range controlled by utilizing Modification filters. This method could also be used to quickly evaluate spatial and spectral light emission uniformity of light sources by using uniform photochromic filter. It is fast, efficient and could be automated for testing photosensitive materials in quality control departments.

Because photochromes do not require external power supply sources for operation, can be embedded into a thin organic film and are sensitive to the light, there is a high probability that they will gain more importance as a various components in opto-electronic systems as all-optical parallel light modulators.

Conclusions

The purpose of this thesis was to describe both the results of investigation into the functions of the human visual system, and our resulting proposal and development of a novel photonic device, the Adaptive Filter. To this end a theory was developed to support the design and implementation of the filter as a photosensitive device, a Photochromic Adaptive Filter, that controls and modifies images in a parallel fashion. This work was documented and the experimental results were presented. We opted for the implementation of the Adaptive Filter using photosensitive materials because they are self-adjusting, do not require additional electrical power to operate and can be implemented into standard image acquiring systems without increasing the complexity of the electronic processing system. These are all important constraints, as the ultimate goal of this research is to implement the filter as part of an artificial eye. The thesis intended to provide a guide on how solutions implemented by nature could be used to improve existing man-made systems.

The work described above was motivated by a desire to improve the limited dynamic range of modern image acquisition systems by bridging the gap between biological and artificial visual systems. Based on the knowledge we gained from studying the light adaptation processes in biological visual systems over a wide spectrum of disciplines, we proposed a new type of image acquisition system. The system we developed is made of a very sensitive photodetector array and modulating filter that adjust the image intensity in high ambient light intensities to match the detector's operating range.

Contributions

The major contribution made by this thesis was the presentation of a novel photonic device, the Adaptive Filter. The general theoretical model of the Adaptive Filter concept was proposed and evaluated. Adaptive Filters can extend the dynamic range of operation and improve the contrast ratio of any existing standard video cameras.

We implemented the Adaptive Filter in the form of a Photochromic Adaptive Filter. We also developed a simple, fast and accurate procedure for evaluating properties of the photosensitive materials that were fabricated as part of the research. By using the method we developed to measure the filter's photochromic response from a series of pictures of lamp we determined the maximum photochromic response of the filter tested in the local adaptation mode as $OD=0.8$. The photochromic response of the filter is limited by a number of factors, such as thermal fading, optical bleaching and the maximum concentration of the photochromic molecules.

There is a limit for the maximum concentration of the photochromic materials that can be embedded in the polymeric environment. Depending on the fabrication process the saturation of the photochromic solution can occur at levels of 5-10% concentration. By testing different polymeric systems we raised the level of the concentration from initial 1-2% to more than 10% while maintaining good optical quality and clear base state. We also fabricated filters with the concentration levels as high as 20%; however, at that concentration level agglomeration of the molecules occurs, which causes coloration of the filter in the base state, and as a result gives smaller photochromic response. Increase in the thickness of the filter with lower photochrome load is not a viable option because the excited molecules strongly absorb the exciting radiation (300-400 nm) and in this way they deplete the light intensity in that spectral region.

To reduce thermal fading process we utilized an infra-red blocking filter; however, at high light intensities the thermal fading process overcomes the darkening process as the temperature of the filter increases locally.

A test bed for evaluating the Photochromic Adaptive Filter was designed and developed and the concept of implementing optically addressed PAF successfully tested. As a result of utilization of the Photochromic Adaptive Filter the dynamic range was extended and negative side-effects such as blooming and flare within the image were reduced. This approach has several advantages over existing methods (Mann, 1991), because optical pre-processing of the image does not change the electronic circuit design complexity and

it is autonomous. In particular it can be applied to any photodetector array.

Details of experimental results which provide spectral and temporal properties as well as composition of several developed PAF's complete this part of the thesis.

In the other part of the thesis the saturation of the signal in the glare phenomena was used by us to reveal the highly complex structure of the retina. Our investigation led to an estimation of the horizontal cell connections density along the diameter of the human retina and a space constant of the horizontal cell lattice. We predict a decline in the density of horizontal cell connection from the fovea as $1/x^2$ (where x is the distance from the fovea). The deduced profound decline is plausible in view of our knowledge of cone and ganglion cells density, and some partial estimation of horizontal cells density. As the horizontal cells are embedded in the middle of the neural structure of the retina, it is a very difficult task to actually count the cell distribution. Using our model we can predict this distribution using a non-invasive method.

In this work we also presented a systematic compilation of the biological phenomena found in the living visual systems and corresponding implementations in the man-made systems. We presented adaptation mechanisms, that are yet to be implemented, which can improve the dynamic range of the operation for low light intensities.

No artificial image acquiring system can match the biological visual system in terms of the dynamic range of light intensities it can effectively operate. By implementing adaptation mechanisms into artificial systems we reduced the gap between the two systems, but we can not match yet the versatility of the human eye.

Advantages of photochromic systems

The use of passive adaptive filters offers several advantages over other solutions leading to extension of the dynamic range of operation. The most important is that they can be added to any existing image acquiring system without changing the electronic architecture.

The existing systems with wide dynamic range use focal-plane electronic post-processing. These systems incorporate local processing circuitry to perform signal conditioning and image filtering. This post-processing mimics different adaptation mechanisms on the level of photoreceptors themselves, or as an electronic neural net processing information from the photodetector arrays. Those additional processing systems, although fast,

add an element of complication to the design of a photodetector array. They also take some space on the focal plane, thus decreasing the ratio of array surface available for the detection (so called *fill factor*), and they require additional energy supply. Another option of utilizing classical computer-oriented processing system suffers from the inherent speed problems.

The optically-induced image processing utilizes light to affect optical properties in the photo-reactive filter which is subsequently used for image processing. They automatically adjust to different light conditions and they do not require any additional power supply to operate. Adaptive filter provides parallel conversion, essential for fast image processing. For some type of applications, such as the artificial eye, it can be very important that the photochromic systems have a response time very similar to that of the human eye.

Spatial image modulation by photochromic filters is practically only diffraction limited. Intrinsic resolution of the inorganic photochromic film is known to exceed 2000 lp/mm, for organic photochromes the resolution limit is more like 5000 lp/mm. Photochromic filters can be inexpensively manufactured using standard techniques. As a result of using photochromic opto-optic modulators we extended the dynamic range of operation of image acquiring systems. Application of the PAF can also protect such systems against excessive light intensities.

Limitations of organic photochromic systems

One has to carefully consider material advantages and disadvantages when using photochromic systems. These materials are relatively slow reacting – with relaxation times varying from minutes to days. They are very sensitive to environmental factors – temperature being the most important. Organic photochromes last a limited number of cycles between both energy states before they dissociate*. Those organic materials can be destroyed by excessive illumination in process of photolysis. Finite life of the thin film and practically no control over the thin film properties once the filter is built are other limiting factors.

It is a difficult task to build a filter with a grey-like characteristic using organic pho-

* Photodegradation process can be drastically slowed down by adding specific inhibitors to the polymer, however.

tochromic components, because they have a rather narrow peak of absorption in the visible part of spectrum and different dynamic properties. Main limitation of the organic photochromic materials is speed of coloration and relaxation. No photochromic lens is instantaneous in action. However the time response of the photochromic filter is similar to the time response of the human eye. This can be an advantage when considering the properties of the filter with respect to the long-term goal of utilization of the filter into design of the artificial eye. Slow alterations rates are required for psychologically acceptable changes in the illumination level. Maximum Optical Density attainable in the colored state is another confining factor in wide-spread utilization of the new device.

Future work

In this thesis we demonstrated the feasibility of using Photochromic Adaptive Filter as a novel component of the opto-electronic systems in the scale-up arrangements. Next major step would be to implement the photochromic film directly on the surface on the image acquiring array and solve a new set of problems related to materials compatibility, film stability, technological improvements and changes to accommodate this additional component. Ideally the thin-layer filter would be fabricated using standard IC fabrication process, as a one additional production step. A lot of work remains to be done in the optimization of the components, the design of the photochromic filter and improvements in performance.

Design improvements

One of the most visible (literally) problems when dealing with the organic photochromic materials is the problem of coloration. As photochromic materials are absorbing in a narrow range of wavelengths, it is difficult to design filter with grey-like properties. One of the possible solutions to this problem is shown in Figure 4.1. We propose to utilize the concept of splitting the image into three equal light-beams and processing them independently in different regions of the visible spectrum.

New photochromic systems with better properties should be investigated. Finally, the use of an anti-reflection (AR) coating, (designed for the peak absorption wavelengths) on the surface of the filter would improve the collection of the light and the response of the

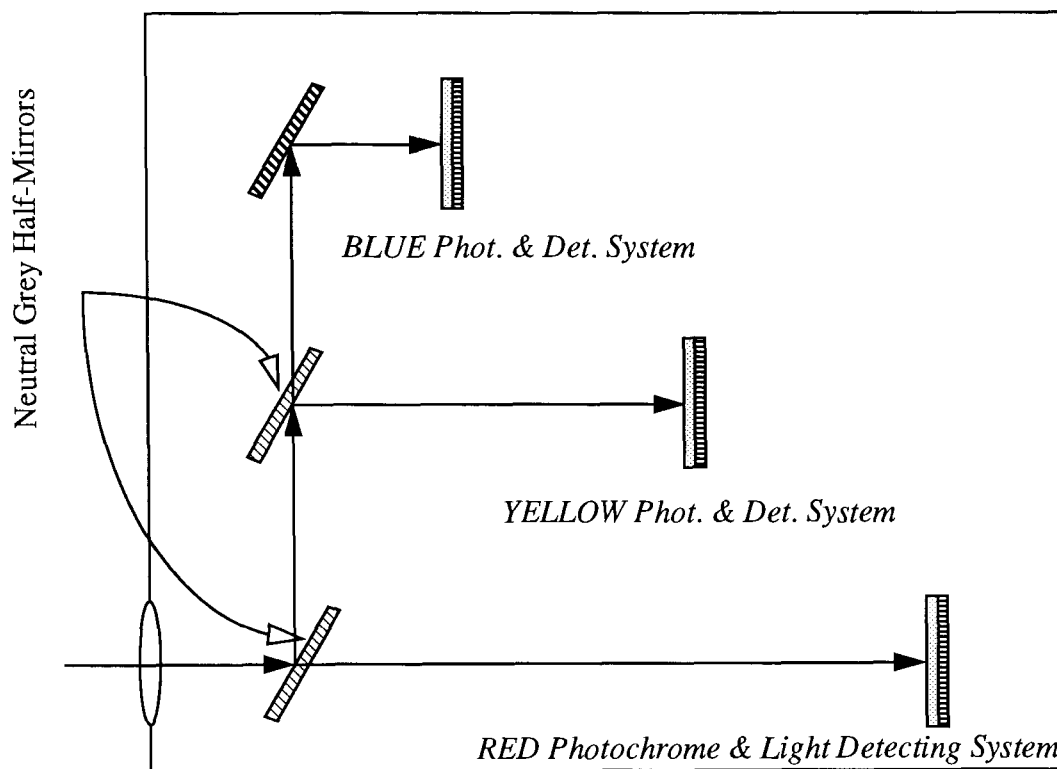


Figure 4.1 Organic photochromes based color image processing

filter. Introduction of photochromic stabilizers may significantly decrease the fatigue rate, and increase the number of activation cycles.

Attention should be given to protection of the thin film from harmful environmental conditions. As an example a simple process of covering thin layers with a PVA coating, which prevents oxygen diffusion (Irie, 1994), can radically increase fatigue resistance of organic systems.

Technological improvements

It is well acknowledged that using different methods of fabrication, such as molding, can improve the quality and properties of the photochromic filter. A preferred method (McArdle, 1992) for making plastic photochromic lenses is to dissolve the photochromic material into an organic resin (and perhaps solvent) such as an acrylic resin, and then apply this

solution to the lens surface by any of several techniques such as dip, spray, spin etc. Another process for applying an optical coating containing a photochromic is by “in-mold coating” (McArdle, 1992).

Synthesis of new compounds that have sensitivity at longer wavelengths (650-830 nm) will provide components necessary to fabricate truly grey-like filter made of mixture of photochromes. Another improvements would be to apply suitable AR coatings to reduce reflection losses on the thin film to air interface. In fact, it might be possible to utilize the anti-reflection property when designing media for photochromic materials.

Another viable option would be to develop a thin layer silver-halide filter with grey-like filter characteristic.

Applications of photochromic systems

Photochromic processes encompasses many disciplines and are found in both living and non-living matter. The research in that field has shown steady growth, because of the potential usefulness of photochromes in a variety of applications. On the one hand possible applications are limited by the properties of the organic photochromic systems, such as poor performance with regard to fatigue, thermal reversibility, speed of response and viable system integration. On the other hand fatigue-free silver halide glasses can produce a grey scale image with resolution exceeding 2000 lp/mm with contrast ratios exceeding 30:1.

Photochromic materials have already found numerous applications in very diverse fields such as:

1. radiation intensity control
2. data storage (short and medium term memory)
3. optical computing and image processing
4. dynamic holography (Tomlinson, 1972)
5. optically controlled waveguides and optical lenses

We proposed to use a passive system utilizing photochromes to build an example of the Adaptive Filter – the Photochromic Adaptive Filter. Photochromic systems are naturally seen as a feasible component, as they are already used for that purpose (Young, 1993). Millions of people enjoy and wear photochromic glasses to help adjust their living visual

systems to different, especially excessive light intensities. The usage of photochromic lenses reduces squinting and eyestrain. They also protect human eyes from UV rays. For this purpose lenses are used as a globally adapting filter. In our project we went a step further; we proposed to utilize a photochromic thin-layer film as a locally adapting filter that stretches the dynamic range of the system. This has several advantages over globally adaptive filter, which only shifts the operating range.

In recent years, society has become aware of the harmful effects of ultraviolet radiation. Photochromic materials by their nature may be used to protect humans, and equipment, from UV radiation. As a human eye is insensitive to the UV radiation, the photochromic filter can be used in the same time to indicate UV presence and intensity and as a result to allow individuals protect themselves from this harmful radiation.

A promising future exists for photochromic materials in many fields, especially in information processing and storage. We postulated to use these materials as a component of photonic device: a thin-layer Photochromic Adaptive Filter, and we successfully proved that application of the adaptive filter is a viable alternative to other approaches. Some obvious applications for such system with enhanced dynamic range include: security systems, autonomous robots and other types of smart image acquisition systems. Photochromic filters by their nature are good candidates as elements of the artificial retinas, as they don't require power supply and won't increase much the architectural complexity of the 3-D detecting structure.

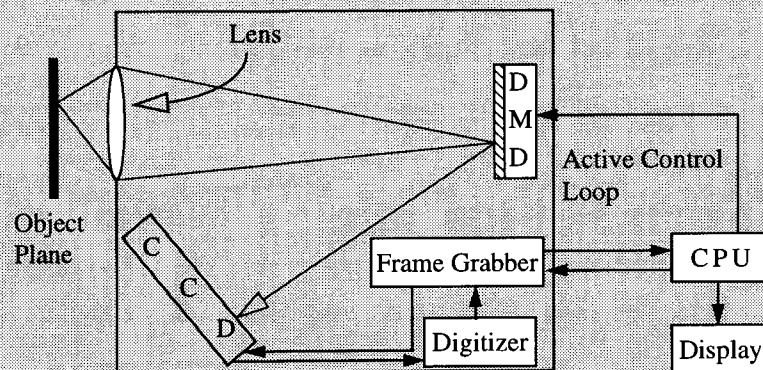
Related studies

Some of the limitations of photochromic adaptive filter can be avoided using Active Adaptive Filter^{*}. As opposed to PAF's, light modulation can be performed for any light conditions and in a way that we can control. Modern Spatial Light Modulators can potentially increase the dynamic range of the camera up to two decades. Using recently developed components, such as the Digital Micromirror Device and long exposure CCD makes it possible to build compact systems for image acquisition with unique properties.

* See section *"Investigating possible implementation of an Active Adaptive Filter"* in the Appendix.

Appendix

| | |
|--|------------|
| Errors discussion and summary | 100 |
| Development of the inorganic PAF | 103 |
| Investigating possible implementation of the Active Adaptive Filter | 109 |



Errors discussion and summary

All the experimental data values presented in this project are related to some type of errors. They can be treated as: measurement, methodology and instrumentation errors, or as related to the performed calculations. Systematic description is presented in Table A.1. We analyzed different types of errors and in case that there are few independent ones, the maximum cumulative value is shown (Equation A.1).

$$\Delta x = |\Delta_{\Sigma}x| = |\Delta_1x| + |\Delta_2x| + |\Delta_3x| + |\Delta_jx| \quad (\text{Eq. A.1})$$

Where:

Δx – absolute maximum error [%]

$\Delta_{i=1\dots j}x$ – different components of measurement error [%]

Throughout the thesis numerical data are presented with the last significant digit given. For example, if the accuracy of the measurement is ± 0.01 , we present values in 9.99 form.

The most important are errors that are intrinsic to the developed image processing system (see Figures 3.10, A.1). In this system the processing and imaging part are separat-

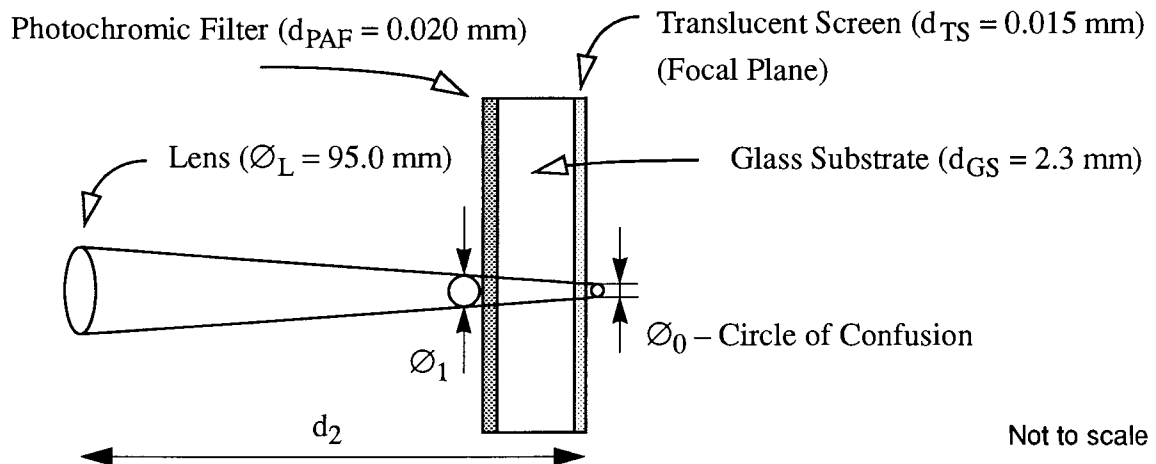


Figure A.1 Spatial separation of image processing and display

ed by the thickness of the glass substrate, host both to the PAF and screen. As a result the light intensity that induces coloration of the photochromic filter may have different value

that light intensity on the screen, that is detected and used to scale the measured functions. An object at a distance d_1 from the lens will produce an image on the frosted side of glass plate at a distance d_2 on the other side of the lens that has focus length f (Figure A.1). If we assume that the object is in the plane, a sharp and inverted image will be presented. If the object is not exactly in focus, the image become fuzzy. The size of the blurred spot, assumed circular in shape, is an inverse measure of the resolving power of lens. It is a measure of the quality of the image. We determine the focusing error ε using Equation A.2. The next step is to determine the size of the blurred spot, sometimes described as a circle of confusion, from Equation A.3.

$$\varepsilon = \frac{1}{d_1} + \frac{1}{d_2} - \frac{1}{f} \quad (\text{Eq. A.2})$$

$$\varnothing_0 = \varepsilon \cdot \varnothing_L \cdot d_2 \quad (\text{Eq. A.3})$$

Where:

ε – focusing error

\varnothing_0 – diameter of the blurred spot

\varnothing_1 – diameter of the spot on the PAF plane, where image processing takes place

\varnothing_L – diameter of the circular aperture of the lens

d_1 – object plane

d_2 – image plane

f – focal length of the lens

By substituting data for a typical experiment, we estimated the maximum circle of confusion: $\varnothing_0 = 1.5$ mm. Next, using geometrical relation we estimated $\varnothing_1 = 3.0$ mm. By comparing surface ratio of these two circular spots we estimated that the maximum light intensity ratio may reach as much as 4:1. This important factor must be considered when functions of the light intensity (such as presented in Figures 3.21-3.24) are determined.

Of course such discrepancy in light intensity occurs only in case when large spatial gradient of light intensity exists across the plane surface. For a spatially uniform light distribution the corresponding light intensities on both planes (screen & PAF) are equal. During experiments made to determine the Transformation Function, we minimized the intensity ratio by moving the screen to intentionally increase the circle of confusion.

Table A.1 Errors overview

| # | Source | Variable x [units] | Δx | Variable y [units] | Δy | Notes |
|----|----------------------------------|--|--|---|--|---|
| 1 | Eq. 1.3 Fig. 1.5 | eccentricity [arc min] | $\pm 0.5^{*\ddagger}$ | Glare Constant | Estimation of the GC depends on many variables and it is not very precise. | |
| 2 | Fig. 1.7 | | | surface density [mm^{-2}] | $\pm 100^*$ | Experimental data comes from the retina of monkey. |
| 3 | Fig. 2.4 Fig. 2.5 Fig. 2.6 | pixel position [-] | exact | grey level [-] | $\pm 1^\dagger$ | Grey level range: (0-256) |
| 4 | Fig. 2.7 | Input Light Inten. | $\pm 1^\dagger$ | Output Light Intensity | $\pm 1^\dagger$ | arbitrary units |
| 5 | Tab. 3.4 | C_{wt} [%] | $\pm 0.1^{\dagger\ddagger}$ | spinning speed [rpm] | $\pm 10^{*\ddagger}$ | Thickness error depends of the method used. The overall difference in the thickness across the sample may reach 0.5 [μm]. |
| | | time [s] | $\pm 1^{*\ddagger}$ | thickness [μm] | $\pm 0.1^\dagger$ | |
| 6 | Tab. 3.5 | thickness [μm] | $\pm 0.05^\dagger$ | surface density [mm^{-2}] | $\pm 0.01^*$ | Refr. index error \equiv zero error. |
| | | C_{wt} [%] | $\pm 1^*$ | refractive index [-] | $\pm 0.01^\ddagger$ | |
| 7 | Tab. 3.6 Fig. 3.4 | wavelength [nm] | $\pm 0.5^*$ | transmittance [%] | $\pm 0.01^*$ | reading every 0.05 [s] & 2 [nm] scanning speed 2,400 [nm/min] |
| | | time [s] | $\pm 0.05^*$ | | | |
| 8 | Tab. 3.7 | peak wavel. [nm] | $\pm 2^\dagger$ | ϵ [$10^{-3}\text{dm}^{-3}\text{mol}^{-1}\text{cm}^{-1}$] | $\pm 3^*$ | |
| 9 | Tab. 3.8 | quasi time constant [s] | Relaxation process is not a simple exponential function, so presented time constants are a first approximation, given for comparison only. | | | |
| | Fig. 3.5 | time [s] | $\pm 0.05^*$ | Optical Density [-] | $\pm 0.005^*$ | DU 600 SpecPhot Specifications |
| 10 | Fig. 3.6 | wavelength [nm] | $\pm 0.5^*$ | transmittance [%] | $\pm 0.01^*$ | scanning speed 2,400 [nm/min] |
| 11 | Eq. 3.5 Fig. 3.9 | absorption peak wavelength [nm] | $\pm 2^\dagger$ | refractive index [-] | $\pm 0.01^\ddagger$ | Profilometer specifications: offset: -1.0 [μm] measurement error: ± 0.5 [μm] |
| | | m is exact [-] | n/a | thickness [μm] | $\pm 0.05^\dagger$ | |
| 12 | Fig. 3.12 | wavelength [nm] | $\pm 0.25^*$ | transmittance [%] | $\pm 0.01^*$ | scanning speed 1,200 [nm/min] |
| 13 | Fig. 3.15 ----- Fig. 3.20 | pixel position [-] | exact | grey level [-] | $\pm 1^*$ | Grey level range: (0-256) For very high and low intensity values the error may reach $\pm 3^*$ |
| | Fig. 3.21 | | | light intensity [a.u.] | $\pm 1^*$ | Light Intensity range: (0-256) |
| 15 | Fig. 3.22 | light intensity [mW/mm^2] | $\pm 0.1^*$ | light inten. [mW/mm^2] | $\pm 0.1^*$ | Max offset $\pm 0.25^{*\ddagger}$ [mW/mm^2] Errors increase significantly towards low light intensities, due to nonlinearity of operation of the detecting device (CCD). |
| 16 | Fig. 3.23 | | | light intensity ratio [-] | $\pm 0.01^\dagger$ | |
| | Fig. 3.24 | | | Optical Density [-] | $\pm 0.01^\dagger$ | |
| | Eq. 3.6 | transmittance [%] | $\pm 0.01^*$ | | | |
| 17 | Fig. 3.25 | light intensity | $\pm 0.005^*$ | light intensity | $\pm 0.005^*$ | arbitrary units |
| 18 | Fig. A.2 | wavelength [nm] | $\pm 0.5^*$ | transmittance [%] | $\pm 0.01^*$ | scanning speed 2,400 [nm/min] |

* Indication, scale, measuring or instrument reading error (intrinsic to measurement technique)

† Miscount and estimation error (related to the performed calculation)

‡ Zero error

Development of the inorganic PAF

Variety of inorganic compounds show photochromism, including metal oxides, alkaline earth metal sulfides, titanates, copper compounds, certain minerals and other compounds (Davey, 1980). Inorganic photochromic materials are mainly manufactured as silver halide photochromic glasses to make ophthalmic lenses. The glasses contain small crystallites (5-20 nm in diameter) of silver halides suspended in a host glass matrix (Araujo, 1987). The average spacing between crystallites is 100 nm. To achieve satisfying change in the optical density 100 μm film thickness is a minimum value for this type of glass. A small amount of copper increases the darkening sensitivity by several orders of magnitude and is included in almost all the transparent glasses. For ordinary photochromic ophthalmic lenses the overall change in the transmittance from day to night is $\Delta T = 50\%$, across visible region.

Photochromic process

Photochromic process can be divided into three steps:

- - formation of electron-hole pair by excitation process;
- - formation of the color centers by trapping of free electrons;
- - bleaching of color centers by various recombination processes.

We can summarize the process of darkening and fading of the glass as follows:

Darkening Process:

- - Formation of electron-hole pairs in particles of $\text{AgCl}_x\text{Br}_{1-x}$ by UV radiation;
- - Photo-electrons transferred from halogen ions and copper ions reduce metal ions within the silver halide, or at the silver halide – glass interface;
- - Reduced silver atoms aggregate at ambient temperature to form submicroscopic, light absorbing metal particles;
- - Kinetics of the darkening is in the simplest case, governed by a first-order equation.
- - The darkening process reverts when irradiation ceases.

Bleaching Process:

- - Fading is a diffusion controlled process;
- - Holes (Cu^{2+} , Cl^0) diffuse to within efficient electron tunneling distances from the silver metal specks;

- - Trapped hole recombines with an electron from the silver speck;
- - To maintain neutrality silver ion (Ag^+) diffuses away;
- - Kinetics of the bleaching process is more than second order reaction.

Overall photochromic reaction can be presented as* :



Unlike the organic photochromic systems which are capable of rapid darkening and recovery, photochromic glasses have a long time constant ranging from minutes to hours. The speed of relaxation can be controlled by changing dimension of the crystals, and in that way the total diffusion path. With few exceptions the photochromism is a structure-sensitive phenomenon.

In organic systems the photochromic element can be concentrated in one narrow layer of the filter so as to remove the effect of surface non-uniformities on the evenness of the tint. In glass systems the photochromic material must be uniformly dispersed in the volume, what limits the minimum thickness of the filter and may cause the non-uniformities in spatial transmittance due to the difference in the thickness.

Glass is a durable material, unaffected in most cases by weathering, and has a good scratch resistance. Unlike the organic systems, inorganic photochromic glasses never fatigue, even after being subjected to more than 300,000 darkening and bleaching cycles (Brown, 1971).

Spectral properties of inorganic photochromic film

The inorganic photochromic materials are characterized by a large band gap: 3-12 eV. As a result, glasses that contains photochromic materials are transparent in the base state (Megla, 1966). We can classify photochromic materials as insulators or semiconductors. The optical excitation leads to the formation of metastable color centers. The spectral absorbance of those centers will depend directly on the properties of the material used. In case of silver halide materials it will be spectral absorbance of silver, which is a nearly perfect absorber, i.e. it absorbs uniformly through the VIS spectrum. This properties: full transparency in the base state and dark silver grey tint when activated (see Figure A.1),

* The exact overall process of reversible coloring is not fully understood at present time.

make them very desired materials for image processing. It is a difficult task to build a filter with a grey-like spectral characteristic using organic components that have rather narrow peak of absorption in the visible part of spectrum, but it is rather easy to design such a system using silver compounds. AgCl based photochromic filter very little changes a spectral distribution of light, in other words colors are preserved. This property is yet to be matched by recently developed plastic photochromic lenses. Figure A.1 presents spectral

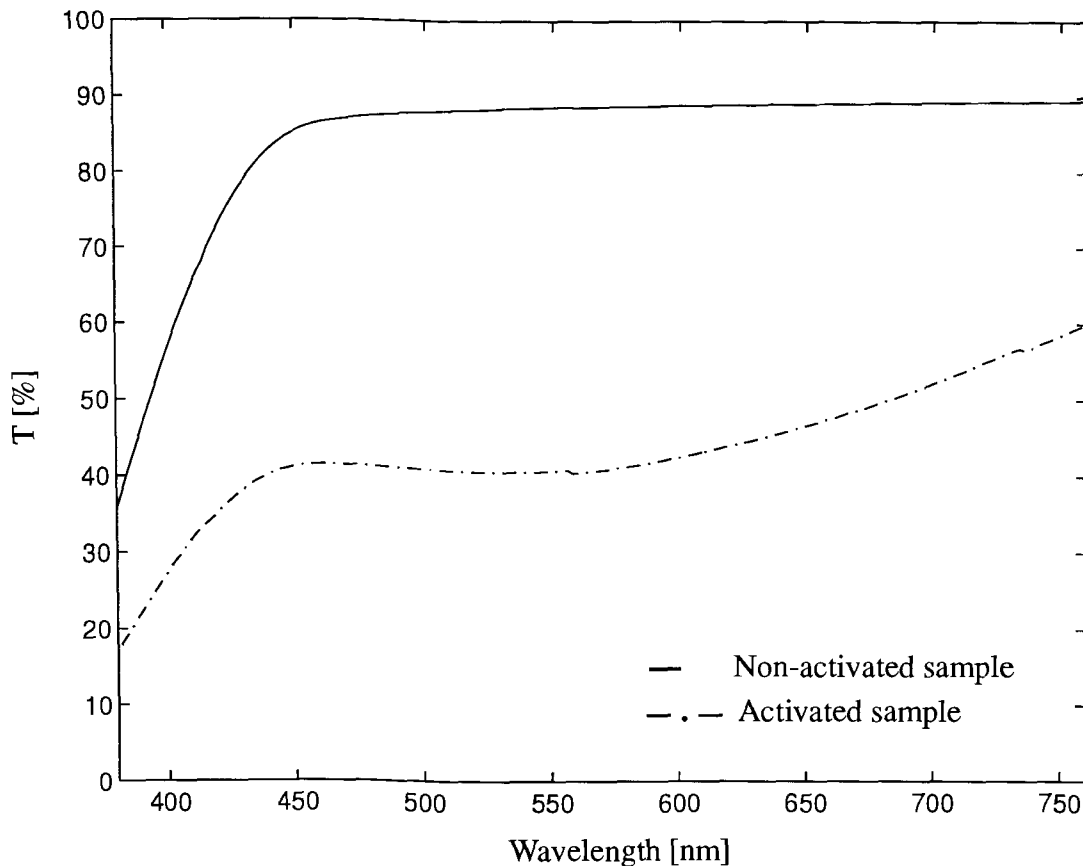


Figure A.2 Spectral characteristic data for SOLA PhotoGray Extra[®] lens

transmittance of the photochromic ophthalmic lens* in both energy states.

Crystalline inorganic solids may be activated by wavelengths anywhere in the spectrum, ranging from infrared to X-rays to gamma rays, although, ultraviolet activation is most common. Inorganic solids commonly absorb in the visible and infrared.

* For measurement details see *Part III – “Spectral properties of photochromic filters”*.

Formation of Photochromic Glasses

The process of making glass with photochromic properties uses the standard glass-forming techniques from melts.

First a system of salts of silver, copper, and chloride are added to the molten batch materials together with sensitizers (Araujo, 1987; Smith, 1967). Such a system is analogous to a solution of sodium chloride in water. Due to highly corrosive nature and high temperatures, the whole process has to be carried out in inert atmosphere (nitrogen) and platinum crucibles. During extensive heat treatment precipitates of silver-halide are formed.

A great care must be exercised with regard to maintaining precise control of the ingredients. Some of them are generally present in amounts much less than 1% by weight, sometimes less than a tenth of a percent. The additives precipitate in response to controlled heating. Careful control of the melting conditions must be maintained to kept the volatilization and oxidation state of the dopants constant (Borelli et al., 1991). At the end, generally press-formed product needs to be chemically strenghtened or tempered. Large thin photochromic sheets can also be made by suitably supporting the glass, such as on the air hearth, during heat treatment (Borelli et al., 1991). All these manufacturing methods require specialized hardware and laboratory facilities. In our research we were testing other methods of fabrication, that could be implemented using our existing laboratory. We concentrated our efforts on two techniques: sputtering and sol-gel processes, which are described in more detail below.

Sputtering deposition of inorganic PAF

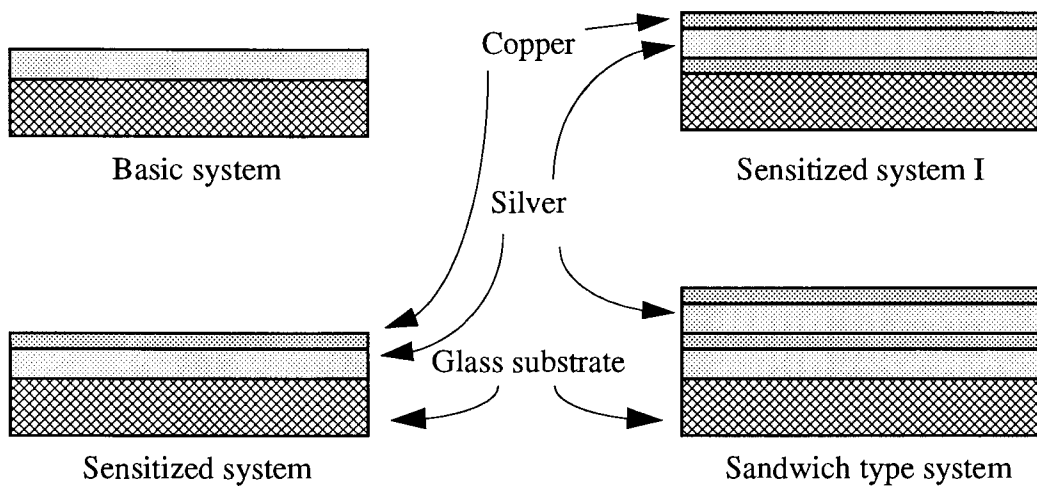
Sputtering is rapidly supplanting vacuum evaporation for metal deposition, because it is a well controllable process, provides adherent films, and enables better coverage of complex-shaped objects (Harper et al., 1994). Sputtering is a more versatile process than other vacuum deposition techniques. It allows not only high-vapor-pressure metals to be deposited but also refractory metals, alloys, inorganic compound, and ceramics. In Radio Frequency (RF) sputtering materials other than electrically conductive metals can be deposited.

Initially we attempted to sputter a thin layer of silver-halide film and in the next step to cover it with a glass to create an inorganic photochromic film. Similar works on AgCl,

Cu^+ doped thin films have been made at Corning (Prassas, 1994), but no experimental details have been published so far.

A Silver-Chloride target was prepared and attached to a copper substrate. Using RF sputtering we deposited that material on the glass substrates. However during the process we discovered that stoichiometric proportion and the form of the material were not preserved during a deposition process. We received silver enriched layers and process of chlorine depletion was observed on the target. To get back a silver halide on the substrate, we designed a process of transforming the thin silver layer back into silver halide. We converted the silver thin layer into AgCl crystallites by a HCl vapor treatment.

Different configurations were tested to find the system with good adhesion of the film to the glass substrate. Figure A.3 presents cross sections of several configurations that



Not to scale

Figure A.3 Multilayered structures fabricated using sputtering technique

were designed and fabricated. The multilayered structure of silver halide and copper was eventually covered with materials like Spin on Glass (SOG), different polymeric layers or sputtered glass, to protect chlorine (Cl) from departing the film, and this way to assure reversibility of the whole process. Unfortunately the sputtering process of the glass has very low deposition ratio. Another obstacle was the porosity of such deposited film.

In another attempt we tried to create a thin glass layer on top of AgCl layer using Spin on Glass technology. Fairly complex heat treatment process required to solidify the

SOG was causing damage to the fabricated photosensitive layer and this approach was abandoned.

By controlling the thickness of the film we could at the same time control the optical response of the film to exciting radiation. Fabricated samples had thickness between 1-6 μm . Because of the big size of silver halide crystallites, the thin layer in the not activated state was opaque to the visible light and as such was not suited to be used as optical modulator. Another problem was reversibility. Fabricated coating darkened by UV irradiation, forming Ag crystallites. However this process was not completely reversible in a room temperature. We found that by thermally heating the layer at 300°C we could erase stored image making it possible for use in erasable holograms, but it was not good enough for self-adjusting filters.

Preparation of a Photochromic Glass via a Sol-Gel process

The Sol-Gel process has been suggested more than 20 years ago as an alternative to other methods for applying coatings (Vossen et al., 1991). The process consists of the preparation of a solution homogeneous at the molecular level and solution-to-gel conversion near room temperature (Sakka, 1992). Densification of the gel, usually in elevated temperatures, completes the process.

In first part chemical ingredients are mixed to produce a sol with only slightly higher than the water viscosity. Hydrolysis and polycondensation of the sol form the 3-D network of gel. After aging, a further drying step eliminates the interstitial liquid from the gel body. Finally, the dry gel is heat-treated to change the porous solid into a dense homogeneous glass. Lower reaction temperature, high purity, homogeneity, high efficiency and possibility of many new composites are main potential advantages of sol-gel processing.

We utilized this technique to create the Sol-Gel derived AgCl-doped SiO_2 photochromic filters. In one process small AgCl crystallites were embedded in Sol-Gel material. By slow evaporation we turned this system into glass. In another experiment we mixed colloid of small silver halide crystallites with Spin on Glass* (SOG). Next, we used this volume for multiple coatings of substrate glass. This led to uniform photochromic film. However sensitivity of such developed materials was found not satisfactory enough for the purpose of using it as an image transformation filter. The low optical response and long reaction constant were other obstacles. The developed Sol-Gel glass was mi-

* SOG's are used primarily for planarization in IC fabrication process.

porous and quite fragile due to significant shrinkage of the sample during fabrication process.

Following recent development in the of Sol-Gel processes, we noticed a lot of improvements that might increase applicability of this fabrication method to produce photochromic thin layer filters. By adding specific additives, porosity and drying stress maybe minimized, and as a result cracking prevented. Still, this is a new method, and number of processing variables must be understood, controlled and evaluated before the advantages of Sol-Gel-derived composites can be realized.

Summary

The interest in inorganic photochromic materials for image processing, is attributed to such factors as:

1. Photochromic materials are dry-process imaging systems.
2. The image is formed upon direct exposure while the reverse reaction, i.e. spontaneous fading occurs in darkness.
3. Selective absorption occurs in specific regions of the spectrum.
4. Spatial resolution of the image can be very high.

Inorganic photochromic glasses find application in electronics, optics and decorative arts (Trotter, 1991). They have many advantages over organic plastic materials, such as no fatigue and grey filter characteristics when activated. However production process is more complicated on the laboratory scale than very well known polymeric technology. The minimum thickness of 100 μm of photochromic glass, as compared to 5 μm thickness of the organic films, may be a limiting factor for some specific applications. Inorganic photochromic filter may find numerous applications, such as:

1. Extending dynamic range of operation of image acquiring systems and protecting components of such systems against excessive light intensities
2. Testing an opto-electronic equivalent of adaptation mechanism and sensitivity change process that occur in the biological visual systems
3. Holograms

In overall, inorganic photosensitive samples that we developed and tested were found to be not suitable for the main project.

Investigating possible implementation of the Active Adaptive Filter

A Spatial Light Modulator (SLM) is a device which can impress information on an optical wavefront. The applications of light modulators are numerous; they include coherent optical processing applications, data routing, data input to optical processing systems and information display. The 2-Dimensional (2-D) SLM's play a major role in optical information processing by providing means to construct optical architectures.

Spatial light modulation can be accomplished via the electro-optic, acousto-optic, magneto-optic, opto-mechanical, photorefractive, optical absorption and interference effects in a variety of materials (Horner, 1987). Modulation is essential to many practical electro-optic devices and applications. Spatial light modulators already are used to transform image for Fourier transform etc. We propose to use them as Active Adaptive Filters for implementation of adaptation mechanisms. The proposed adaptive system consists of an imaging system, a modulator and a photodetector array.

Within the broad set of modulators we focused on two types: Opto-Mechanical (O-M), and Electro-Optic (E-O). Digital Micromirror Device is an example of the O-M design. LCD is one example of E-O modulators, which translate information from electronic domain to the optical domain, accompanied by other, such as plasma displays, liquid crystal over nMOS array (McKnight et al., 1989), electrochromic displays, etc. (Ziegler et al., 1994).

Liquid Crystal Displays (LCD's)

Early LCD's were prohibitively expensive, what limited their application for research and application purposes. Technological breakthroughs in the last few years and recent advances in microelectronics and liquid crystals have caused a significant reduction in price. LC Display (LCD) consists of many individually addressable LC intensity modulators arranged in an array – in that form it is referred to as a Spatial Light Modulator. The advantage of using Liquid Crystals (LC) materials for SLM's include their high birefringence and low voltage operation. Especially interesting are LCD's of types using Thin Film Transistors (TFT's), due to their increased contrast ratio. They all exploit the anisotropic medium of Liquid Crystals (LC's). These properties allow large optical effects to be induced in pixels only a few wavelengths thick.

Nowadays Liquid Crystals (LC's) are among the most successful materials used for SLM implementations. It is mostly due to high sensitivity, large dimensions of the array and relatively low cost. Additional advantage of these displays is low power consumption. Other advantages of using LC display are: very wide absorption in the visible spectrum and fast reaction time. Like other E-O modulators, LC modulators can modify the polarization, phase and intensity of the light. When placed in the path of broad light beam, the spatial light modulator generates spatially changing intensity patterns in the light.

Although LCD SLM were used so far mainly for implementing Fourier transformations – LCD SLM could be used in a straightforward fashion to implement an Adaptive Filter (Figure A.4).

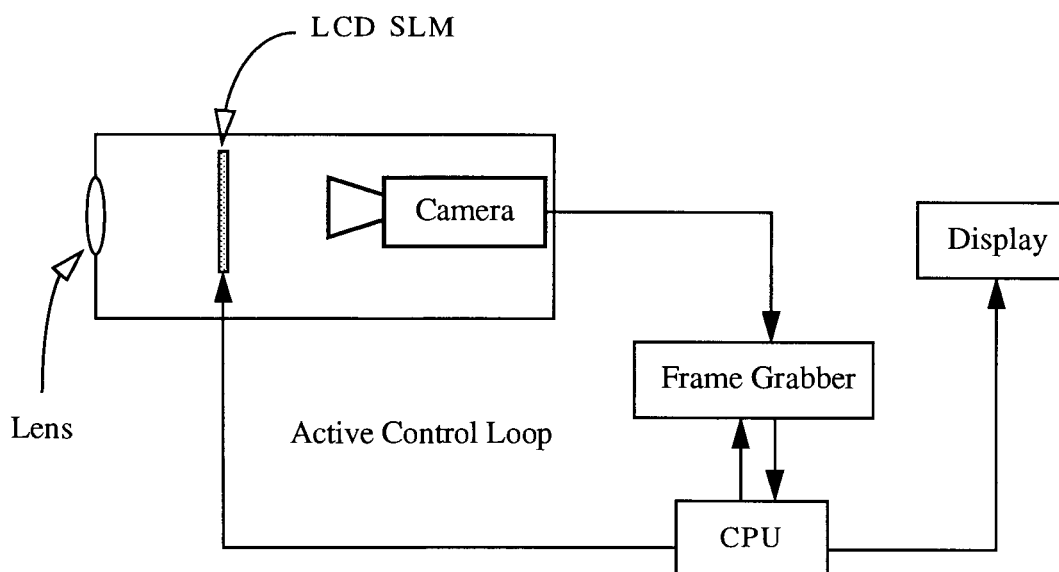


Figure A.4 General layout of an image processing system utilizing LCD as an Active Adaptive Filter

We propose to use SLM for the hybrid optical implementation of the Adaptive Filter to increase the dynamic range of a system. A standard digital computer is used to determine the spatial light distribution, then it drives the SLM with the predetermined function. Because each pixel is modified in parallel by LCD, this allows for the real-time correction. This implementation uses a digitized sample of the original image to generate a new trans-

mittance function on an SLM used as a spatial mask. The grey-levels of the output image emerging from the SLM will then be the transformation of the original grey-level image.

LCD SLM's have shown a big progress in recent years, bigger matrices with higher contrast ratio are produced. Recently available on the market are SLM with pixel pitch: $330 \times 330 \mu\text{m}$, and contrast ratio reaching 100:1 (SHARP, 1994; InFocus, 1994).

Using Ferroelectric Liquid Crystals (FLC), optic beam shutters are produced with the Contrast Ratio (CR) range from 200-500:1 (Johnson, 1992). Such CR's are well within acceptance values for certain optical processing applications. If flat panel displays made of such LC's are developed, utilizing them will expand the dynamic range of acquisition systems up to 5 decades. With the integration technology improving, it will be possible to fabricate a 3-D structure with LCD SLM placed directly on the top of a photosensitive array, as visualized in Figure 2.1.

Digital Micromirror Device (DMD)

Digital Micromirror Device* (DMD) was designed and manufactured for large projection systems utilizing Digital Light Processing (DLP). It consists of a 2-D array of micromirrors (Younse, 1993), each individually mounted and controlled by an on-chip circuitry. This revolutionary, new opto-mechanical technology for digital display, that may have a significant impact on the market, is founded on a spatial modulator invented in 1987. In broad outline, tilting of the small deflectable mirror modulates the light incident on the surface. The mirrors are programmed to remain at the "on" or "off" reflective angle for exact time periods within a single frame of motion. This permits grey-scale projection of more than 24 bits of depth of the image.

This electrically addressed system, which combines VLSI electronics with mechanical motion of pixel-size mirror, was intended for high-definition display, and as such it has a high contrast ratio ($>110:1$, for recently improved design), short response time ($\sim 10 \mu\text{s}$) and large number of active pixels ($>2.3 \times 10^6$ active pixels) (Feather, 1995). One additional factor that does not find practical application as a projection system is a possibility of permanent switching the pixels to off-state, in other words: zero on-time (Lin, 1994). This is very important in proposed by us application of the DMD as an Active Adaptive Filter (Figure A.5). DMD combined with a focusing system, detecting array and controlling system, can be used to build active implementation of the Adaptive Filter. In proposed set-up

* Sometimes called Deformable Mirror Device.

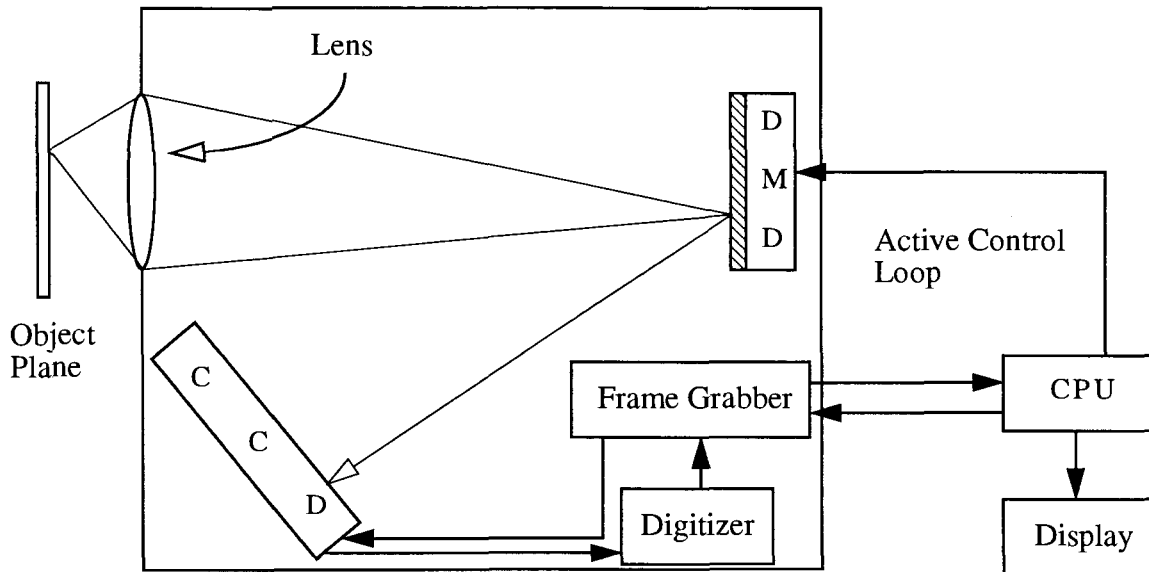


Figure A.5 General layout of an image processing system utilizing DMD as an Active Adaptive Filter

each mirror is related to an individual pixel of photodetector array. Object is focused on the Digital Mirror Device, whose mirrors are switched “on” or “off” according to the digital information written to the device’s memory circuits. The mirrors then reflect the modulated image onto a focal plane of a photodetector array*.

We propose to implement the DMD in two modes. In the simplest case, an image-sample would be analyzed for region(s) that are oversaturated. At that point algorithm would be applied to extract those part(s) from the picture by switching off the mirrors that correspond to that region(s) to redirect and trap excessive light. Finally, substitution of maximum values in the output signal for those selected pixels would complete the modulation process. In this way no alteration of the image would be made but the overall quality of the image would improve due to minimization of blooming phenomenon and suppressing flare. This set-up can find an application in situations where light sources appear within the image.

* Using VLSI technology and FLC materials a custom 128x128 SLM was developed by Boulder Nonlinear Systems (BNS) that could be used in the same processing system. In this device electrodes which control the FLC material serve at the same time as mirrors which outputs the SLM’s signal by reflection, since the back-plane made of silicon is non-transmissive (Serrati et al., 1993).

More complicated version of the system would implement global and local adaptation in real time without the need to relocate the DMD from the position. Shades of grey would be accomplished by clocking the mirrors with a type of pulse-width modulation, so they remain in the on-state during each frame for a time that is proportional to the desired grey level. To reduce smearing of the image due to mirrors tilting, the integration time of the photosensors would have to be much longer than frame rates of DMD.

Another immediate application would be to replace the standard CCD with a long exposure, on chip light-integration CCD (Southworth, 1992, Williams, 1995). In this case the system would be perfect for enhancing parts of the image that are underexposed. We expect that the system of camera combined with the adaptive filter might also find applications into imaging in astronomy, for producing long term exposure pictures, with the brightest object eliminated from the field of vision to expose more dim stars.

A size and weight advantage

Liquid Crystal Displays (LCD's) are well-suited and cost effective for spatial light modulation. The use of LCD SLM will allow to build reconfigurable architecture, that can be easily adjusted for different task, such as expansion of the dynamic range, image transformation for pattern recognition etc. LCD is a continuously evolving technology which benefits from the advances of electronic integration, optics miniaturization, and material control. This seems to indicate that LCD's technologies will increase their capabilities in the coming years. A system utilizing LCD SLM can be easily upgraded by changing modulator and adapting the system.

DMD-based system promises to have a number of advantages. First it offers a competitive cost and display-quality solutions. Additional size and weight advantages coupled with increased contrast ratio hold the promise for DMD solutions to build a compact camera with enhanced functionality. Technical characteristics of resolution, contrast ratio and grey scale will provide a new possibilities for in-camera image pre-processing. Additional advantage when comparing DMD with LCD is amount of light that is lost during modulation process. DMD provide higher efficiency (two to three times) of the modulation process due to the high reflectivity of the micromirrors (more than 90% of VIS light), and a high fill-factor of the device.

Summary

Spatial Light Modulators are important tools for the implementation of optical processors. They provide means to modulate two-dimensional incident light beams, and they enable to take advantage of the inherent parallelism of the optical processors. They can be used to achieve reprogrammable architectures that can be easily changed without the need to adjust other components of the optical set-up. Implementing electrically controlled spatial light modulators as an Active Adaptive Filter can drastically change the way we detect and analyze images, similarly to changes that utilization of the Adaptive Optics brought.

Different technologies are available for the realization of SLM's but Liquid Crystals are among the most successful materials used for SLM implementations. Progress in the development of LCD SLM's, in particular for optical processing, has accelerated dramatically in the last few years. Advances in LCD properties and minimization of the dimensions of the individual pixels and improvements in the contrast ratio and the switching speed make them good potential candidates for novel opto-electronic acquisition systems. DMD-based systems also promise to have a number advantages, such as a competitive cost and high contrast ratio, that combined with unique properties could be utilized for implementation of the Adaptive Filter.

Bibliography

- Abrahamsson, Maths and Sjöstrand, Johan **Impairment of Contrast Sensitivity Function (CSF) as a Measure of Disability Glare**, In: Invest. Ophthalmol. Vis. Sci., 1986; Vol. 27, Pages: 1131-1136.
- Adelson, Edward H. **Saturation and adaptation in the rod system**, In: Vision Research 1982; Vol. 22, Pages: 1299-1312.
- Ammermüller, J. and Möckel, W. and Rujan, P. **A geometrical description of horizontal cell networks in the turtle retina**, In: Brain research, JUL 09 1993; Vol. 616, No. 1/2, Pages: 351-359.
- Araujo, Roger J. *Encyclopedia of Physical Science and Technology*, Vol. 10, chapter: Photochromic Glasses, Academic Press, 1987.
- Attwell, David and Borges, Salvador and Wu, Samuel M. and Wilson, Martin **Signal clipping by the rod output synapse**, In: Nature, AUG 06 1987; Vol. 328, Pages: 522-524.
- Auty, G. and Corke, P. and Dunn, P. and Jensen, M. and Macintyre, I. and Mills, D. and Nguyen, H. and Simons, B. **An Image Acquisition System for Traffic Monitoring Applications**, In: Cameras and Systems for Electronic Photography and Scientific Imaging, FEB 1995; Proc. SPIE, Vol. 2416, Pages: 119-133.

- Barlow, Robert B. and Birge, Robert R. and Kaplan, Ehud and Tallent, Jack R. **On the molecular origin of photoreceptor noise**, In: Nature, NOV 04 1993; Vol. 366, Pages: 64-66.
- Beckman, C. and Scott, R. and Garner, L.F. **Comparison of three methods of evaluating glare**, In: Acta Ophthalmologica, FEB 1992; Vol. 70, No. 1, Pages: 53-59.
- van den Berg, T.J.T.P. **On the relation between glare and straylight**, In: Documenta Ophthalmologica, 1991; Vol. 78, No. 3/4, Pages: 177-181.
- Birge, Robert R. **Protein-Based Optical Computers**, In: Scientific American, MAR 01 1995; Vol. 272, No. 3, Pages: 90-95.
- Borelli, N.F. and Seward III, T.P. **Ceramic and Glasses, Engineered Materials Handbook**, Vol. 4, chapter: Photosensitive Glasses and Glass-Ceramics, ASM Int., 1991.
- Boynton, R.M. and Whitten, D.N. **Visual Adaptation in Monkey Cones: Recordings of Late Receptor Potentials**, In: Science, DEC 25 1970; Vol. 170, Pages: 1423-1426.
- Brown, Glenn H. **Photochromism**, John Wiley & Sons, 1971.
- Burton, G.J. **Evidence for non-linear response processes in the human visual system from measurements on the thresholds of spatial beat frequencies**, In: Vision Research, 1973; Vol. 13, Pages: 1211-1225.
- Buser, P.A. and Imbert, M., Eds. **Vision**, A Bradford Book, The MIT Press, 1992.
- Byzow, A.L. and Shura-Bura, T.M. **Spread of potentials along the network of horizontal cells in the retina of the turtle**, In: Vision research, 1983; Vol. 23, No. 4, Pages: 389-397.
- Cathey, W.T. and Ishihara, S. and Lee, S.Y. and Chrostowski, J. **Optical information processing systems**, In: IEICE Trans. Fundam. E75-A, APR 1992; Vol. 1, Pages: 28-36.
- Chen, Zhongping and Birge, Robert R. **Protein-Based Artificial Retinas**, In: Trends in Biotechnology, JUL 1993; Vol. 11, Pages: 292-300.
- Cohen, B. and Bodis-Wollner, I., Eds. **Vision and the brain: the organization of the central visual system**, Dowling, John E. chapter: Functional and Pharmacological Organization of the Retina: Dopamine, Interplexiform Cells, and Neuromodulation, Raven Press, Ltd., New York, 1990.
- Colorado Video, Inc. *Model 503 – exposure control unit specifications*, 1994.

- Crawford, B.H. and Granger, G.W. and Weale R.A., Eds. ***Techniques of photostimulation in biology***, Amsterdam, North-Holland Pub. Co., New York, Wiley & Sons, 1968.
- Crook, J.M. and Lee, B.B. and Tigwell, D.A. and Valberg, A. **Thresholds to chromatic spots of cells in the macaque geniculate nucleus as compared to detection sensitivity in man**, In: *Journal of Physiology*, 1987; Vol. 392, Pages: 193-211.
- Curcio, C.A. and Sloan, K.R. and Kalina R.E. and Hendrickson, A.E. **Human photoreceptor topography**, In: *The Journal of Comparative Neurology*, 1990a; Vol. 292, Pages: 497-523.
- Curcio, C.A. and Allen, K.A. **Topography of ganglion cells in the human retina**, In: *The Journal of Comparative Neurology*, 1990b; Vol. 300, Pages: 5-25.
- Davey, J.B. **Photochromics: the state of the art**, In: *Manufacturing optics international*, AUG/SEP 1980; Pages: 31-53.
- Dawson, W.W. and Enoch, J.M. ***Foundations of sensory science***, Berlin: Springer-Verlag, 1984.
- Dowling, John E. ***The retina: an approachable part of the brain***, The Belknap Press of Harvard University Press, Cambridge, Massachusetts, and London, England, 1987.
- Dürr, Heinz and Bouas-Laurent, Henri ***Photochromism – Molecules and Systems***, ELSEVIER, 1990.
- Efron, U. and Fisher, A.D. and Warde, C. **Spatial light modulators for optical information processing: Introduction by the feature editors**, In: *Applied Optics*, NOV 1989; Vol. 28, No. 22, Page: 4739.
- Elliott, D.B. and Whitaker, D. **Changes in macular function throughout adulthood**, In: *Documenta Ophthalmologica*, 1990-1991; Vol. 76, No. 3, Pages: 251-259.
- Etienne-Cummings, R.R. and Fernando, S.A. and Van der Spiegel, J. and Mueller, P. **Real-time 2D analog motion detector VLSI circuit**, JUN 1992; *Proc. IJCNN*, Vol. 4, Pages: 426-431.
- Feather, Gary A. **Micromirrors and Digital Processing**, In: *Photonics Spectra*, MAY 1995; Vol. 29, Iss. 5, Pages: 118-124.
- Fichou, D. and Nunzi, J-M. and Charra, F. and Pfeffer, N. **α -Sexithiophene: A New Photochromic Material for a Prototype Ultrafast Incoherent-to-Coherent Optical Converter**, In: *Advanced Materials*, JAN 01 1994; Vol. 6, No. 1, Pages: 64-67.

- Fry, G.A. and Alpern, M. **The effect of a peripheral glare source upon the apparent brightness of an object**, In: Journal of the Optical Society of America, 1953; Vol. 43, Pages: 189-195.
- Fry, G.A. **A revaluation of the scattering theory of glare**, In: Journal of the illuminating engineering society, 1954; Vol. XLIX, No. 2, Pages: 89-102.
- Goldstein, E. Bruce *Sensation and Perception*, Wadsworth Publishing Company: Belmont, California; A Division of Wadsworth Inc., 1984.
- Gorden, Shepherd M., Ed. *The Synaptic Organization of the Brain*, Oxford University Press, Boston, Massachusetts, 1990.
- Harper, C.A. and Sampson, R.M., Eds. *Electronic Materials & Processes Handbook*, Licari, J.J. chapter: Thin and Thick Films, McGraw-Hill, Inc., New York, 1994.
- Held, Richard and Richards, Whitman, Eds. *Recent progress in perception*, W.H. Freeman and Company, San Francisco, 1976.
- Hemenger, Richard P. **Sources of intraocular light scatter from inversion of an empirical glare function**, In: Applied optics, JUL 01 1992; Vol. 31, No. 19, Pages: 3687-3693.
- Hess, R.F. and Sharpe, L.T. and Nordby, K., Eds. *Night vision: basic, clinical, and applied aspects*, Cambridge University Press, 1990.
- Holladay, L.L. **The fundamentals of glare and visibility**, In: Journal of the Optical Society of America, 1926; Vol. 12, Pages: 271-319.
- Hood, D.C. and Birch, D.G. **Computational Models of Rod-Driven Retinal Activity**, In: IEEE engineering in medicine and biology magazine, JAN 01 1995; Vol. 14, No. 1, Pages: 59-66.
- Hornak, Lawrence A. *Polymers for lightwave and integrated optics*, Marcel Dekker, Inc. New York, Basel, Hong Kong, 1992.
- Horner, J., Ed. *Optical Signal Processing*, Academic, San Diego, 1987.
- Horspool, William M. *CRC Handbook of Organic Photochemistry and Photobiology*, CRC Press, 1995.
- Hübel, David H. *Eye, Brain and Vision*, Scientific American Library book #22, 1988.
- InFocus LitePro[®]500 LCD overhead display specifications, 1994.

- Irie, M., Ed. ***Photo-reactive Materials for ultrahigh Density Optical Memory***, part: Photochromic Materials, ELSEVIER Amsterdam, 1994.
- Johansson, T. and Abbasi, M. and Huber, R.J. and Normann, R.A. **A three-dimensional architecture for a parallel processing array (silicon retina application)**, DEC 1992; IEEE Transactions on Biomedical Engineering, Vol. 39, Iss. 12, Pages: 1292-1297.
- Johnson, Kristina M. **Flat panel displays or bust?**, In: Physics world, SEP 01 1992; Vol. 5, No. 9, Pages: 37-42.
- Jones, Clark R. **Quantum Efficiency of Human Vision**, In: J. Opt. Soc. Am. A, JUL 1959; Vol. 49, No. 7, Pages: 645-653.
- Kohley, R. and Reif, K. and Pohlmann, T. and Müller, P. **Operating a large area MPP-CCD with anti-blooming**, In: Charge-Coupled Devices and Solid State Optical Sensors V, FEB 1995; Proc. SPIE, Vol. 2415, Pages: 67-76.
- Kolb, H. and Fernandez, E. and Schouten, J. and Ahnelt, P. and Linberg, K.A. and Fisher, S.K. **Are There Three Types of Horizontal Cell in the Human Retina?**, In: The journal of comparative neurology, MAY 15 1994; Vol. 343, No. 3, Pages: 370-386.
- Krebs, W. and Krebs, I., Eds. ***Primate Retina and Choroid – Atlas of Fine Structure in Man and Monkey***, New York: Springer-Verlag, 1991.
- Krongauz, V.V. and Trifunac, A.D., Eds. ***Processes in Photoreactive Polymers***, Chapman & Hall, 1995.
- Lakowski, Roni *University of British Columbia*, Private communication, 1992.
- Lankheet, M.J.M. and van Wezel, R.J.A. and Prickaerts, J.H.H.J. and van de Grind, W.A. **The dynamics of light adaptation in cat horizontal cell responses**, In: Vision Research, JUN 1993a; Vol. 33, Iss. 9, Pages: 1153-1171.
- Lankheet, M.J.M. and Przybyszewski, A.W. and van de Grind, W.A. **The lateral spread of light adaptation in cat horizontal cell responses**, In: Vision Research, JUN 1993b; Vol. 33, Iss. 9, Pages: 1173-1184.
- Lessard, Roger A. and Changkakoti, R. and Roberge, Danny and Manivannan, G. **Photopolymers in Optical Computing: Materials and Devices**, In: Optical Computing, JUN 1992; Proc. SPIE, Vol. 1806, Pages: 2-13.
- Leybovic, K.N., Ed. ***Science of Vision***, New York: Springer-Verlag, 1990.

- Lin, Tsen-Hwang *Texas Instruments Inc.*, Private communication, 1994.
- MacLeod, Donald I. and Chen, Bing and Crognale, Michael **Spatial organization of sensitivity regulation in rod vision**, In: *Vision research*, 1989; Vol. 29, No. 8, Pages: 965-978.
- MacLeod, Donald I. and He, Sheng **Visible flicker from invisible patterns**, In: *Nature*, JAN 21, 1993; Vol. 361, Pages: 256-258.
- Mahowald, Misha A. and Mead, Carver **The Silicon Retina**, In: *Scientific American*, MAY 01 1991; Vol. 264, No. 5, Pages: 76-84.
- Malatesta, V. and Ranghino, G. and Romano, U. and Allegrini, P. **Photochromic Spiro-naphthoxazines: A Theoretical Study**, In: *Int. J. of Quantum Chemistry*, 1992; Vol. 42, Pages: 879-887.
- Mann, J.A. **Implementing early visual processing in analog vlsi: light adaptation**, In: *Visual Information Processing*, APR 1991; Proc. SPIE, Vol. 1473, Pages: 128-136.
- March, Jerry *Advanced Organic Chemistry*, John Wiley & Sons, New York, 1985.
- Mathur, B.P. and Koch, C.H., Eds. **Visual information processing: From neurons to chips**, APR 1991; Proc. SPIE, Vol. 1473.
- McArdle, C.B. *Applied photochromic polymer systems*, Glasgow: Blackie; New York: Chapman and Hall, 1992.
- McKnight, D.J. and Vass, D.G. and Sillitto, R.M. **Development of spatial light modulator: a randomly addressed liquid-crystal-over-nMOS array**, In: *Applied optics*, NOV 15 1989; Vol. 28, No. 22, Pages: 4757-4762.
- Mead, C. *Analog VLSI and neural systems*, Addison-Wesley Publishing Company, 1989.
- Megla, G.K. **Optical Properties and Applications of Photochromic Glass**, In: *Applied Optics*, JUN 1966; Vol. 5, No. 6, Pages: 945-960.
- Melzack, Ronald **Phantom Limbs**, In: *Scientific American*, APR 01 1992; Pages: 120-126.
- Nadler, M.P. and Miller, D. and Nadler, D.J., Eds. *Glare And Contrast Sensitivity For Clinicians*, New York: Springer-Verlag, 1990.
- Neff, J.A. and Athale, R.A. and Lee, S.H. **Two Dimensional Spatial Light Modulators – A Tutorial**, Proc. IEEE, 1990; Vol. 78, Page: 826.

- Nerger, J.L. and Cicerone, C.M. **The ratio of L cones to M cones in the human parafoveal retina**, In: Vision research, MAY 1992; Vol. 32, No. 5, Pages: 879-888.
- Normann, R.A. and Werblin, F.S. **Control of retinal sensitivity: I. Light and dark adaptation of vertebrate rods and cones**, In: Journal of Physiology, 1974; Vol. 63, Pages: 37-61.
- Pham, V.P. and Manivannan, G. and Po, R. **Real-time dynamic polarization holographic recording on auto-erasable azo-dye doped PMMA storage media**, In: Optical materials, MAR 01 1995; Vol. 4, No. 4, Page: 467.
- Phipson, T.L. In: Chem. News, 1881; Vol. 44, Page: 293.
- Polyak, Stephen Lucian, *The vertebrate visual system: its origin, structure, and function and its manifestation in disease with an analysis of its role in the life of animals and in the origin of man, preceded by a historical review of investigations of the eye, and of the visual pathways and centers of the brain*, Chicago: University of Chicago Press, 1957.
- Potts, A.M., Ed. *The assessment of Visual Functions*, Keeney, A.H. chapter 9: Assessment of special visual function, The C.V. Mosby Company, Saint Louis, 1972.
- Prassas, Michel *Corning Europe Inc.*, Private communication, 1994.
- Rawicz, Andrew H. *Simon Fraser University*, Private communication, 1991.
- Ray, Sidney F. *The Photographic Lens*, Focal Press – London, 1979.
- Rodieck, R.W. *The Vertebrate Retina*, San Francisco: Freeman, 1973.
- Röhrenbeck, J. and Wässle, H. and Boycott, B.B. **Horizontal Cells in the Monkey Retina: Immunocytochemical staining with antibodies against calcium binding proteins**, In: European journal of neuroscience, SEP 01 1989; Vol. 1, No. 5, Pages: 407-420.
- Rose, Albert **Quantum and Noise Limitations of the Visual Process**, In: J. Opt. Soc. Am. A, SEP 1953; Vol. 43, No. 9, Pages: 715-716.
- Ross III, Denwood F. **Ophthalmic lenses: accurately characterizing transmittance of ophthalmic and other common lens materials**, In: Applied Optics, SEP 01 1991; Vol. 30, No. 25, Pages: 3673-3677.
- Sakka, Sumio **Current status of the preparation of optical solids by the sol-gel method**, In: Sol-Gel Optics II, 1992; Proc. SPIE, Vol. 1758, Pages: 2-13.

- Schnapf, Julie L. and Baylor, Denis A. **How Photoreceptor Cells Respond to Light**, In: Scientific American, APR 1987; Vol. 256, No. 4, Pages: 40-47.
- Serati, S.A and Ewing, T.K. and Serati, R.A. and Johnson, K.M. and Simon, D.M. **Programmable 128x128 ferroelectric-liquid-crystal spatial-light-modulator compact correlator**, In: Optical Pattern Recognition IV, APR 1993; Proc. SPIE, Vol. 1959, Pages: 55-68.
- SHARP *QA-1650 LCD overhead display specifications*, 1994.
- Sharpe, Lindsay T. and Fach, Clemens and Nordby, Knut and Stockman, Andrew **The Incremental Threshold of the Rod Visual System and Weber's Law**, In: Science, APR 21, 1989; Vol. 244, Pages: 354-356.
- Sjöstrand, Fritiof S. *Deducing function from structure*, San Diego: Academic Press, 1990.
- Skrzypek, Josef **Lightness Constancy: Connectionist Architecture for Controlling Sensitivity**, In: IEEE Transactions on Systems, Man, and Cybernetics, SEP/OCT 1990; Vol. 20, No. 5, Pages: 957-967.
- Sloane, M.E. and Owsley, C. and Jackson, C.A. **Aging and luminance-adaptation effects on spatial contrast sensitivity**, In: Journal of the Optical Society of America A, 1988; Vol. 5, No. 12, Pages: 2181-2190.
- Siminoff, R. **Simulated bipolar cells in fovea of human retina, I. Computer simulations**, In: Biological Cybernetics, 1991; Vol. 64, No. 6, Pages: 497-504.
- Smith, G.P. **Photochromic Glasses: Properties and Applications**, In: Journal of Material Science, 1967; Vol. 2, Pages: 139-152.
- Southworth, Glen **Time Exposures Boost Sensitivity**, In: Lasers & Optronics, OCT 1992; Pages: 17-18.
- Stiles, S.W. **The effect of glare on the brightness difference threshold**, In: Tech. rep., Dept. Sci. Ind. Res. Illum. Res. Tech. Paper No. 8. H. M., Stationery Office – London, 1929.
- Tomlinson, W.J. **Phase Holograms in Photochromic Materials**, In: Applied Optics, APR 1972; Vol. 11, No. 4, Pages: 823-831.
- Trotter, D.M. Jr. **Photochromic and Photosensitive Glass**, In: Scientific American, APR 01 1991; Vol. 264, No. 4, Pages: 124-129.

- Tsukamoto, Yoshihiko and Sterling, Peter **Spatial summation by ganglion cells: some consequences for the efficient encoding of natural scenes**, In: Neuroscience Research, Supp. 1991; Vol. 15, Pages: S185-S198.
- Tunimanova, I.V. and Voronin, F.V. and Chetvergoy, N.P. and Shevlyagina, M.M. and Papunoshvili, N.A. **Photochromic glasses in systems for controlling high-intensity emitting objects**, In: Soviet Journal of Optical Technology, MAY 1991; Vol. 58, Pages: 290-292.
- Ueda, Takaharu and Yamamoto, Tetsu and Adachi, Mitsunori **CCD Array Scanning Servomechanism for a High Resolution Camera-Type Color Image**, In: JSME international journal, Series III, MAR 01 1990; Vol. 33, No. 1, Page: 89.
- Uhlmann, D.R. and Kreidl, N.J., Eds. **Optical properties of glass**, chapter: Photochromic Glasses, The American Ceramic Society, 1991.
- De Valois, Russell L. **Spatial Vision**, New York: Oxford University Press, 1988.
- Vimal, R.L.P. and Pokorny, J. and Smith, V.C. and Shevell, S.K. **Foveal Cone Threshold**, In: Vision research, 1989; Vol. 29, No. 1, Pages: 61-78.
- Vollhardt, Peter K. **Organic Chemistry**, W.H. Freeman and Company, New York, 1987.
- Vossen, J.L. and Kern, W., Eds. **Thin Film Processes II**, chapter: Sol-Gel Coatings, Academic Press, 1991.
- Wandell, Brian A. **Foundations of Vision**, Sinauer Associates, Inc., Sunderland, Massachusetts, 1995.
- Ward, V. and Syrzycki, M. and Chapman, G. **CMOS Photodetector With Built-in Light Adaptation**, In: Microelectronics journal, AUG 01 1993; Vol. 24, No. 5, Page: 547.
- Wässle, H. and Boycott, B.B. and Röhrenbeck, J. **Horizontal Cells in the Monkey Retina: Cone connections and dendritic network**, In: European journal of neuroscience, SEP 01 1989; Vol. 1, No. 5, Pages: 421-435.
- Wilkinson, F. and Hopley, J. and Naftaly, M. **Photochromism of Spiro-naphthoxazines: Molar Absorption Coefficients and Quantum Efficiencies**, In: J. Chem. Soc. Faraday Trans., 1992; Vol. 88, Iss. 11, Pages: 1511-1517.
- Williams, George M. and Blouke, Morley M. **How to capture low-light-level images without intensifiers**, In: Laser Focus World, SEP 1995; Pages: 129-138.

- Winslow, R.L. and Knapp, A.G. **Dynamic models of the retinal horizontal cell network**, In: *Progress in Biophysics & Molecular Biology*, 1991; Vol.56, Iss. 2, Pages: 107-133.
- Wysokinski, T.W. *Survey of "Smart Retina" Concept*, Technical Report, Prepared for Andrew Engineering Inc., OCT 02, 1994; Pages: 34.
- Wysokinski, T.W. and Rawicz, A.H. and Letowski, S. **Dynamic Range Extension of Photosensitive Device Array**, In: *Applications of Photonic Technology*, Eds. Lampropoulos, G.A. et al., Plenum Press, New York and London, 1995a; Proc. of International Conference on Applications of Photonic Technology – ICAPT'94, Toronto – June 1994, Sponsoring society: IEEE & IEE, Pages: 531-534.
- Wysokinski, T.W. and Rawicz, A.H. and Letowski, S. **Modelling and Testing of a Light-Induced Spatial Light Modulator in Hybrid Optoelectronic Systems**, In: *Micro-wave and Optical Technology Letters*, JUN 05 1995b; Vol. 9, No. 2, Pages: 72-77.
- Wysokinski, T.W. and Letowski, S. and Czyzewska, E. and Rawicz, A.H. **Characterization of a Transformation Function of a Photochromic Adaptive Filter**, In: *Spectroscopy Letters*, MAR 1996a; Vol. 29, No. 2, Pages: 337-344.
- Wysokinski, T.W. and Czyzewska, E. and Rawicz, A.H. **Development, Properties and Applications of a Photochromic Adaptive Filter**, Submitted to: *Thin Solid Films*, 1996b.
- Yang, Xiong-Li and Wu, Samuel M. **Modulation of Rod-Cone Coupling by Light**, In: *Science*, APR 21, 1989; Vol. 244, Pages: 352-354.
- Yeh, Chai *Applied Photonics*, San Diego: Academic Press, 1994.
- Young, John M. *Contemporary Photochromic Lenses*, Course Text for Opticians, NAO, 1993.
- Younse, Jack M. **Mirrors on a chip**, In: *IEEE Spectrum*, NOV 1993; Vol. 30, No. 11, Pages: 27-31.
- Ziegler, John P. and Howard, Bruce M. **Flat Panel Display Technology**, In: *The Electrochemical Society Interface*, SUMMER 1994; Vol. 3, No. 2, Pages: 27-35.